

International Journal of Modern Physics D
 © World Scientific Publishing Company

EXTENDED GRAVITY COSMOGRAPHY

SALVATORE CAPOZZIELLO

*Dipartimento di Fisica, Università di Napoli “Federico II”, and Istituto Nazionale di Fisica Nucleare, Sez. di Napoli, Via Cinthia 9, I-80126 Napoli, Italy,
 Gran Sasso Science Institute, Via F. Crispi 7, I-67100, L’Aquila, Italy,
 Laboratory for Theoretical Cosmology,
 Tomsk State University of Control Systems and Radioelectronics (TUSUR),
 634050 Tomsk, Russia,
 Tomsk State Pedagogical University, ul. Kievskaya, 60, 634061 Tomsk, Russia.
 capozziello@na.infn.it*

ROCCO D’AGOSTINO

*Istituto Nazionale di Fisica Nucleare, Sez. di Roma “Tor Vergata”, Via della Ricerca Scientifica
 1, I-00133, Roma, Italy.
 rocco.dagostino@roma2.infn.it*

ORLANDO LUONGO

*Istituto Nazionale di Fisica Nucleare, Laboratori Nazionali di Frascati, 00044 Frascati, Italy.
 Scuola di Scienze e Tecnologie, Università di Camerino, 62032 Camerino, Italy.
 NNLOT, Al-Farabi Kazakh National University, Al-Farabi av. 71, 050040 Almaty, Kazakhstan.
 orlando.luongo@lnf.infn.it*

Received Day Month Year
 Revised Day Month Year

Cosmography can be considered as a sort of a model-independent approach to tackle the dark energy/modified gravity problem. In this review, the success and the shortcomings of the Λ CDM model, based on General Relativity and standard model of particles, are discussed in view of the most recent observational constraints. The motivations for considering extensions and modifications of General Relativity are taken into account, with particular attention to $f(R)$ and $f(T)$ theories of gravity where dynamics is represented by curvature or torsion field respectively. The features of $f(R)$ models are explored in metric and Palatini formalisms. We discuss the connection between $f(R)$ gravity and scalar-tensor theories highlighting the role of conformal transformations in the Einstein and Jordan frames. Cosmological dynamics of $f(R)$ models is investigated through the corresponding viability criteria. Afterwards, the equivalent formulation of General Relativity (Teleparallel Equivalent General Relativity) in terms of torsion and its extension to $f(T)$ gravity is considered. Finally, the cosmographic method is adopted to break the degeneracy among dark energy models. A novel approach, built upon rational Padé and Chebyshev polynomials, is proposed to overcome limits of standard cosmography based on Taylor expansion. The approach provides accurate model-independent approximations of the Hubble flow. Numerical analyses, based on Monte Carlo Markov Chain integration of cosmic data, are presented to bound coefficients of the cosmographic series. These techniques are thus applied to reconstruct $f(R)$ and $f(T)$ functions and to frame the late-time expansion history of the universe with no *a priori* assumptions on

2 *S. Capozziello, R. D'Agostino, O. Luongo*

its equation of state. A comparison between the Λ CDM cosmological model with $f(R)$ and $f(T)$ models is reported.

Keywords: Extended gravity; cosmography; dark energy; cosmological observations.

Contents

1. Introduction 2

2. The cosmological puzzle 4

 2.1. Issues with the Λ CDM model 7

 2.2. Dark energy 9

3. Extended theories of gravity: the case of $f(R)$ gravity 10

 3.1. The metric formalism and its viability conditions in cosmology 12

 3.2. The Palatini formalism and viability conditions 15

 3.3. Equivalence between $f(R)$ gravity and scalar-tensor theories 17

4. Gravity with torsion 20

 4.1. Teleparallel Equivalent of General Relativity 23

 4.2. $f(T)$ gravity 26

5. Cosmography 28

 5.1. Limits of standard cosmography 30

 5.2. Improving standard cosmography 31

 5.2.1. The method of Padé polynomials 31

 5.2.2. The method of Chebyshev polynomials 32

 5.2.3. The convergence radius of rational approximations 36

 5.3. Observational constraints 37

 5.4. The E_i s method 39

6. Model-independent reconstruction of $f(R)$ gravity 43

 6.1. The metric formalism case 43

 6.2. The Palatini formalism case 54

7. Model-independent reconstruction of $f(T)$ gravity 58

 7.1. Comparison with previous $f(T)$ models 67

8. Final outlook 69

Appendix A. Experimental data compilations 72

Appendix B. Padé approximations of the luminosity distance 73

Appendix C. Rational Chebyshev approximations of the luminosity distance 73

1. Introduction

The present picture of the universe is based on the homogeneous and isotropic Friedmann-Lemaître-Robertson-Walker (FLRW) metric, which represents a solution of the Einstein field equations of General Relativity (GR). The success of the Big Bang model¹ comes from its remarkable match with the available cosmological observations. However, some shortcomings of this picture, emerged in the last thirty years, have made scientists doubt on the appropriateness of achieve a comprehensive picture of the universe simply based on GR and standard perfect fluid

matter. A crucial role in this respect is played by the relation between cosmology and quantum field theory. The Big Bang singularity along with issues such as the monopole, horizon, and flatness problems² undermine the standard model of particle physics and the standard model of cosmology as an adequate description of the universe at high-energy regimes. On the other hand, a fundamental theory to describe space-time in its full quantum aspects cannot be represented by a classical theory like GR. Therefore, the lack of a definitive quantum theory of gravity is the reason to consider alternative gravitational theories where GR can be reproduced in the semiclassical limit. The so-called Extended Theories of Gravity (ETG), based on corrections and extensions of the Einsteins theory, are the most fruitful paradigms following the aforementioned receipt. The idea behind this approach is essentially to consider some effective quantum gravity action adding higher order curvature invariants and scalar fields minimally or nonminimally coupled to the gravity sector recovering GR at local scales and in the weak field limit.³ In this perspective, it is more correct to deal with *Extended Gravity*^a instead of modified gravity.⁴ The presence of non-minimal couplings and high-order terms appears necessary in any scheme trying to unify fundamental interactions (*e.g.* supergravity and superstring theories).⁵ These contributions come from first or higher-order loop corrections in the high curvature regime.⁵ Quantization of matter fields in curved space-time leads to corrections of the Hilbert-Einstein Lagrangian due to the interactions between the background geometry and quantum scalar fields.⁶

A revision of standard cosmological scenarios is necessary also at late-time epochs. In fact, observations of Supernovae Ia (SNeIa)^{7,8} suggested that the expansion of the universe has recently entered an accelerated phase that cannot be explained only by the dynamics of ordinary matter and radiation as constituents of the cosmic fluid.⁹ On the other hand, Cosmic Microwave Background (CMB) anisotropies^{10,11} strongly suggest a universe with flat spatial curvature.

Within the framework of GR, the simplest explanation for the cosmic speed up would be the well known cosmological constant,¹² which defines the concordance Λ Cold Dark Matter (Λ CDM) model. Although very effective in fitting most of the cosmological data, the Λ CDM model is plagued by some fundamental issues related to its nature.^{13,17} One possible attempt to fix these problem is to replace the cosmological constant with a slowly rolling scalar field, known as *quintessence*.^{19,21} However, even the quintessence approach presents some issues related to the *coincidence problem*.

^a A typical example of extended theory is $f(R)$ gravity. Assuming $f(R) = R$ means that GR is a particular theory in a wide family of model. On the other hand, considering $f(R) = R + \alpha R^2$ means that, if R^2 term is negligible, GR is recovered. Regarding $f(T)$ gravity, the situation is similar because $f(T) = T$ means recovering TEGR (Teleparallel Equivalent General Relativity). In this case, dynamics is given by the torsion scalar T , instead of the curvature scalar R . However the description is equivalent. We intend with "modified gravity" or "alternative gravity", theories which do not reproduce GR in a given energy regime or choice of models. This can be the case of some gauge theories of gravity.

4 *S. Capozziello, R. D'Agostino, O. Luongo*

Furthermore, there exists a different way to approach the cosmic acceleration problem. In fact, the observed behaviour of the late-time expansion might not be due to new species in the cosmic fluid, but rather the signal of a breakdown of standard gravity at infrared regimes. In this respect, modifications of the Friedmann equations give rise to alternative paradigms where effective models with generalizations of the gravity action (e.g. high-order curvature terms) can yield to quintessence behaviour.²⁵ Moreover, the cosmological constant behaviour may be the consequence of including torsion fields starting from the so called Teleparallel Equivalent General Relativity (TEGR).²⁶

In these alternative approaches, the philosophy is that conceptual shortcomings in cosmic evolution are overcome deriving negative pressure scenarios naturally originated from the further geometric degrees of freedom that these models contain with respect to standard GR.

In this review paper, we want to discuss how a cosmographic approach, besides observations coming from *Precision Cosmology*, can contribute to select self-consistent cosmological models based on extensions of GR and TEGR.

The structure of the paper is as follows. In Sec. 2, we review the concordance cosmological model and the issues related to the nature and origin of dark energy. In Sec. 3, we discuss $f(R)$ gravity as a straightforward extension of GR introduced to approach shortcomings of the standard cosmological scenario. In particular, we discuss dynamics and observational viability of such theories in both metric and Palatini formulations. Gravity with torsion is considered in Sec. 4. Specifically, we present the teleparallel equivalent of Einstein's theory (TEGR) and extend the discussion to generic functions of torsion scalar in presence, eventually, of scalar fields coupled to gravity. In Sec. 5, we present the cosmographic method as a model-independent tool to discriminate among dark energy models. The limits of the standard cosmographic approach are discussed and a new method, based on rational polynomials, is presented. The approach is aimed to alleviate the convergence issues at high-redshift epochs. Finally, in Secs. 6 and 7, the cosmographic method is applied to reconstruct gravitational action in a model-independent way starting from the cosmological constraints of the late-time universe.

Throughout the text, we use the metric signature $(+, -, -, -)$ and units such that $c = \hbar = 1$, unless differently specified. We also use the notation $\kappa \equiv 8\pi G = M_{\text{P}}^{-2}$, where G is the Newton constant and M_{P} is the reduced Planck mass.

2. The cosmological puzzle

The standard cosmological model is based on the *cosmological principle*, which consists of two principles of spatial invariance. The first invariance is the isomorphism under translations. This means assuming the universe to be *homogeneous* on large scales, with no special points and galaxies evenly distributed in space. The second invariance is the isomorphism under rotations. This implies an *isotropic* universe with no special spatial directions, where the galaxies are evenly distributed in dif-

ferent angular directions at large scales.

The cosmological principle provides us with the simplest cosmological models, the homogeneous and isotropic universe described by the FLRW metric:²⁷⁻³⁰

$$ds^2 \equiv g_{\mu\nu} dx^\mu dx^\nu = dt^2 - a(t)^2 \left[\frac{dr^2}{1 - kr^2} + r^2(d\theta^2 + \sin^2 \theta d\phi^2) \right], \quad (1)$$

where t is the cosmic time, $a(t)$ is the dimensionless scale factor normalized to unity at the present time ($a(t_0) = 1$), and k defines the spatial curvature:

$$k = \begin{cases} -1 & \text{open universe,} \\ 0 & \text{flat universe,} \\ +1 & \text{closed universe.} \end{cases} \quad (2)$$

To determine the dynamics of the gravitational field for a homogeneous and isotropic universe, we write the Einstein field equations:

$$R_{\mu\nu} - \frac{1}{2}Rg_{\mu\nu} = \kappa T_{\mu\nu}, \quad (3)$$

where $R_{\mu\nu}$ is the Ricci tensor, $R = g_{\mu\nu}R^{\mu\nu}$ is the Ricci (scalar) curvature. $T_{\mu\nu}$ is the energy-momentum tensor which, for a perfect fluid^b, takes the form

$$T_{\mu\nu} = (\rho + P)u_\mu u_\nu - Pg_{\mu\nu}, \quad (4)$$

where ρ and $P(\rho)$ are the density and pressure of the *barotropic* fluid, respectively, which depend on the cosmic time only in agreement with the symmetry properties of the FLRW metric. The four-velocity field u^μ refer to an observer moving inside the light cone and, hence, it is normalized according to

$$g_{\mu\nu}u^\mu u^\nu = 1. \quad (5)$$

In a reference frame which is at rest with respect to the fluid ($u^i = 0$), the relation $u_0 u^0 = 1$ holds and one then has

$$T_{\mu\nu} = \text{diag}(\rho, -P, -P, -P). \quad (6)$$

SNeIa observations at the end of the 90's indicated that the universe is currently undergoing a phase of accelerated expansion.^{7,8} This implies that

$$\rho + 3P < 0. \quad (7)$$

Clearly, this condition cannot be satisfied if the cosmic fluid were made only of radiation and pressureless non-relativistic matter. Therefore, cosmological sources have to include a further component with negative pressure ($P < -\rho/3$), which is today dominant over the other species. This component is dubbed *dark energy*.¹⁸⁻²²

^bA 'perfect' fluid is an ideal fluid characterized by zero viscosity, no shear stresses and vanishing vorticity.

6 *S. Capozziello, R. D'Agostino, O. Luongo*

The simplest model that can describe the dark energy behaviour is a model with the cosmological constant Λ , characterized by the equation of state

$$w_\Lambda \equiv \frac{P_\Lambda}{\rho_\Lambda} = -1 . \quad (8)$$

The gravitational contribution of the cosmological constant can be added into the Einstein-Hilbert action as

$$\mathcal{S} = \int d^4x \sqrt{-g} \left[\frac{1}{\kappa} \left(\frac{R}{2} - \Lambda \right) + \mathcal{L}_m \right] , \quad (9)$$

where \mathcal{L}_m is the matter Lagrangian density. The field equations are obtained by varying the above action with respect to the metric:

$$G_{\mu\nu} - \Lambda g_{\mu\nu} = \kappa T_{\mu\nu} , \quad (10)$$

where $G_{\mu\nu} \equiv R_{\mu\nu} - \frac{1}{2}g_{\mu\nu}R$ is the *Einstein tensor*. Writing Eq. (10) for the FLRW metric, one obtains the Friedmann equations as

$$H^2 = \frac{\kappa}{3}\rho + \frac{\Lambda}{3} - \frac{k}{a^2} , \quad (11)$$

$$\frac{\ddot{a}}{a} = -\frac{\kappa}{6}(\rho + 3P) + \frac{\Lambda}{3} . \quad (12)$$

We thus define the density parameters associated to curvature, matter and cosmological constant as, respectively,

$$\Omega_k \equiv -\frac{k}{a^2 H^2}, \quad \Omega_m \equiv \frac{\kappa \rho_m}{3H^2}, \quad \Omega_\Lambda \equiv -\frac{\Lambda}{3H^2} \quad (13)$$

obeying the cosmic rule

$$1 = \Omega_m + \Omega_k + \Omega_\Lambda , \quad (14)$$

derived from (11). We can finally write the Hubble expansion rate in the form^c

$$H(a) = H_0 \left[\frac{\Omega_{r0}}{a^4} + \frac{\Omega_{m0}}{a^3} + \frac{\Omega_{k0}}{a^2} + \Omega_{\Lambda 0} \right]^{1/2} , \quad (15)$$

where the subscript ‘0’ denotes the corresponding present values of the density parameters. The combinations of low-redshift data and CMB anisotropy measurements portray a universe with the following features:

- vanishing spatial curvature: $\Omega_{k0} \approx 0$;
- very small amount of residual radiation: $\Omega_{r0} \approx 5 \times 10^{-5}$;
- about 30% of matter-energy density, mainly constituted of cold dark matter and a small contribution of baryonic matter: $\Omega_{m0} = \Omega_{cdm,0} + \Omega_{b0} \approx 0.3$, with $\Omega_{cdm,0} \approx 0.25$ and $\Omega_{b0} \approx 0.05$;
- about 70% of dark energy in the form of cosmological constant: $\Omega_{\Lambda 0} \approx 0.7$.

Such a ”paradigm” is named Λ CDM model and represents the so-called *concordance model of cosmology*.

^cWe here include the contribution of radiation Ω_r , which is usually neglected in the late-time epochs.

2.1. Issues with the Λ CDM model

The simplest explanation for the accelerating universe provided by the cosmological constant, although very effective in fitting all the major cosmological observables, does not give a satisfactory physical interpretation of dark energy for a number of issues.¹⁷ Particle physicists considered the possibility to identify the cosmological constant with the energy of the vacuum. Assuming that the vacuum is a Lorentz-invariant state, its energy-momentum tensor takes the form

$$T_{\mu\nu}^{\text{vac}} = -\rho_{\text{vac}}g_{\mu\nu} , \quad (16)$$

where the vacuum energy density ρ_{vac} is related to an isotropic pressure by

$$P_{\text{vac}} = -\rho_{\text{vac}} . \quad (17)$$

Comparing Eq. (17) with Eq. (8), we find that they are formally equivalent:

$$\rho_{\text{vac}} = \rho_{\Lambda} \equiv \frac{\Lambda}{\kappa} . \quad (18)$$

From the classical point of view, Λ is simply a constant whose value should be determined through experiments. These considerations, however, change once quantum mechanics enters the picture. In fact, from the Planck constant one can define a gravitational length scale named reduced Planck length:

$$L_{\text{P}} = M_{\text{P}}^{-1} = \sqrt{\kappa} . \quad (19)$$

We can thus think about quantum fluctuations in the vacuum. For a non-interacting quantum field, each mode contributes to the vacuum energy and the net result is obtained by integrating over all the modes. This integral is in principle divergent, which implies that the vacuum energy is infinite. To avoid the ultraviolet divergence, one can introduce a cut-off and ignore any contribution above that. Then, one naturally would expect that this cut-off is related to the Planck scale by

$$\Lambda \sim L_{\text{P}}^{-2} , \quad (20)$$

so as to obtain

$$\rho_{\Lambda} \sim M_{\text{P}}^4 \sim (10^{18} \text{ GeV})^4 . \quad (21)$$

On the other hand, measurements of the cosmological constant over the last decades from observations of SNeIa and CMB anisotropies¹¹ indicate the following value for the vacuum energy:

$$\rho_{\Lambda}^{(\text{obs})} \sim (10^{-3} \text{ eV})^4 . \quad (22)$$

Then, comparing (21) with (22), one gets

$$\rho_{\Lambda}^{(\text{obs})} \sim 10^{-120} \rho_{\text{vac}} . \quad (23)$$

This embarrassing discrepancy of 120 orders of magnitude is known as *the cosmological constant problem*.^{13,14}

8 *S. Capozziello, R. D'Agostino, O. Luongo*

The second issue is called *coincidence problem*.^{15,16} The concordance cosmological model provides values for the vacuum energy density and the matter density of the same order of magnitude. However, the two components have very different evolution histories:

$$\frac{\Omega_\Lambda}{\Omega_m} = \frac{\rho_\Lambda}{\rho_m} \propto a^3, \quad (24)$$

which implies that the current acceleration of the cosmic expansion started relatively recently. It becomes immediately clear that the transition between a matter-dominated universe and a universe dominated by dark energy is quite fast. This means that the probability for an observer to live during a period when the two species have the same order of magnitude is very small. Therefore, there is no physical reason for us to be on the verge of such a special moment when these components have a similar order of magnitude.

Another further problem that compromises our understanding of the cosmic speed up concerns the discrepancy between the direct and indirect (model-dependent) measurements of the present expansion rate of the universe.³¹ Since the first determination by Hubble in 1929,³² for decades astronomers derived values for H_0 in the range $50 \div 100$ km/s/Mpc. Improved accuracy in the measurements of H_0 were made over the years thanks to a better control of systematics and the use of different calibration techniques. Using the period-luminosity relation for Cepheids to calibrate a number of secondary distance indicators such as SN Ia and the Tully-Fisher relation, the Hubble Space Telescope Key Project³³ estimated $H_0 = (73 \pm 8)$ km/s/Mpc. The most recent direct estimate of H_0 has been provided in 34: $H_0 = (73.24 \pm 1.74)$ km/s/Mpc. This value is in tension with the most recent result of the Planck collaboration¹¹ for the Λ CDM model, $H_0 = (67.51 \pm 0.64)$ km/s/Mpc, which represents so far the strongest constraint on H_0 . An alternative method to measure the Hubble constant, independent of the local distance ladder, is provided by strong gravitational lenses with time delays between the multiple images. Using this approach, the H0LiCOW collaboration estimated $H_0 = 71.9^{+2.4}_{-3.0}$ km/s/Mpc for Λ CDM.³⁵ This value is in agreement with the direct measurement of³⁴ but in tension with Planck.

During the past years, many attempts have been done to solve the dark energy problem. From particle physics point of view, the lack of observed supersymmetric partners of known particles in accelerators leads to assume that the scale at which supersymmetry was broken is of the order of 10^3 GeV. This then implies the following estimate for the vacuum energy density:

$$\rho_\Lambda \sim M_{\text{SUSY}}^4 \sim (10^{12} \text{ GeV})^4. \quad (25)$$

This result is, however, still 60 orders of magnitude larger than the observed value (22). Other approaches based on string theory or loop quantum gravity^{13,17} require some fine-tuning and, in any case, fail to address the coincidence problem. In 2018 a mechanism for cancelling Λ out has been proposed through the use of a symmetry breaking potential in a Lagrangian formalism in which matter shows

a non-vanishing pressure.³⁶ The model assumes that standard matter provides a pressure which counterbalances the action due to the cosmological constant. It has been shown that this mechanism permits to take vacuum energy as quantum field theory predicts, but removing the huge magnitude through a counterbalance term due to baryons and cold dark matter only. The approach is equivalent to have a dark fluid which degenerates with the standard cosmological model^{37–40} and enters the class of unified dark energy models.^{41–43}

2.2. Dark energy

Another approach that seeks for solving the cosmological constant problem is to consider dynamical properties of dark energy. A dynamical dark energy, however, should be able to mimic the cosmological constant at the present time, as required by cosmological observations. In this sense, similarly to the inflationary mechanism,^{44,45} but at different energies, the simplest candidate is a canonical scalar field, often dubbed *quintessence*.^{46–48} For a homogeneous scalar field minimally coupled to gravity, the Klein-Gordon equation in FLRW space-time reads

$$\ddot{\phi} + 3H\dot{\phi} + V'(\phi) = 0, \quad (26)$$

where $V(\phi)$ is the potential of the scalar field and the ‘prime’ denotes derivative with respect to ϕ . Thus, the energy density and pressure are given by, respectively,

$$\rho_\phi = \frac{1}{2}\dot{\phi}^2 + V(\phi), \quad (27)$$

$$P_\phi = \frac{1}{2}\dot{\phi}^2 - V(\phi). \quad (28)$$

It is clear from Eqs. (27) and (28) that $w_\phi = P_\phi/\rho_\phi$ approaches -1 if the *slow-roll* condition $\dot{\phi}^2 \ll V(\phi)$ is satisfied. Imposing this condition, from Eq. (26), we must have $H \sim \sqrt{V''(\phi)}$. Thus, considering that $\sqrt{V''(\phi)}$ represents the effective mass of the scalar field m_ϕ and that the current value of $V(\phi)$ should be of the order of the observed Λ , one gets

$$m_\phi \sim 10^{-33} \text{ eV}. \quad (29)$$

Since the masses of scalar fields in quantum field theory are several orders of magnitude larger than the value of (29), many doubts remain on whether quintessence could be an actual solution of the cosmological constant problem.

There are also attempts to solve the coincidence problem by adopting specific models of quintessence called *tracker models*.^{49–51} In these models, the coincidence problem is solved as the energy density of the scalar field has the same behaviour of the radiation and matter energy densities for a significant part of the cosmic evolution. These solutions do not suffer from fine-tuning problems related to initial conditions, even though they are dependent on the parameters of the potential.

3. Extended theories of gravity: the case of $f(R)$ gravity

An alternative approach to address the dark energy issues is to consider modifications or extensions of the l.h.s of Einstein's field equations. We here discuss such a possibility to cure the shortcomings of the concordance cosmological model. We start presenting some historical reasons that brought first to consider extensions of GR at ultraviolet (UV) scales, and to infrared (IR) scales.

- **UV scales**

Due to their empirical success in describing the physical phenomena, GR and Quantum Field Theory (QFT) represent the two main pillars which modern physics is built on. While GR is the theory of gravitating systems and non-inertial frames on large scales, QFT provides a description of the world on small scales and at high energy regimes. As a classical theory, GR does not take into account the quantum nature of matter; on the other hand, QFT assumes that the space-time contains quantum fields. The key point is, thus, to figure out how quantum fields behave in presence of gravity or, in other words, whether these two theories are compatible. Non-classical effects are expected to be relevant for gravity at Planck's scale, which is unfortunately inaccessible by current experiments. Nevertheless, investigating the fundamental nature of space-time on very small scales is unescapable to shed light on the physics of the universe from the Big Bang to Planck's era.

At the end of the 1950s, the necessity to build up some unified theory capable of describing all the fundamental interactions under the standard of QFT made recognize the need for a quantum theory of gravity. So far, any unification scheme trying to include gravity has revealed unsuccessful or not completely satisfactory. The difficulties are mainly due the fact that the gravitational field describes the background space-time where the same gravitational degrees of freedom, that is the space-time itself, have to be considered as dynamical variables. The assumed mutual interaction between geometry and quantum matter fields necessarily leads to modifications of the standard Einstein-Hilbert action, that is, to consider *Extended Theories of Gravity* (ETG).^{56,57} Such theories represent a semi-classical approach where GR is recovered in the low-energy limit. As GR, these models are gauge invariant and consist of adding higher-order curvature invariants (such as R^2 , $R_{\mu\nu}R^{\mu\nu}$, $R_{\alpha\beta\mu\nu}R^{\alpha\beta\mu\nu}$, $R\Box R$, $R\Box^k R$) and minimally or non-minimally coupled terms between scalar fields and geometry (such as $\phi^2 R$), which come out from the effective action of Quantum Gravity.^{4,58}

- **IR scales**

Einstein's theory has proven successful over many years of experimental tests. GR is in remarkable agreement with precision tests of gravity done in the solar system and consistent with gravitational waves detection.⁵⁹ However, GR has not been tested independently on cosmological scales. The

observational evidences that the main amount of the present matter content of our universe is in the form of unknown particles that are not included in the standard model of particles and interactions, and the discovery of the present accelerated expansion of the universe, have led cosmologists to consider the possibility that GR might not be, in fact, the correct theory of gravity to describe the universe at larger scales. In order to address this issue, two different kinds of phenomena have been proposed: the so-called ‘dark energy models’ and modifications to GR. While the former introduce a new fluid or field from which the apparent cosmological constant could originate, the latter refers to modifying the l.h.s. of Einstein’s equations, i.e., GR itself, by modifying or improving the Einstein-Hilbert action. The ETG theories have thus attracted great interest in cosmology. The related cosmological models, in fact, provide inflationary scenarios able to overcome the shortcomings of standard model based on GR, and the theoretical predictions match with the CMB observations.^{60–62} Moreover, conformal transformations allow to reformulate the higher-order and non-minimally coupled terms into GR term plus one or multiple minimally coupled scalar fields.^{63–65} However, modifications of standard gravitational theory are characterized by mathematical difficulties since the corrections to the standard Lagrangian increase the non-linearity of the field equations, which often produce differential equations higher than the second order.

The possibility to include higher-order curvature invariants in the gravitational action was firstly considered in the 1960s as an attempt to quantize gravity. It was shown that renormalization at the one-loop level requires adding higher-order curvature terms to the Einstein-Hilbert action.⁶⁶ It was initially expected that such terms were suppressed by small couplings and their relevance was confined only to the strong gravity regimes. More recently, however, the dark energy problem related to the late-time acceleration of the universe has revived interest in considering these modifications as possible extensions of GR. We can account for higher-order curvature invariants by generalizing the standard gravitational action to any function of the Ricci scalar, that is:

$$\mathcal{S} = \frac{1}{2\kappa} \int d^4x \sqrt{-g} f(R) + \mathcal{S}_m(g_{\mu\nu}, \psi) , \quad (30)$$

where \mathcal{S}_m is the action of the matter fields ψ . This example of ETG is called $f(R)$ gravity^{67–71} and can be considered a straightforward example of extension or modification of GR.

There exists two variational approaches to derive the field equations of $f(R)$ gravity. The standard procedure is to derived the field equations by varying the gravitational action with respect to the metric $g_{\mu\nu}$, which represents the only dynamical variable of the theory. In this standard approach, called *metric formalism*, one assumes that the connection is symmetric ($\Gamma_{\mu\nu}^\alpha = \Gamma_{\nu\mu}^\alpha$) and metric compatible ($\nabla_\mu g_{\nu\alpha} = 0$). This leads to the torsion-less Levi-Civita connection, which is

completely determined by the metric components.

In principle, the metric and the connection are two independent quantities: the former governs the causal structure of space-time, while the latter defines the geodesic structure. This is the idea behind the *Palatini formalism*,⁷² in which the action is varied with respect to both metric and connection. In the case of GR, the two formalisms are equivalent: the field equations for the connection gives exactly the Levi-Civita connections of the metric in the Einstein-Hilbert case. The situation is, however, different for more general action including non-linear terms in R or scalar fields non-minimally coupled to gravity. In these cases, the two formalisms provide different field equations and different physics.^{4, 73–75}

Finally, there is actually a third variational approach in which the matter action is assumed to be $\mathcal{S}_m(g_{\mu\nu}, \Gamma_{\mu\nu}^\lambda, \psi)$. This is a full *metric-affine formalism*^{76–78} and represents the most general case that reduces to metric or Palatini formalisms under certain assumptions.

In the following sections, we will derive the field equations for $f(R)$ gravity in the metric and Palatini formalisms. It is possible to show that the two versions of $f(R)$ gravity can be recast as scalar-tensor theories with specific values of the Brans-Dicke parameter.

3.1. *The metric formalism and its viability conditions in cosmology*

Let us now derive the field equations of $f(R)$ gravity in the metric formalism. Varying the action 30 with respect to the metric $g_{\mu\nu}$, one obtains

$$f'(R)R_{\mu\nu} - \frac{1}{2}f(R)g_{\mu\nu} - (\nabla_\mu \nabla_\nu - g_{\mu\nu} \square) f'(R) = \kappa T_{\mu\nu} , \quad (31)$$

where

$$T_{\mu\nu} = \frac{-2}{\sqrt{-g}} \frac{\delta \mathcal{S}_m}{\delta g^{\mu\nu}} . \quad (32)$$

Here, the ‘prime’ denotes derivative with respect to R . The field equations (31) are clearly fourth-order partial differential equations in the metric. When $f(R)$ is a linear function of R , the last two terms on left-hand side vanish and we recover GR. Taking the trace of Eq. (31) yields

$$f'(R)R - 2f(R) + 3\square f'(R) = \kappa T, \quad (33)$$

where $T = g^{\mu\nu} T_{\mu\nu}$. We note that R and T are related to each other through a differential equation, contrary to the algebraic relation $R = -\kappa T$ of GR. This means that solutions in $f(R)$ constitute a larger set compared to Einstein’s theory. It is useful to rewrite Eq. (31) in form of Einstein’s equations with a total effective energy-momentum tensor accounting for matter and curvature terms:

$$G_{\mu\nu} = \kappa \left(T_{\mu\nu}^{(m)} + T_{\mu\nu}^{(curv)} \right), \quad (34)$$

where we have identified

$$T_{\mu\nu}^{(m)} = \frac{T_{\mu\nu}}{f'(R)}, \quad (35)$$

$$T_{\mu\nu}^{(curv)} = \frac{1}{\kappa f'(R)} \left[\frac{f(R) - Rf'(R)}{2} g_{\mu\nu} + \nabla_\mu \nabla_\nu f'(R) - g_{\mu\nu} \square f'(R) \right]. \quad (36)$$

From Eq. (35), we immediately find that the effective gravitational constant in $f(R)$ gravity is given as

$$G_{eff} = \frac{G}{f'(R)}, \quad (37)$$

which imposes the condition $f'(R) > 0$.

The $f(R)$ theories of gravity have been largely invoked in cosmology to explain the current acceleration of the universe without the need of dark energy. To study the cosmological evolution at the background level, we assume the FLRW metric restricting our attention to the flat case ($k = 0$), which is favoured by the data.¹¹ Using the FLRW metric implies the following relation between the Ricci scalar and the Hubble parameter:

$$R = -6 \left[\frac{\ddot{a}}{a} + \left(\frac{\dot{a}}{a} \right)^2 \right] = -6(\dot{H} + 2H^2). \quad (38)$$

Furthermore, assuming that $T_{\mu\nu}^{(m)}$ is given by Eq. (6), the modified Friedmann equations read

$$H^2 = \frac{\kappa}{3} \left[\frac{\rho_m}{f'(R)} + \rho_{curv} \right], \quad (39)$$

$$2\dot{H} + 3H^2 = -\kappa \left[\frac{p_m}{f'(R)} + p_{curv} \right], \quad (40)$$

where

$$\rho_{curv} = \frac{1}{f'(R)} \left[\frac{1}{2} (f(R) - Rf'(R)) - 3H\dot{R}f''(R) \right], \quad (41)$$

$$p_{curv} = \frac{1}{f'(R)} \left[2H\dot{R}f''(R) + \ddot{R}f''(R) + (\dot{R})^2 f'''(R) - \frac{1}{2} (f(R) - Rf'(R)) \right] \quad (42)$$

are the energy density and pressure of the effective curvature fluid, respectively. Thus, from Eqs. (41) and (42) one obtains the effective equation of state

$$w_{DE} \equiv \frac{p_{curv}}{\rho_{curv}} = -1 + \frac{\ddot{R}f''(R) + (\dot{R})^2 f'''(R) - H\dot{R}f''(R)}{(f(R) - Rf'(R))/2 - 3H\dot{R}f''(R)}, \quad (43)$$

which is supposed to fuel the effective dark energy fluid associated to the curvature. For $f(R) \propto R - 2\Lambda$, $w_{DE} = -1$ as in the cosmological constant scenario.

Modelling matter as dust ($p_m = 0$), the conservation equation for the total energy density can be written as

$$\dot{\rho}_{tot} + 3H(\rho_{tot} + p_{curv}) = 0, \quad (44)$$

14 *S. Capozziello, R. D'Agostino, O. Luongo*

where $\rho_{tot} = \rho_m/f'(R) + \rho_{curv}$. Then, assuming no interaction between matter and curvature fluid, the conservation equation for the matter energy density is

$$\dot{\rho}_m + 3H\rho_m = 0, \quad (45)$$

whose solution gives the standard behaviour

$$\rho_m = \rho_{m0}a^{-3} = 3H_0^2\Omega_{m0}(1+z)^3. \quad (46)$$

Inserting Eq. (45) into Eq. (44) and using Eq. (46), we obtain the continuity equation for the effective curvature fluid:

$$\dot{\rho}_{curv} + 3H(1+w_{DE})\rho_{curv} = 3H_0^2\Omega_{m0}(1+z)^3 \frac{\dot{R}f''(R)}{(f'(R))^2}. \quad (47)$$

It is finally convenient to combine Eqs. (39) and (40) into a single equation:

$$\dot{H} + \frac{1}{2f'(R)} \left[3H_0^2\Omega_{m0}(1+z)^3 - H\dot{R}f''(R) + \ddot{R}f''(R) + (\dot{R})^2f'''(R) \right] = 0, \quad (48)$$

where we have used the definitions (41) and (42).

In the last years, many attempts with the aim to construct quintessence-like $f(R)$ models were proved to produce both early and late-time acceleration.⁵⁷

It has been shown that the model $f(R) = R + \alpha R^2$ ($\alpha > 0$) is consistent with the temperature anisotropies observed in CMB and it can be a viable alternative to the scalar field models of inflation.^{60,79} The quadratic term αR^2 , in fact, gives rise to an asymptotically exact de Sitter solution, and inflation ends when it becomes subdominant with respect to the linear term R . However, this model is not suitable to explain the present cosmic acceleration because the quadratic term is much smaller than R today.

Models of type $f(R) = R - \alpha R^{-n}$ ($\alpha > 0, n > 0$) were proposed to explain the late-time cosmic acceleration,^{25,68,80} but it has been shown that they do not satisfy local gravity constraints because of the instability arising from negative value of $f''(R)$.^{81,82,100} Moreover, these models do not possess a standard matter-dominated epoch because of a large coupling between matter and dark energy.⁸³ However, cosmological viability of $f(R)$ gravity as an ideal fluid and its compatibility with a matter dominated phase has been demonstrated for a large class of models.⁸⁴

We can thus summarize the conditions that $f(R)$ models have to satisfy to be viable for dark energy. It has to be:

$$(1) \quad f'(R) > 0, \quad R \geq R_0 > 0,$$

where R_0 is the value of the Ricci scalar at the present time. This condition is required in order to avoid negative values of the effective gravitational constant (cf. Eq. (37)).

$$(2) \quad f''(R) > 0, \quad R \geq R_0 > 0.$$

This arises from the constraints of gravity in the solar system,^{85,86} and the con-

sistency with the presence of a standard matter-dominated epoch.⁸⁷ Moreover, this condition guaranties the stability of cosmological perturbations.

$$(3) \quad f'(R) \longrightarrow 1, \quad R \gg 1.$$

This condition is expected to be fulfilled to ensure that viable $f(R)$ model tends to Λ CDM at large curvatures, as required by CMB observations.^{91–93}

However, one of the main issues is to reconstruct early and late cosmology through the same approach. In the framework of $f(R)$ gravity, as firstly reported in 94, it is possible to select a class of realistic models describing inflation and the onset of late accelerated expansion. Specifically, power-law $f(R)$ gravity models, describing inflation, can be related to Λ CDM in a quite natural way.⁹⁵ In 96, exponential non-singular $f(R)$ models are discussed in order to connect early- and late-time accelerated expansions.

3.2. The Palatini formalism and viability conditions

As we have already discussed earlier in this section, the field equations can be derived by applying the variational principle to the metric and the connection, treated as independent variables. In the Palatini formalism, in fact, the curvature tensor is built up from independent connections. To avoid confusion with the metric formalism, we denote the Ricci tensor constructed by independent connections as $\mathcal{R}_{\mu\nu}$, and the corresponding Ricci scalar as $\mathcal{R} = g^{\mu\nu}\mathcal{R}_{\mu\nu}$. The action thus takes the form

$$\mathcal{S} = \frac{1}{2\kappa} \int d^4x \sqrt{-g} f(\mathcal{R}) + \mathcal{S}_m(g_{\mu\nu}, \psi), \quad (49)$$

which reduces to GR when $f(\mathcal{R}) = \mathcal{R}$. The variation of Eq. (49) with respect to the metric provides

$$F(\mathcal{R})\mathcal{R}_{(\mu\nu)} - \frac{1}{2}f(\mathcal{R})g_{\mu\nu} = \kappa T_{\mu\nu}, \quad (50)$$

where $F(\mathcal{R}) \equiv df/d\mathcal{R}$ and $(\mu\nu)$ denotes symmetrization over the indices μ and ν . Taking the trace of Eq. (50) yields the following useful relation:

$$F(\mathcal{R})\mathcal{R} - 2f(\mathcal{R}) = \kappa T. \quad (51)$$

On the other hand, the variation with respect to the connection gives

$$\delta\mathcal{R}_{\mu\nu} = \bar{\nabla}_\lambda \delta\Gamma_{\mu\nu}^\lambda - \bar{\nabla}_\nu \delta\Gamma_{\mu\lambda}^\lambda, \quad (52)$$

where $\bar{\nabla}_\mu$ indicates the covariant derivative defined with respect to the independent connection $\Gamma_{\mu\nu}^\lambda$. Therefore, variation of (49) with respect to the connection yields

$$\bar{\nabla}_\lambda (\sqrt{-g} F(\mathcal{R})g^{\mu\nu}) - \bar{\nabla}_\sigma (\sqrt{-g} F(\mathcal{R})g^{\sigma\mu}) \delta_\lambda^\nu = 0. \quad (53)$$

Contracting the above equation over λ and μ results in⁹⁷

$$\bar{\nabla}_\sigma (\sqrt{-g} F(\mathcal{R})g^{\sigma\mu}) = 0. \quad (54)$$

16 *S. Capozziello, R. D'Agostino, O. Luongo*

This naturally leads to introduce a new metric conformally related to $g_{\mu\nu}$ being

$$\sqrt{-g} F(\mathcal{R})g^{\mu\nu} = \sqrt{-h} h^{\mu\nu} , \quad (55)$$

which implies

$$h_{\mu\nu} = F(\mathcal{R})g_{\mu\nu} . \quad (56)$$

Thus, Eq. (54) becomes the definition of the Levi-Civita connection of the metric $h_{\mu\nu}$:

$$\Gamma_{\mu\nu}^{\lambda} = \frac{1}{2}h^{\lambda\sigma} (\partial_{\mu}h_{\nu\sigma} + \partial_{\nu}h_{\mu\sigma} - \partial_{\sigma}h_{\mu\nu}) . \quad (57)$$

The independent connection (57) can be written in terms of the metric $g_{\mu\nu}$ as

$$\Gamma_{\mu\nu}^{\lambda} = \{\lambda_{\mu\nu}\} + \frac{1}{2F} \left[2\delta_{(\mu}^{\lambda} \partial_{\nu)} F - g_{\mu\nu} g^{\lambda\sigma} \partial_{\sigma} F \right] , \quad (58)$$

where $\{\lambda_{\mu\nu}\}$ are the Christoffel symbols of the metric $g_{\mu\nu}$. Considering how the Ricci tensor transforms under conformal transformations, we can write

$$\mathcal{R}_{\mu\nu} = R_{\mu\nu} + \frac{3}{2} \left[\frac{(\nabla_{\mu} F)(\nabla_{\nu} F)}{F^2} \right] - \frac{1}{F} \left(\nabla_{\mu} \nabla_{\nu} + \frac{1}{2} g_{\mu\nu} \square \right) F , \quad (59)$$

and contracting with $g_{\mu\nu}$, one obtains

$$\mathcal{R} = R + \frac{3}{2} \left[\frac{(\nabla_{\mu} F)(\nabla^{\mu} F)}{F^2} \right] - \frac{3}{F} \square F . \quad (60)$$

Note that, when $f(\mathcal{R}) = \mathcal{R}$, F is constant and the theory reduces to GR as $\mathcal{R}_{\mu\nu} = R_{\mu\nu}$ and $\mathcal{R} = R$. Finally, substituting Eqs. (59) and (60) into Eq. (50) leads to

$$\begin{aligned} G_{\mu\nu} &= \frac{\kappa}{F} T_{\mu\nu} - \frac{1}{2} g_{\mu\nu} \left(\mathcal{R} - \frac{f}{F} \right) - \frac{3}{2F^2} \left[(\nabla_{\mu} F)(\nabla_{\nu} F) - \frac{1}{2} g_{\mu\nu} (\nabla_{\mu} F)(\nabla^{\mu} F) \right] \\ &+ \frac{1}{F} (\nabla_{\mu} \nabla_{\nu} - g_{\mu\nu} \square) F . \end{aligned} \quad (61)$$

Cosmic dynamics can be studied assuming that the universe is described by the flat FLRW metric and it is filled with a perfect fluid with an energy-momentum tensor given by Eq. (6). Thus, combining the modified Friedmann equations calculated as the (0,0) and (i,j) components of Eq. (61), one obtains⁹⁸

$$\left(H + \frac{1}{2} \frac{\dot{F}}{F} \right)^2 = \frac{1}{6} \left[\frac{\kappa(\rho + 3p)}{F} + \frac{f}{F} \right] . \quad (62)$$

Assuming that matter is dust and neglecting the contribution of radiation, we have $p = 0$ and $\rho = \rho_m$. Then, the time derivative of Eq. (51) reads

$$\dot{\mathcal{R}}(\mathcal{R}F_{\mathcal{R}} - 2f) = \kappa \dot{\rho}_m , \quad (63)$$

where we have used that $\dot{F} = F_{\mathcal{R}} \dot{\mathcal{R}}$, being $F_{\mathcal{R}} \equiv dF/d\mathcal{R} = d^2 f/d\mathcal{R}^2$. Making use of the continuity equation $\dot{\rho}_m + 3H\rho_m = 0$ and again of Eq. (51), from Eq. (63) one gets

$$\dot{\mathcal{R}} = - \frac{3H(\mathcal{R}F - 2f)}{\mathcal{R}F_{\mathcal{R}} - 2F} . \quad (64)$$

Thus, substituting the above expression for $\dot{\mathcal{R}}$ into Eq. (62), we finally obtain

$$H^2 = \frac{1}{6F} \frac{2\kappa\rho_m + \mathcal{R}F - f}{\left[1 - \frac{3}{2} \frac{F_{\mathcal{R}}(\mathcal{R}F - 2f)}{F(\mathcal{R}F_{\mathcal{R}} - F)}\right]^2}, \quad (65)$$

where $\rho_m = 3H_0^2\Omega_{m0}(1+z)^3$.

In the Palatini formalism, the field equations are second-order and are then free from the instabilities due to negative values of $f''(R)$.^{110,111} Several works addressing the dynamics of Palatini $f(R)$ gravity at background level showed that the correct sequence of cosmological eras is realized even for the model $f(R) = R - \alpha R^{-n}$ with $n > 0$.^{112,113} Dark energy models from Palatini $f(R)$ gravity are not compatible with large-scale structure observations for substantial deviations from the Λ CDM model, because of a large coupling between non-relativistic matter and dark energy.^{114–116} Also, the non-perturbative corrections to the matter action introduced by such a large coupling appear in conflict with the Standard Model of particle physics.¹¹⁷

Moreover, while in metric $f(R)$ gravity the Cauchy problem is well-posed both in vacuo and with matter, in Palatini $f(R)$ gravity the Cauchy problem is unlikely to be well-formulated, unless for null derivatives of the trace of the energy-momentum tensor. This is due to the presence of higher derivatives of matter fields in the field equations.⁶⁹ In any case, the well-position and the well-formulation of the Cauchy problem in Palatini $f(R)$ gravity can be correctly addressed considering specific forms of sourcing fluids.¹⁰²

3.3. Equivalence between $f(R)$ gravity and scalar-tensor theories

Similarly to classical mechanics where one can redefine variables in order to make equations easier to handle, in field theory, it is also possible to redefine fields and rewrite action and field equations in a different form. Theories that, under a suitable transformation of fields, preserve action and equations of motion are said dynamically equivalent. Such theories give the same results and can be seen as different representations of the same theory. In this section, we show the equivalence between $f(R)$ gravity and scalar-tensor theories of gravity.

A general scalar-tensor theory of gravity is described by the action

$$\mathcal{S}_{ST} = \frac{1}{2\kappa} \int d^4x \sqrt{-g} \left[\phi R - \frac{\omega(\phi)}{\phi} \partial_\mu \phi \partial^\mu \phi - V(\phi) \right] + \mathcal{S}_m(g_{\mu\nu}, \psi), \quad (66)$$

where V is the potential of the scalar field ϕ and $\omega(\phi)$ is some arbitrary function of ϕ . Varying action (66) with respect to the metric provides

$$G_{\mu\nu} = \frac{\kappa}{\phi} T_{\mu\nu} - \frac{V(\phi)}{2\phi} g_{\mu\nu} + \frac{1}{\phi} (\nabla_\mu \nabla_\nu \phi - g_{\mu\nu} \square \phi) + \frac{\omega(\phi)}{\phi^2} \left(\nabla_\mu \phi \nabla_\nu \phi - \frac{1}{2} g_{\mu\nu} \nabla^\alpha \phi \nabla_\alpha \phi \right), \quad (67)$$

18 *S. Capozziello, R. D'Agostino, O. Luongo*

while variation with respect to the scalar field yields

$$\square\phi = \frac{\phi}{2\omega(\phi)} [V'(\phi) - R] + \frac{1}{2} \left[\frac{1}{\phi} - \frac{\omega'(\phi)}{\omega(\phi)} \right] \nabla^\mu\phi \nabla_\mu\phi \quad (68)$$

The trace of Eq. (67) can be used to replace R in Eq. (68) obtaining thus

$$[2\omega(\phi) + 3]\square\phi = \kappa T + \phi V'(\phi) - \omega'(\phi) \nabla^\alpha\phi \nabla_\alpha\phi - 2V(\phi) . \quad (69)$$

From the general action Eq. (66) one can retrieve a Brans-Dicke-like theory⁹⁹ with a scalar-field potential by setting $\omega(\phi) = \omega_{BD}$:

$$\mathcal{S}_{BD} = \frac{1}{2\kappa} \int d^4x \sqrt{-g} \left[\phi R - \frac{\omega_{BD}}{\phi} \partial_\mu\phi \partial^\mu\phi - V(\phi) \right] + \mathcal{S}_m(g_{\mu\nu}, \psi) , \quad (70)$$

where the Brans-Dicke parameter ω_{BD} plays the role of a coupling constant.

The equivalence between $f(R)$ gravity, in the metric formalism, and scalar-tensor theories can be achieved as follows. We can introduce a new scalar field χ and consider the following action:¹⁰⁰

$$\mathcal{S}_{met} = \frac{1}{2\kappa} \int d^4x \sqrt{-g} [f(\chi) + f'(\chi)(R - \chi)] + \mathcal{S}_m(g_{\mu\nu}, \psi) . \quad (71)$$

Varying with respect to χ yields

$$f''(\chi)(R - \chi) = 0 , \quad (72)$$

which implies that $\chi = R$ if $f''(\chi) \neq 0$. This reproduces action (30) and proves that the theory is dynamically equivalent to the original. Then, one can redefine the field χ by setting

$$\begin{aligned} \phi &= f'(\chi) , \\ V(\phi) &= \phi\chi(\phi) - f(\chi(\phi)) . \end{aligned} \quad (73)$$

Hence, (71) takes the form

$$\mathcal{S}_{met} = \frac{1}{2\kappa} \int d^4x \sqrt{-g} [\phi R - V(\phi)] + \mathcal{S}_m(g_{\mu\nu}, \psi) , \quad (74)$$

which is equivalent to a Brans-Dicke-like theory with $\omega_{BD} = 0$.⁶⁴ In such a case, field equations (67) read

$$G_{\mu\nu} = \frac{\kappa}{\phi} T_{\mu\nu} - \frac{1}{2\phi} g_{\mu\nu} V(\phi) + \frac{1}{\phi} (\nabla_\mu \nabla_\nu \phi - g_{\mu\nu} \square\phi) , \quad (75)$$

and Eq. (69) becomes

$$3\square\phi + 2V(\phi) - \phi V'(\phi) = \kappa T . \quad (76)$$

Furthermore, as usual in scalar-tensor theories, one can perform a conformal transformation and move from the *Jordan frame* to the *Einstein frame*. In fact, through the conformal transformation

$$\tilde{g}_{\mu\nu} = f'(R) g_{\mu\nu} \equiv \phi g_{\mu\nu} , \quad (77)$$

and the redefinition of field

$$\tilde{\phi} = \sqrt{\frac{2\omega_{BD} + 3}{2\kappa}} \ln\left(\frac{\phi}{\phi_0}\right), \quad (78)$$

we obtain the Einstein frame, in which the new field $\tilde{\phi}$ has a kinetic energy and it is minimally coupled to gravity:

$$\mathcal{S}_{BD}^{(Ein)} = \int d^4x \sqrt{-\tilde{g}} \left[\frac{\tilde{R}}{2\kappa} - \frac{1}{2} \partial^\mu \tilde{\phi} \partial_\mu \tilde{\phi} - U(\tilde{\phi}) \right]. \quad (79)$$

For $\omega_{BD} = 0$, corresponding to $f(R)$ gravity in the metric formalism, one has

$$\phi \equiv f'(R) = e^{\sqrt{\frac{2\kappa}{3}}\tilde{\phi}}, \quad (80)$$

$$U(\tilde{\phi}) = \frac{Rf'(R) - f(R)}{2\kappa(f'(R))^2}, \quad (81)$$

and the action reads

$$\mathcal{S}_{met}^{(Ein)} = \int d^4x \sqrt{-\tilde{g}} \left[\frac{\tilde{R}}{2\kappa} - \frac{1}{2} \partial^\mu \tilde{\phi} \partial_\mu \tilde{\phi} - U(\tilde{\phi}) \right] + \mathcal{S}_m(e^{-\sqrt{\frac{2\kappa}{3}}\tilde{\phi}} \tilde{g}_{\mu\nu}, \psi). \quad (82)$$

We want to stress that actions (30), (74) and (82) are equivalent representations of the same theory. However, the issue on which conformal frame (Jordan or Einstein) is the ‘physical’ one has been the subject of much debate and the answers are still controversial. A detailed discussion on this can be found in 101 and the references therein.

Let us now examine the equivalence between the Palatini formulation of $f(R)$ gravity and a scalar-tensor theory. Adopting a similar procedure to the one presented above, we consider the action for the field χ :

$$\mathcal{S}_{Pal} = \frac{1}{2\kappa} \int d^4x \sqrt{-g} [f(\chi) + f'(\chi)(\mathcal{R} - \chi)] + \mathcal{S}_m(g_{\mu\nu}, \psi). \quad (83)$$

A variation with respect to χ yields $\chi = \mathcal{R}$. Then, redefining the field as in Eq. (73), the action takes the form

$$\mathcal{S}_{Pal} = \frac{1}{2\kappa} \int d^4x \sqrt{-g} [\phi \mathcal{R} - V(\phi)] + \mathcal{S}_m(g_{\mu\nu}, \psi). \quad (84)$$

and Eq. (60) in terms of the new field ϕ reads

$$\mathcal{R} = R + \frac{3}{2\phi^2} (\nabla_\mu \phi)(\nabla^\mu \phi) + \frac{3}{\phi} \square \phi. \quad (85)$$

Therefore, plugging the above relation into Eq. (84) and neglecting a total divergence, one obtains

$$\mathcal{S}_{Pal} = \frac{1}{2\kappa} \int d^4x \sqrt{-g} \left(\phi R + \frac{3}{2\phi} \partial_\mu \phi \partial^\mu \phi - V(\phi) \right) + \mathcal{S}_m(g_{\mu\nu}, \psi). \quad (86)$$

Comparing this with (70) we deduce that $f(R)$ gravity in the Palatini formalism is equivalent to a Brans-Dicke theory with $\omega_{BD} = -3/2$. Thus, the field equations

20 *S. Capozziello, R. D'Agostino, O. Luongo*

that one obtains from varying the action with respect to the metric and the scalar field are, respectively,

$$G_{\mu\nu} = \frac{\kappa}{\phi} T_{\mu\nu} - \frac{3}{2\phi^2} \left(\nabla_\mu \phi \nabla_\nu \phi - \frac{1}{2} g_{\mu\nu} \nabla^\lambda \phi \nabla_\lambda \phi \right) + \frac{1}{\phi} (\nabla_\mu \nabla_\nu \phi - g_{\mu\nu} \square \phi) - \frac{V(\phi)}{2\phi} g_{\mu\nu}, \quad (87)$$

$$\square \phi = \frac{\phi}{3} (R - V'(\phi)) + \frac{1}{2\phi} \nabla^\mu \phi \nabla_\mu \phi. \quad (88)$$

Moreover, Eq. (69) takes the simpler form

$$2V(\phi) - \phi V'(\phi) = \kappa T. \quad (89)$$

Finally, performing conformal transformation (77) one can rewrite action 86 in the Einstein frame:

$$\mathcal{S}_{Pal}^{(Ein)} = \int d^4x \sqrt{-\tilde{g}} \left[\frac{\tilde{R}}{2\kappa} - U(\phi) \right] + S_m(\phi^{-1} \tilde{g}_{\mu\nu}, \psi), \quad (90)$$

where

$$U(\phi) = \frac{1}{2\kappa} \frac{V(\phi)}{\phi^2}. \quad (91)$$

An important issue has to be stressed at this point. The equivalence between $f(R)$ and scalar-tensor gravity can be lost, even mathematically, in the presence of singularities. As discussed in 103, big rip singularities can emerge in these models related to phantom scalar fields. Furthermore, it is possible to demonstrate that $f(R)$ gravity singularities in Jordan and Einstein frames correspond.¹⁰⁴ Finally, even if equivalence is fulfilled, the physical interpretation may be different in the two frames.^{84,105}

Recently, it has been considered the possibility to combine metric and Palatini formalism considering a theory of gravity as

$$\mathcal{F} = R + f(\mathcal{R}), \quad (92)$$

where R is formulated in metric formalism and $f(\mathcal{R})$, that is the extra terms with respect to GR, are formulated in Palatini formalism.^{106–108} This combined approach (the so called Hybrid Gravity) allows to bypass some shortcomings of both the scenarios.¹⁰⁹

4. Gravity with torsion

The issue about the symmetry of the space-time connection has led to consider the role of torsion in the description of the gravitational interaction. Quantum effects are not taken into account in a classical theory as GR. However, those effects cannot be neglected one deals with any theory involving gravity at a fundamental level. A straightforward generalization including in GR matter spin fields is obtained when one considers a four-dimensional space-time manifold with torsion. In

such a picture, mass-energy and spin are, respectively, the sources of curvature and torsion. A relevant example towards this direction is represented by the Einstein-Cartan-Sciama-Kibble (ECSK) theory.¹¹⁸ Also, higher dimensional paradigms such as Kaluza-Klein theories^{119–121} take into account torsion in unification schemes with gravity and electromagnetism. Moreover, torsion must be included in any gravity theory with the presence of twistors,^{122, 123} and in supergravity where curvature is considered together with torsion and matter fields.^{124, 125}

Besides, several authors take seriously into account the role played by torsion in the early universe with the observational consequences at the present time. The repulsive contributions of torsion to the energy-momentum tensor yield cosmological models which are free from singularities.^{126–128} Topological defects originated from torsion, in a universe characterized by phase transitions,^{129–131} are reflected today into the angular momenta of cosmic structures. Furthermore, the energy-momentum contribution of torsion influences the cosmological perturbations giving rise to characteristic lengths in the spectrum.¹³² The presence of torsion also modifies the evolution equations of shear, expansion and other kinematic quantities.¹³⁵

To describe the dynamics of space-time with torsion, it is possible to introduce tetrad fields e_A^μ . Denoting by $A, B, C \dots$ the coordinates of the tangent space-time, the tetrad fields are dynamical variables which form an orthonormal basis at each point x^μ of the manifold.¹³³ One thus defines the co-tetrad field e_μ^A with the following properties:

$$e_A^\mu e_\nu^A = \delta_\nu^\mu, \quad (93)$$

$$e_A^\mu e_\mu^B = \delta_A^B. \quad (94)$$

The metric of tetrad fields is

$$\eta_{AB} = \eta^{AB} = \text{diag}(1, -1, -1, -1), \quad (95)$$

from which one can construct the metric tensor as

$$g_{\mu\nu} = \eta_{AB} e_\mu^A e_\nu^B. \quad (96)$$

We thus consider simple bivectors which are obtained by skew-symmetric tensor product of two vectors. A bivector $B^{\mu\nu}$ is simple if it satisfies the condition

$$B^{[\mu\nu} B^{\rho]\sigma} = 0. \quad (97)$$

It is possible to construct the $N(N-1)/2$ simple bivectors through tetrad vectors in a N -dimensional manifold as

$$F_{AB}^{\mu\nu} = e_A^{[\mu} e_B^{\nu]}, \quad (98)$$

while any bivector $B^{\mu\nu}$ takes the form

$$B^{\mu\nu} = B^{AB} e_A^\mu e_B^\nu, \quad (99)$$

being $B^{AB} = -B^{BA}$.

22 *S. Capozziello, R. D'Agostino, O. Luongo*

From the antisymmetric part of the affine connection, we define the torsion tensor $T_{\mu\nu}{}^\rho$ as

$$T_{\mu\nu}{}^\rho = \frac{1}{2} (\Gamma_{\mu\nu}^\rho - \Gamma_{\nu\mu}^\rho) \equiv \Gamma_{[\mu\nu]}^\rho. \quad (100)$$

We note that $T_{\mu\nu}{}^\rho = 0$ is postulated in GR. It is often useful to define the *contorsion tensor* as

$$K_{\mu\nu}{}^\rho = -T_{\mu\nu}{}^\rho - T_{\mu\rho}{}^\nu + T_{\nu\rho}{}^\mu = -K_{\mu\rho}{}^\nu, \quad (101)$$

and the *modified torsion tensor* as

$$\hat{T}_{\mu\nu}{}^\rho = T_{\mu\nu}{}^\rho + 2\delta_{[\mu}{}^\rho T_{\nu]}, \quad (102)$$

where $T_\mu \equiv T_{\mu\nu}{}^\nu$. From the above definition, we can write the affine connection as

$$\Gamma_{\mu\nu}^\rho = \left\{ \begin{smallmatrix} \rho \\ \mu\nu \end{smallmatrix} \right\} - K_{\mu\nu}{}^\rho, \quad (103)$$

where $\left\{ \begin{smallmatrix} \rho \\ \mu\nu \end{smallmatrix} \right\}$ are the Christoffel symbols of the symmetric Levi-Civita connection defined in GR. Since torsion is present in the affine connection, the covariant derivatives of a scalar field ϕ do not commute:

$$\tilde{\nabla}_{[\mu} \tilde{\nabla}_{\nu]} \phi = -T_{\mu\nu}{}^\rho \tilde{\nabla}_\rho \phi, \quad (104)$$

while one has the following relations for a vector v^μ and a covector w_μ :

$$(\tilde{\nabla}_\mu \tilde{\nabla}_\nu - \tilde{\nabla}_\nu \tilde{\nabla}_\mu) v^\rho = R_{\mu\nu\sigma}{}^\rho v^\sigma - 2T_{\mu\nu}{}^\sigma \tilde{\nabla}_\sigma v^\rho, \quad (105)$$

$$(\tilde{\nabla}_\mu \tilde{\nabla}_\nu - \tilde{\nabla}_\nu \tilde{\nabla}_\mu) w_\sigma = R_{\mu\nu\rho}{}^\sigma w_\sigma - 2T_{\mu\nu}{}^\sigma \tilde{\nabla}_\sigma w_\rho, \quad (106)$$

where the Riemann tensor is given as

$$R_{\mu\nu\rho}{}^\sigma = \partial_\mu \Gamma_{\nu\rho}^\sigma - \partial_\nu \Gamma_{\mu\rho}^\sigma + \Gamma_{\mu\lambda}^\sigma \Gamma_{\nu\rho}^\lambda - \Gamma_{\nu\lambda}^\sigma \Gamma_{\mu\rho}^\lambda. \quad (107)$$

Also, torsion contributes to the Riemann tensor as

$$R_{\mu\nu\rho}{}^\sigma = R_{\mu\nu\rho}{}^\sigma(\{\}) - \nabla_\mu K_{\nu\rho}{}^\sigma + \nabla_\nu K_{\mu\rho}{}^\sigma + K_{\mu\lambda}{}^\sigma K_{\nu\rho}{}^\lambda - K_{\nu\lambda}{}^\sigma K_{\mu\rho}{}^\lambda, \quad (108)$$

where $R_{\mu\nu\rho}{}^\sigma(\{\})$ is the tensor of the symmetric connection. Here, $\tilde{\nabla}$ and ∇ denote the covariant derivative with and without torsion, respectively. Thus, the Ricci tensor reads

$$R_{\mu\nu} = R_{\mu\nu}(\{\}) - 2\nabla_\mu T_\nu + \nabla_\nu K_{\mu\rho}{}^\rho + K_{\mu\lambda}{}^\rho K_{\nu\rho}{}^\lambda - 2T_\lambda K_{\mu\rho}{}^\lambda \quad (109)$$

and the Ricci scalar is given by

$$R = R(\{\}) - 4\nabla_\mu T^\mu + K_{\rho\lambda\nu} K^{\nu\rho\lambda} - 4T_\mu T^\mu. \quad (110)$$

To understand the geometrical meaning of torsion, we can think in terms of parallelograms breaking.¹³⁴ In a curved space, an infinitesimal parallelogram is formed when two parts of geodesics are displaced one along the other. Thus, curvature determines the difference obtained by the parallel transport of a field across both paths. However, the same procedure applied in a twisted space produces a gap between the extremities of the two geodesics, *i.e.* breaking the infinitesimal parallelogram Fig. 1.

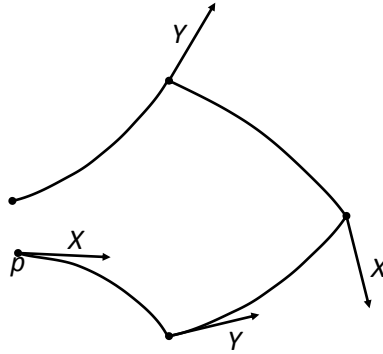


Fig. 1. Representation of parallelograms determined by torsion.

4.1. Teleparallel Equivalent of General Relativity

Bearing in mind the considerations made above, let us here summarize the so called Teleparallel Equivalent of General Relativity (TEGR) as an alternative approach to describe the gravitational interaction (see²⁶ for a review). This scenario was first studied by Einstein himself as an equivalent alternative to GR and it represents a gauge theory for the translation group.^{136,137} Within this approach, tetrad fields are used to define the free-curvature Weitzenböck connection.¹³⁹ It is worth mentioning that curvature and torsion are properties of the connection and, within the same space-time, it is possible to define several different connections.¹⁴⁰ While the Riemannian structure is related to the Levi-Civita connection, the teleparallel structure is related to Weitzenböck connection. These geometrical structures are linked to the gravitational interaction due to its universality.

Although gravity can be equivalently described in terms of curvature and torsion, conceptual differences occur. In teleparallel theories, torsion accounts for the gravitational interaction acting like a *force*, rather than providing a geometric picture of space-time as in GR. In the teleparallel version of GR, in fact, the geodesic equation can be seen as the Lorentz force law of electrodynamics.

To describe the teleparallel equivalent of GR, we adopt the notation in which the Greek indices ($\mu, \nu, \rho, \dots = 0, 1, 2, 3$) are related to space-time, and the capital Latin indices ($A, B, C, \dots = 0, 1, 2, 3$) denote the tangent space. We assume that the tangent space is Minkoskian with metric

$$\eta_{AB} = \text{diag}(+1, -1, -1, -1). \quad (111)$$

Introducing the translation generators $P_A = \partial/\partial x^A$, one can define a local translation on the tangent-space as follows:

$$\delta x^A = \delta \alpha^B P_B x^A, \quad (112)$$

Then, for a given matter field Ψ , we define its gauge covariant derivative as

$$\mathcal{D}_\mu \Psi = e^B{}_\mu \partial_B \Psi, \quad (113)$$

24 *S. Capozziello, R. D'Agostino, O. Luongo*

where

$$e^B{}_{\mu} = \partial_{\mu}x^B + A^B{}_{\mu} , \quad (114)$$

with $A^B{}_{\mu}$ being the gauge potentials. As in the standard Abelian gauge theories, the field strength reads

$$F^B{}_{\mu\nu} = \partial_{\mu}A^B{}_{\nu} - \partial_{\nu}A^B{}_{\mu} , \quad (115)$$

satisfying the following relation:

$$[\mathcal{D}_{\mu}, \mathcal{D}_{\nu}]\Psi = F^B{}_{\mu\nu}P_B\Psi . \quad (116)$$

The teleparallel structure on space-time is induced by nontrivial tetrad fields, which allow to define the *Weitzenböck connection*:

$$\hat{\Gamma}^{\rho}{}_{\mu\nu} = e^A{}_{\rho}\partial_{\nu}e^A{}_{\mu} , \quad (117)$$

characterized by torsion with no curvature. As a consequence, the Weitzenböck covariant derivative of the tetrad field is identically zero:

$$\nabla_{\nu}e^A{}_{\mu} \equiv \partial_{\nu}e^A{}_{\mu} - \hat{\Gamma}^{\rho}{}_{\mu\nu}e^A{}_{\rho} = 0 . \quad (118)$$

The above condition is known as absolute parallelism. Moreover, one can write the expression for the torsion related the Weitzenböck connection as

$$T^{\rho}{}_{\mu\nu} = \hat{\Gamma}^{\rho}{}_{\nu\mu} - \hat{\Gamma}^{\rho}{}_{\mu\nu} , \quad (119)$$

and the corresponding gravitational "force" is

$$F^A{}_{\mu\nu} = e^A{}_{\rho}T^{\rho}{}_{\mu\nu} . \quad (120)$$

One can use a nontrivial tetrad field to define also the torsionless Levi-Civita connection of the space-time metric:

$$\overset{\circ}{\Gamma}^{\sigma}{}_{\mu\nu} = \frac{1}{2}g^{\sigma\rho}[\partial_{\mu}g_{\rho\nu} + \partial_{\nu}g_{\rho\mu} - \partial_{\rho}g_{\mu\nu}] . \quad (121)$$

The relation between the Weitzenböck and the Levi-Civita connections is

$$\hat{\Gamma}^{\rho}{}_{\mu\nu} = \overset{\circ}{\Gamma}^{\rho}{}_{\mu\nu} + K^{\rho}{}_{\mu\nu} , \quad (122)$$

where $K^{\rho}{}_{\mu\nu}$

$$K^{\rho}{}_{\mu\nu} = \frac{1}{2}(T_{\mu}{}^{\rho}{}_{\nu} + T_{\nu}{}^{\rho}{}_{\mu} - T^{\rho}{}_{\mu\nu}) \quad (123)$$

is the contorsion tensor. From the identity

$$R^{\rho}{}_{\lambda\mu\nu} = \partial_{\mu}\hat{\Gamma}^{\rho}{}_{\lambda\nu} + \hat{\Gamma}^{\rho}{}_{\sigma\mu}\hat{\Gamma}^{\sigma}{}_{\lambda\nu} - (\mu \leftrightarrow \nu) \equiv 0 , \quad (124)$$

substituting the expression for $\hat{\Gamma}^{\rho}{}_{\mu\nu}$ given in (122), we find

$$R^{\rho}{}_{\lambda\mu\nu} = \overset{\circ}{R}{}^{\rho}{}_{\lambda\mu\nu} + Q^{\rho}{}_{\lambda\mu\nu} \equiv 0 , \quad (125)$$

where $\overset{\circ}{R}{}^{\rho}{}_{\lambda\mu\nu}$ is the Riemann tensor of the Levi-Civita connection, and $Q^{\rho}{}_{\lambda\mu\nu}$ is expressed in terms of Weitzenböck connection only:

$$Q^{\rho}{}_{\lambda\mu\nu} = D_{\mu}K^{\rho}{}_{\lambda\nu} - D_{\nu}K^{\rho}{}_{\lambda\mu} + K^{\sigma}{}_{\lambda\nu}K^{\rho}{}_{\sigma\mu} - K^{\sigma}{}_{\lambda\mu}K^{\rho}{}_{\sigma\nu} \quad (126)$$

Here, D_μ is the teleparallel covariant derivative, whose explicit form can be obtained by operating on a space-time vector V^μ :

$$D_\rho V^\mu \equiv \partial_\rho V^\mu + \left(\hat{\Gamma}^\mu_{\lambda\rho} - K^\mu_{\lambda\rho} \right) V^\lambda . \quad (127)$$

The equivalence between the teleparallel and the Riemann descriptions is clearly expressed in Eq. (125): the contribution from the Levi-Civita connection ($\overset{\circ}{R}{}^\rho_{\lambda\mu\nu}$) compensates the one from the Weitzenböck connection ($Q^\rho_{\lambda\mu\nu}$), so that $R^\rho_{\lambda\mu\nu}$ is identically zero.

Therefore, we can write the Lagrangian of the gravitational field as

$$\mathcal{L}_G = \frac{e}{2\kappa} S^{\rho\mu\nu} T_{\rho\mu\nu} , \quad (128)$$

where $e = \det(e^a_\mu)$ and

$$S^{\rho\mu\nu} = -S^{\rho\nu\mu} \equiv \frac{1}{2} \left(K^{\mu\nu\rho} - g^{\rho\nu} T^{\lambda\mu}_\lambda + g^{\rho\mu} T^{\lambda\nu}_\lambda \right) \quad (129)$$

Using relation (122) and identifying $e = \sqrt{-g}$, the Lagrangian (128) results to be equivalent to the Einstein-Hilbert Lagrangian of GR modulo divergence:

$$\mathcal{L} = -\frac{1}{2\kappa} \sqrt{-g} \overset{\circ}{R} . \quad (130)$$

The teleparallel version of the gravitational field is obtained by varying \mathcal{L}_G with respect to the gauge field $A_B{}^\rho$:

$$\partial_\sigma (e S_B{}^{\sigma\rho}) - 4\pi G (e j_B{}^\rho) = 0 , \quad (131)$$

where $S_B{}^{\sigma\rho} \equiv e_B{}^\lambda S_\lambda{}^{\sigma\rho}$. The quantity

$$e j_B{}^\rho \equiv \frac{\partial \mathcal{L}_G}{\partial e^B{}_\rho} = -\frac{1}{4\pi G} e e_B{}^\lambda S_\mu{}^{\nu\rho} T^\mu{}_{\nu\lambda} + e_B{}^\rho \mathcal{L}_G \quad (132)$$

represents the gauge current which coincides with the energy and momentum of the gravitational field.¹⁴¹ The quantity $e S_B{}^{\sigma\rho}$ is called *superpotential* as its derivative provides the gauge current $e j_B{}^\rho$, which is conserved:

$$\partial_\rho (e j_B{}^\rho) = 0 . \quad (133)$$

Using the following identity

$$\partial_\rho e \equiv e \overset{\circ}{\Gamma}{}^\nu{}_{\nu\rho} = e \left(\hat{\Gamma}^\nu{}_{\rho\nu} - K^\nu{}_{\rho\nu} \right) , \quad (134)$$

Eq. (133) can be written as

$$D_\rho j_B{}^\rho \equiv \partial_\rho j_B{}^\rho + \left(\hat{\Gamma}^\rho{}_{\lambda\rho} - K^\rho{}_{\lambda\rho} \right) j_B{}^\lambda = 0 , \quad (135)$$

It is interesting to relate the above gauge approach with canonical GR. To do that, we use Eq. (117) to express $\partial_\rho e_A{}^\lambda$ and rewrite Eq. (131) in the form

$$\partial_\sigma (e S_\lambda{}^{\sigma\rho}) - 4\pi G (e t_\lambda{}^\rho) = 0 , \quad (136)$$

26 *S. Capozziello, R. D'Agostino, O. Luongo*

where

$$et_{\lambda}{}^{\rho} = \frac{e}{4\pi G} \Gamma^{\mu}{}_{\nu\lambda} S_{\mu}{}^{\nu\rho} + \delta_{\lambda}{}^{\rho} \mathcal{L}_G \quad (137)$$

represents the standard energy-momentum pseudotensor of the gravitational field.^{142,143} Using Eq. (122), one can rewrite Eq. (136) in terms of the Levi-Civita connection. Thus, from the equivalence of the Lagrangians, we can reproduce the Einstein field equations:

$$\frac{e}{2} \left[\overset{\circ}{R}_{\mu\nu} - \frac{1}{2} g_{\mu\nu} \overset{\circ}{R} \right] = 0. \quad (138)$$

This result proves the equivalence of the two approaches and justifies the name ‘‘Teleparallel Equivalent of General Relativity’’ (TEGR).¹³⁸

4.2. $f(T)$ gravity

Among all the models suggested to describe the late-time accelerated expansion, the *teleparallel* description of gravity has recently reached much attention.^{144–147} As for the $f(R)$ theories of gravity, interesting scenarios arise when one replaces the torsion scalar with a generic function $f(T)$.^{148–150} In particular, one considers the action

$$\mathcal{S} = \int d^4x e \left[\frac{f(T)}{2\kappa} + \mathcal{L}_m \right], \quad (139)$$

where $e = \sqrt{-g} = \det(e_{\mu}^A)$. The field equations are thus obtained by varying the action (139) with respect to the vierbein fields:

$$e_A^{\rho} S_{\rho}{}^{\mu\nu} (\partial_{\mu} T) f'' + \left[\frac{1}{e} \partial_{\mu} (e e_A^{\rho} S_{\rho}{}^{\mu\nu}) - e_A^{\lambda} T^{\rho}{}_{\mu\lambda} S_{\rho}{}^{\nu\mu} \right] f' + \frac{1}{4} e_A^{\nu} f = \frac{\kappa}{2} e_A^{\rho} T^{(m)}{}_{\rho}{}^{\nu}, \quad (140)$$

where $T^{(m)}{}_{\rho}{}^{\nu}$ represents the energy-momentum tensor of matter, and the ‘primes’ indicate derivatives with respect to T .

Assuming a spatially flat FLRW background manifold, the vierbein takes the form

$$e_{\mu}^A = \text{diag}(1, a, a, a), \quad (141)$$

while the dual vierbein is given by $e_A^{\mu} = \text{diag}(1, a^{-1}, a^{-1}, a^{-1})$. From this choice, one obtains the well-known metric

$$ds^2 = dt^2 - a^2(t) \delta_{ij} dx^i dx^j. \quad (142)$$

Under this assumption, the torsion scalar is related to the Hubble parameter through

$$T = -6H^2. \quad (143)$$

Moreover, considering a perfect fluid for matter and neglecting radiation, the modified Friedmann equations are thus given as

$$H^2 = \frac{1}{3}(\rho_m + \rho_T), \quad (144)$$

$$2\dot{H} + 3H^2 = -\frac{1}{3}(p_m + p_T), \quad (145)$$

where ρ_T and p_T are, respectively, the torsional energy density and pressure:

$$\rho_T = Tf' - \frac{f}{2} - \frac{T}{2}, \quad (146)$$

$$p_T = \frac{f - Tf' + 2T^2f''}{2(f' + 2Tf'')}. \quad (147)$$

The above quantities can be then used to define an effective dark energy fluid with equation of state parameter

$$w_{DE} \equiv \frac{p_T}{\rho_T} = -1 + \frac{(f - 2Tf')(f' + 2Tf'' - 1)}{(f + T - 2Tf')(f' + 2Tf'')}. \quad (148)$$

In particular, when $f' = 1$, one gets $w_{DE} = -1$ which corresponds to the Λ CDM case.

The prescription described above can be even extended to consider *teleparallel dark energy models*, in which a scalar field non-minimally coupled to gravity is responsible for the cosmic acceleration.^{151–153} Although a single scalar field is commonly employed, multiple field models can be also considered to explain late-time acceleration and inflation.¹⁵⁷ In GR, through a suitable conformal transformation, the Lagrangian can be written in a particular frame, *i.e.* Einstein frame, in which the coupling does not show up. The situation is different in teleparallel gravity, where no Einstein frames exist even in the case of a single field model.^{160, 161}

We thus can write the generic action for a scalar field ϕ and the kinetic term $X \equiv \nabla_\mu \phi \nabla^\mu \phi$ in the form¹⁶²

$$\mathcal{S} = \int d^4x e \left[\frac{1}{2}f(T, \phi, X) + \mathcal{L}_m \right], \quad (149)$$

Variation of the above action with respect to the vierbein fields gives

$$\begin{aligned} \Theta_A^\mu &= \frac{1}{2}f e_A^\mu + f_T \left[e^{-1} \partial_\nu \left(e e_A^\rho S_\rho^{\mu\nu} \right) - e_A^\gamma S^{\rho\beta\mu} T_{\rho\beta\gamma} \right] + e_A^\rho S_\rho^{\nu\mu} \partial_\nu f_T \\ &\quad - \frac{1}{2} f_X e_A^\nu \partial^\mu \phi \partial_\nu \phi, \end{aligned} \quad (150)$$

where $f_T \equiv \partial f / \partial T$, $f_X \equiv \partial f / \partial X$ and

$$\Theta_\nu^\mu = e^A_\nu \Theta_A^\mu = -e^A_\nu \delta \mathcal{L}_m / \delta e^A_\mu \quad (151)$$

is the matter energy-momentum tensor. On the other hand, varying the action (149) with respect to the scalar field yields

$$\square \phi + \frac{\partial_\alpha f_X}{f_X} \partial^\alpha \phi - \frac{f_\phi}{f_X} = 0, \quad (152)$$

28 *S. Capozziello, R. D'Agostino, O. Luongo*

where $\square\phi = \partial_\mu(\sqrt{-g}\partial^\mu\phi)/\sqrt{-g}$. Then, we can write a covariant representation of Eq. (150) as

$$\Theta_\alpha{}^\mu = f_T G_\alpha{}^\mu + \frac{1}{2}\delta_\alpha^\mu(f - f_T T) + S_\alpha{}^{\nu\mu}\partial_\nu f_T - \frac{1}{2}f_X \partial^\mu\phi \partial_\alpha\phi, \quad (153)$$

being $G_\alpha{}^\mu$ the Einstein tensor. Requiring the symmetry and the local invariance of the energy-momentum tensor under Lorentz transformation, one obtains that

$$(S_\alpha{}^{\lambda\nu}g^{\alpha\mu} - S_\alpha{}^{\lambda\mu}g^{\alpha\nu})\partial_\lambda f_T = 0. \quad (154)$$

The form of the field equations under the assumptions (141) and (142) is

$$\rho_m = 3H^2 f_T - \frac{1}{2}(f - f_T T) + \frac{1}{2}f_X \dot{\phi}^2, \quad (155)$$

$$p_m = -(3H^2 + 2\dot{H})f_T + \frac{1}{2}(f - f_T T) - H\partial_0 f_T, \quad (156)$$

$$0 = \ddot{\phi} + \left(3H + \frac{\partial_0 f_X}{f_X}\right)\dot{\phi} - \frac{f_\phi}{f_X}, \quad (157)$$

under the hypothesis that ϕ depends only on time at the background level. By means of the definitions

$$\begin{aligned} \rho_{DE} &= 3H^2(1 - f_T) + \frac{1}{2}(f - f_T T) - \frac{1}{2}f_X \dot{\phi}^2, \\ p_{DE} &= -(3H^2 + 2\dot{H})(1 - f_T) - \frac{1}{2}(f - f_T T) + H\partial_0 f_T, \end{aligned} \quad (158)$$

Eqs. (155) and (156) read

$$\begin{aligned} \rho_{DE} + \rho_m &= 3H^2, \\ p_{DE} + p_m &= -(3H^2 + 2\dot{H}), \end{aligned} \quad (159)$$

Therefore, we can finally obtain the dark energy equation of state as $w_{DE} = p_{DE}/\rho_{DE}$:

$$w_{DE} = -\frac{1 + \frac{2\dot{H}}{3H^2} + \frac{w_m \rho_m}{3H^2}}{1 - \frac{\rho_m}{3H^2}}, \quad (160)$$

where $p_m = w_m \rho_m$.

5. Cosmography

The above $f(R)$ and $f(T)$ gravity are some examples of the possibilities to address the problem of accelerated speed of the observed universe under the standard of geometry. However, the degeneracy among the cosmological models invoked to feature the dark energy behaviour has made clear the need of model-independent techniques to describe the expansion of the universe. Among all reasonable approaches, *cosmography* has recently attracted a lot of attention.^{163,164} This model-independent technique relies only on the observational assumptions of the cosmological principle

and permits the study of the dark energy evolution without the need of assuming a specific cosmological model.^{1,165–167} The standard cosmographic approach is based on Taylor expansions of observables which can be directly compared to data, and the outcomes of such a procedure are independent of any equation of state postulated to study the cosmic evolution. For these reasons, cosmography turns out to be a powerful tool to break the degeneracy among cosmological models and it is currently widely adopted to understand universe's kinematics.^{168–200}

The cosmological principle demands the scale factor as the only degree of freedom governing the universe. One can thus expand $a(t)$ in Taylor series around the present time:

$$a(t) = 1 + \sum_{k=1}^{\infty} \frac{1}{k!} \left. \frac{d^k a}{dt^k} \right|_{t=t_0} (t - t_0)^k. \quad (161)$$

The above expansion defines the so-called cosmographic series.²⁰¹

$$H(t) \equiv \frac{1}{a} \frac{da}{dt}, \quad q(t) \equiv -\frac{1}{aH^2} \frac{d^2 a}{dt^2}, \quad (162a)$$

$$j(t) \equiv \frac{1}{aH^3} \frac{d^3 a}{dt^3}, \quad s(t) \equiv \frac{1}{aH^4} \frac{d^4 a}{dt^4}, \quad (162b)$$

which are known as the *Hubble*, *deceleration*, *jerk* and *snap* parameters^d. These quantities are used to study the dynamics of the late-time universe. The physical properties of the coefficients can be deduced by the shape of the Hubble expansion. In particular, the sign of the parameter q indicates whether the universe is accelerating or decelerating. The sign of j determines the change of the universe's dynamics, a positive value indicating the occurrence of a transition time during which the universe modifies its expansion. Moreover, the value of s is necessary to discriminate between an evolving dark energy term or a cosmological constant behaviour.

From the definition $z = a^{-1} - 1$ and Eq. (161), one obtains the Taylor expansion of the luminosity distance:

$$d_L(z) = \frac{z}{H_0} \left[1 + \frac{z}{2}(1 - q_0) - \frac{z^2}{6}(1 - q_0 - 3q_0^2 + j_0) + \frac{z^3}{24}(2 - 2q_0 - 15q_0^2 - 15q_0^3 + 5j_0 + 10q_0j_0 + s_0) + \mathcal{O}(z^4) \right]. \quad (163)$$

The above expression can be used to constrain the cosmographic series and frame the expansion of the universe without resorting to any *a priori* cosmological model. In fact, one can insert Eq. (163) into

$$H(z) = \left[\frac{d}{dz} \left(\frac{d_L(z)}{1+z} \right) \right]^{-1}, \quad (164)$$

^dOne may, in principle, consider high-order terms in the series. However, we here limit our study up to the *snap* parameter, as the current observations are not able to properly constrain the next order terms.²⁰²

30 *S. Capozziello, R. D'Agostino, O. Luongo*

and find

$$H(z) \simeq H_0 \left[1 + H^{(1)}z + H^{(2)}\frac{z^2}{2} + H^{(3)}\frac{z^3}{6} \right], \quad (165a)$$

$$H^{(1)} = 1 + q_0, \quad (165b)$$

$$H^{(2)} = j_0 - q_0^2, \quad (165c)$$

$$H^{(3)} = 3q_0^2 + 3q_0^3 - j_0(3 + 4q_0) - s_0. \quad (165d)$$

Useful relations are obtained by expressing the cosmographic series in terms of the time-derivatives of the Hubble rate:

$$q = -1 - \frac{\dot{H}}{H}, \quad (166)$$

$$j = 1 + \frac{\dot{H} + \ddot{H}}{H^2}, \quad (167)$$

$$s = 1 + \frac{2}{H^2} (3\dot{H} + 2\ddot{H}) + \frac{1}{H^4} (3H^2 + \ddot{H}). \quad (168)$$

The above equations permit to calculate the cosmographic coefficients for a given cosmological model.

5.1. *Limits of standard cosmography*

Although powerful and simple to apply, the cosmographic method is plagued with several shortcomings which limit the possibility to use it in certain circumstances. The main problem concerns the inability of the currently available cosmological data to put tight constraints on the cosmographic parameters and fix the kinematic expansion of the universe especially at early stages. Also, the arbitrary order of truncation of the Taylor series might compromise the predictive power of cosmography. Another important issue is the degeneracy between all of the cosmographic coefficients. The impossibility to measure them separately but only the sum leads to different results depending on the probability distribution associated with each coefficient.

Moreover, the role of spatial curvature is crucial in cosmographic constraints. In fact, $\Omega_k \neq 0$ causes a dark energy equation of state evolving with time,^{203, 204} which fixes *a priori* the dark energy term. Due to the close relation between luminosity distance and spatial curvature, one is forced to fix the value of Ω_k in order to constrain the cosmographic parameters. In doing so, the resulting series is the expression of the universe with that assumed curvature. Furthermore, Ω_k is strongly degenerate with the other cosmographic coefficients, which cannot be measured independently if the curvature is not fixed. On the one hand, assuming a precise value of Ω_k may affect the dark energy reconstruction while, on the other hand, convergence issues could arise if Ω_k is not postulated *a priori*.

5.2. Improving standard cosmography

The standard cosmographic approach suffers from severe issues when high-redshift data are used to study the dark energy behaviour.²⁰⁰ The restricted convergence of the Taylor series makes this method poorly predictive for cosmographic analysis at $z > 1$.

5.2.1. The method of Padé polynomials

A way to overcome these restrictions is offered by Padé rational polynomials.²⁰⁵ The method of Padé approximations is built up from the standard Taylor series of a generic function $f(z)$:

$$f(z) = \sum_{i=0}^{\infty} c_i z^i, \quad (169)$$

where $c_i = f^{(i)}(0)/i!$. We thus define the (n, m) Padé approximation of $f(z)$ as

$$P_{n,m}(z) = \frac{\sum_{i=0}^n a_i z^i}{1 + \sum_{j=1}^m b_j z^j}. \quad (170)$$

whose Taylor expansion agrees with Eq. (169) to the highest possible order, i.e.

$$\begin{cases} P_{n,m}(0) = f(0), \\ P'_{n,m}(0) = f'(0), \\ \vdots \\ P_{n,m}^{(n+m)}(0) = f^{(n+m)}(0). \end{cases} \quad (171)$$

The $n+1$ independent coefficients in the numerator and m independent coefficients in the denominator of Eq. (170) make $n+m+1$ the number of total unknown terms. These can be determined by imposing

$$f(z) - P_{n,m}(z) = \mathcal{O}(z^{n+m+1}), \quad (172)$$

from which one obtains

$$(1 + b_1 z + \dots + b_m z^m)(c_0 + c_1 z + \dots) = a_0 + a_1 z + \dots + a_n z^n + \mathcal{O}(z^{n+m+1}). \quad (173)$$

Then, equating the coefficients with the same power provides a set of $n+m+1$ equations for the $n+m+1$ unknown terms a_i and b_i :

$$\begin{cases} a_i = \sum_{k=0}^i b_{i-k} c_k, \\ \sum_{j=1}^m b_j c_{n+k+j} = -b_0 c_{n+k}, \quad k = 1, \dots, m. \end{cases} \quad (174)$$

Recent applications of Padé approximations in the cosmological context have shown the good properties of this technique to alleviate the convergence problems at high redshifts.^{207–209} Also in this approach all physical information got from data, i.e. the cosmographic series, is based on assuming cosmic homogeneity and isotropy only. We can summarize the advantages of Padé rational approximations as follows:

- the series can heal bad convergence issues in the data ranges;
- the series can decrease error propagations outside the interval $z < 1$;
- the series can be calibrated by choosing appropriate orders depending on the specific situation.

Nevertheless, the Padé polynomials suffer from some issues:

- the convergence of the series is not known a priori, and directly comparing with data is necessary in order to specify the appropriate order;
- possible poles characteristic of the series within the observational domain may limit the convergence;
- there could exist a degeneration among different series.

A detailed study of Padé approximations in the cosmographic context has been performed in 210, where the authors showed the advantages of this method by analyzing several Padé expansions and comparing them with different cosmological observables. They obtained bounds on the cosmographic series and investigated how to reduce the errors systematics and to overcome degeneracy between the cosmological parameters. We report in Appendix B some explicit expressions of the Padé approximations of the luminosity distance.

5.2.2. *The method of Chebyshev polynomials*

We have seen that Padé method still leaves a degree of subjectivity in the choice of the highest orders of expansion. In addition, the Padé treatment works much better as one has to approximate non-smooth functions in which other numerical methods fail. This happens as one needs to approximate flexes or discontinuities in domains. Unfortunately, this is not the case of cosmic distances. So that, from the one hand it is possible to heal the convergence problem, but from the other hand one conceptually uses Padé series to approximate well-defined cosmic distances, albeit no poles are effectively involved.

To alleviate these caveats, we proposed in 211 a new cosmographic method based on ratios of Chebyshev polynomials. We showed that they reduce systematics on fitted coefficients, and candidate as a serious alternative to Taylor and Padé series in cosmology. The Chebyshev polynomials $T_n(z)$ are defined as

$$T_n(z) = \cos(n\theta), \quad (175)$$

where $\theta = \arccos(z)$ and $n \in \mathbb{N}_0$. They are orthogonal polynomials with respect to

the function $w(z) = (1 - z^2)^{-1/2}$ for $|z| \leq 1$ such that

$$\int_{-1}^1 T_n(z)T_m(z)w(z) = \begin{cases} \pi , & n = m = 0 \\ \frac{\pi}{2}\delta_{nm} , & \text{otherwise} \end{cases} \quad (176)$$

It is possible to generate the Chebyshev polynomials from the recurrence relation:

$$T_{n+1}(z) = 2zT_n(z) - T_{n-1}(z) . \quad (177)$$

The explicit expressions up to the fifth order are the following:^e

$$\begin{aligned} T_0(z) &= 1 , \\ T_1(z) &= z , \\ T_2(z) &= 2z^2 - 1 , \\ T_3(z) &= 4z^3 - 3z , \\ T_4(z) &= 8z^4 - 8z^2 + 1 ; \end{aligned} \quad (178)$$

which will be employed to build the new expression for $d_L(z)$. The powers of z can be expressed in terms of the Chebyshev polynomials as

$$z^n = 2^{1-n} \sum_{k=0}^{[n/2]} a_k \binom{n}{k} T_{n-2k}(z) , \quad (179)$$

for $n > 0$, being $[n/2]$ the integer part of $n/2$, $a_k = 1/2$ if $k = n/2$ and $a_k = 1$ if $a_k \neq n/2$.

Suppose $f(z) \in L_w^2$, where L_w^2 is the Hilbert space of the square-integrable functions with respect to $w^{-1}(z) dz$. If the truncated Taylor series of $f(z)$ around the point $z = 0$, $g(z)$, is known, it is possible to obtain the polynomial of degree n , $\sum_{k=0}^n c_k T_k$, giving the best approximation of $f(z)$ in the interval $[-1, 1]$ in L_w^2 . Then, the Chebyshev series expansion of $f(z)$ can be written as

$$f(z) = \sum_{k=0}^{\infty} c_k T_k(z) , \quad (180)$$

where

$$\begin{cases} c_0 = \frac{1}{\pi} \int_{-1}^1 g(z) T(z) w(z) dz , \\ c_k = \frac{2}{\pi} \int_{-1}^1 g(z) T(z) w(z) dz , & k > 0 . \end{cases} \quad (181)$$

^eWe here truncate up to the fifth order, since additional contributions go beyond this treatment. In so doing, we arrive to analyse up to snap parameter s_0 .

34 *S. Capozziello, R. D'Agostino, O. Luongo*

Therefore, the (n, m) rational Chebyshev approximant is

$$R_{n,m}(z) = \frac{\sum_{i=0}^n a_i T_i(z)}{1 + \sum_{j=1}^m b_j T_j(z)}. \quad (182)$$

Equating Eq. (180) and Eq. (182) up to the $(n+m)$ -th Chebyshev polynomial, one obtains the unknown coefficients a_k and b_k :

$$f(z) = R_{n,m}(z) + \mathcal{O}(T_{n+m+1}). \quad (183)$$

By doing so, one gets

$$(1 + b_1 T_1 + \dots + b_m T_m)(c_0 + c_1 T_1 + \dots) = a_0 + a_1 T_1 + \dots + a_n T_n + \mathcal{O}(T_{n+m+1}). \quad (184)$$

The products of The Chebyshev polynomials on the left hand side of Eq. (184) can be obtained through the trigonometric identity

$$\cos(n\theta) \cos(m\theta) = \frac{1}{2} \left[\cos[(n+m)\theta] + \cos[(n-m)\theta] \right],$$

leading to

$$T_n(z)T_m(z) = \frac{1}{2} \left[T_{n+m}(z) + T_{|n-m|}(z) \right]. \quad (185)$$

Hence, equating the terms with the same degree of T 's one has

$$\begin{cases} a_i = \frac{1}{2} \sum_{j=0}^m b_j (c_{i+j} + c_{|i-j|}) = 0, & i = 0, \dots, n \\ \sum_{j=0}^m b_j (c_{i+j} + c_{|i-j|}) = 0, & i = n+1, \dots, n+m. \end{cases} \quad (186)$$

The above formalism can be easily generalized for z in an arbitrary interval $[a, b]$. To do that, one can define the generalized Chebyshev polynomials $T_n^{[a,b]}(z) = \cos(n\theta)$, where z is the new variable

$$z = \frac{a(1 - \cos \theta) + b(1 + \cos \theta)}{2}. \quad (187)$$

This is obtained by means of

$$\cos \theta = \frac{2z - (a + b)}{b - a}, \quad (188)$$

so that $\theta \in [-\pi, \pi]$ while $z \in [a, b]$. From the ordinary Chebyshev polynomials it is possible to obtain the generalized polynomials through

$$T_n^{[a,b]}(z) = T_n \left(\frac{2z - (a + b)}{b - a} \right). \quad (189)$$

$T_n^{[a,b]}(z)$ form an orthogonal set with respect to the weighting function²¹³

$$w_{[a,b]}(z) = [(z - a)(b - z)]^{-1/2}, \quad (190)$$

so that

$$\langle T_m^{[a,b]}, T_n^{[a,b]} \rangle = \int_a^b dz w_{[a,b]}(z) T_n^{[a,b]}(z) T_m^{[a,b]}(z) . \quad (191)$$

Then, the orthogonality condition reads

$$\langle T_m^{[a,b]}, T_n^{[a,b]} \rangle = \begin{cases} \pi , & n = m = 0 \\ \frac{\pi}{2} \delta_{nm} , & \text{otherwise} \end{cases} \quad (192)$$

since $T_n^{[a,b]}(z) = \cos(n\theta)$ and $d\theta = -w_{[a,b]}dz$.

To approximate the luminosity distance with Chebyshev polynomials, we need to calculate the coefficients c_k in Eq. (181) where $g(z)$ is the Taylor expansion (163). The fourth-order Chebyshev expansion of the luminosity distance reads

$$d_L(z) = \frac{1}{H_0} \sum_{n=0}^4 c_n T_n(z) , \quad (193)$$

where the coefficients c_n are:

$$\begin{aligned} c_0 &= \frac{1}{64} [18 + 5j_0(1 + 2q_0) - 3q_0(6 + 5q_0(1 + q_0)) + s_0] , \\ c_1 &= \frac{1}{8} (7 - j_0 + q_0 + 3q_0^2) , \\ c_2 &= \frac{1}{48} [14 + 5j_0(1 + 2q_0) - q_0(14 + 15q_0(1 + q_0)) + s_0] , \\ c_3 &= \frac{1}{24} (-1 - j_0 + q_0(1 + 3q_0)) , \\ c_4 &= \frac{1}{192} [2 + 5j_0(1 + 2q_0) - q_0(2 + 15q_0(1 + q_0)) + s_0] . \end{aligned}$$

We report some explicit expressions of the rational Chebyshev approximations of $d_L(z)$ in Appendix C. High-order polynomials leading to more accurate approximations are characterized by more complicated forms. The most suitable choice of Chebyshev approximation lies on assuming the correct set of coefficients which avoids one to encounter poles in the numerical analyses. This strategy can be performed by simply requiring no poles in the investigated redshift domain. Moreover, the underlying request over coefficient priors also gives an indication on which are the most viable orders to use in Chebyshev expansions.

We compare the various Chebyshev approximations with the Λ CDM luminosity distance to check their accuracy. In the case of the standard model, the cosmographic series are calculated in terms of Ω_{m0} :

$$\begin{aligned} q_{0,\Lambda\text{CDM}} &= -1 + \frac{3}{2}\Omega_{m0} , \\ j_{0,\Lambda\text{CDM}} &= 1 , \\ s_{0,\Lambda\text{CDM}} &= 1 - \frac{9}{2}\Omega_{m0} . \end{aligned} \quad (194)$$

36 *S. Capozziello, R. D'Agostino, O. Luongo*

As an indicative example, we fix $\Omega_{m0} = 0.3$. From Eq. (194) one then get

$$\begin{cases} q_0 = -0.55 , \\ j_0 = 1 , \\ s_0 = -0.35 . \end{cases} \quad (195)$$

Adopting the values of Eq. (195), in Fig. 2 we show $\bar{d}_L(z) \equiv H_0 \times d_L(z)$ for different degrees of Chebyshev approximations.

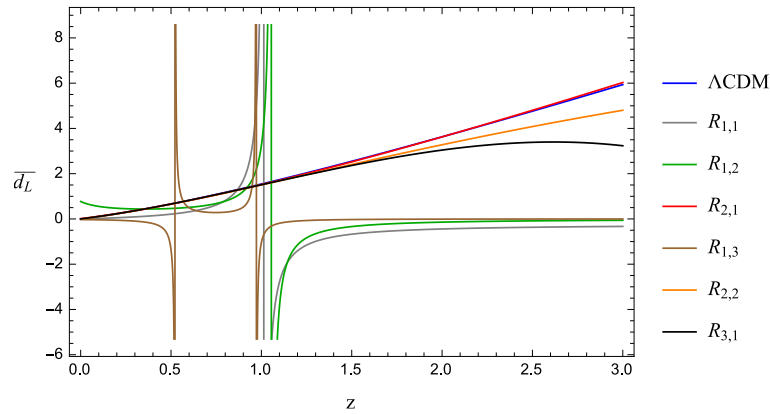


Fig. 2. Dimensionless luminosity distance in terms of the redshift in the case of rational Chebyshev approximations ($R_{1,1}$), ($R_{1,2}, R_{2,1}$) and ($R_{1,3}, R_{2,2}, R_{3,1}$) orders; it is possible to notice the comparison with the Λ CDM model. Choosing a set of values for the free parameters enables to get the correct expansion orders in Chebyshev analyses.

5.2.3. The convergence radius of rational approximations

To verify the effective improvement of the new cosmographic technique in approximating cosmic distances, it is necessary to test the stability of Chebyshev approximations at high-redshift domains. Therefore, one can study the convergence radius ρ of the various cosmographic methods.

As an example, we compare the convergence radius of the (1,1) rational Chebyshev approximation of $d_L(z)$ with the second-order Taylor and the (1,1) Padé approximations. From Eqs. (178) and (182), it follows

$$R_{1,1}(z) = \frac{a_0 T_0(z) + a_1 T_1(z)}{1 + b_1 T_1(z)} = \frac{a_0 + a_1 z}{1 + b_1 z}, \quad (196)$$

where $\{a_0, a_1, b_1\}$ are expressed in terms of the series given in Eq. (C.1). One can recast Eq. (196) as

$$R_{1,1} = \frac{a_0}{1 + b_1 z} + \frac{a_1}{b_1} \left(1 - \frac{1}{1 + b_1 z} \right), \quad (197)$$

which leads to

$$R_{1,1} = \frac{a_1}{b_1} + \left(a_0 - \frac{a_1}{b_1}\right) \sum_{n=0}^{\infty} (-b_1)^n z^n . \quad (198)$$

The convergence radius of the geometric series in Eq. (198) is thus

$$\rho_{R_{1,1}} = \frac{1}{|b_1|} = \left| \frac{-3(7 - j_0 + q_0 + 3q_0^2)}{14 + 5j_0(1 + 2q_0) - q_0(14 + 15q_0(1 + q_0)) + s_0} \right| . \quad (199)$$

For the (1,1) Padé approximation of $d_L(z)$, similar calculations yield

$$\rho_{P_{1,1}} = \frac{2}{1 - q_0} , \quad (200)$$

while, in the case of the second-order Taylor series, one has

$$\rho_{d_{L,2}} = \frac{1 - q_0}{2} . \quad (201)$$

The proper procedure should make use of fitting results over the cosmographic coefficients to compute $\rho_{R_{1,1}}$, $\rho_{P_{1,1}}$ and $\rho_{d_{L,2}}$. However, an immediate check can be done assuming the reference values given by Eq. (194), in which case one finds

$$\begin{cases} \rho_{R_{1,1}} = 1.014 , \\ \rho_{P_{1,1}} = 1.290 , \\ \rho_{d_{L,2}} = 0.775 . \end{cases} \quad (202)$$

The above results demonstrate the improvements obtained in the case of rational polynomials. In Fig. 3 we show the convergence radii for Taylor, Padé and Chebyshev polynomials using a different calibration with respect to the concordance paradigm.

5.3. Observational constraints

In 211 we tested the new method of rational Chebyshev polynomials against other cosmographic approaches by performing a Markov Chain Monte Carlo (MCMC) integration on the combined likelihood of the SN Ia JLA data,²¹⁴ and other low-redshift measurements such as the Observational Hubble data²¹⁵ (OHD) and Baryon Acoustic Oscillations²¹⁶ (BAO) (see Table 6 and Table 7). Assuming the uniform priors listed in Table 1, we show in Table 2 the results of the joint analysis obtained through the Metropolis numerical algorithm implemented by the Monte Python code.²¹⁷ We also show, in Fig. 4, Fig. 5, and Fig. 6, the marginalized contours and posterior distributions for the different cosmographic techniques. As shown in Table 3, the relative uncertainties for the cosmographic parameters are clearly reduced in the case of rational Chebyshev polynomials compared to the other approximation methods.

An interesting fact to note is that, by construction, one uses Chebyshev polynomials with lower orders than Taylor series and Padé approximants. This mostly

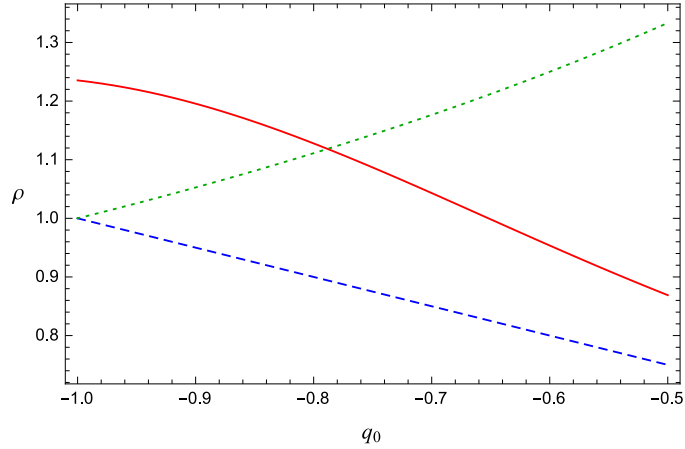


Fig. 3. Convergence radii for different orders. In particular, for second-order Taylor (dashed curve) and equivalent (1,1) Padé (dotted curve) and (1,1) rational Chebyshev (solid curve). In the picture of Chebyshev approximation we took $j_0 = 2$, $s_0 = -1$.

reduces the computational difficulties in implementing cosmic data, although does not accurately fix the highest-order parameter in the approximation. This is the case of s_0 whose error bars are not significantly improved adopting Chebyshev polynomials. To overcome this issue, it would be enough to increase the Chebyshev order to better fix s_0 than Taylor and Padé treatments.

Table 1. Parameter priors used for MCMC, with H_0 in units of Km/s/Mpc and r_d in units of Mpc.

Parameter	Prior
H_0	(50, 90)
q_0	(-10, 10)
j_0	(-10, 10)
s_0	(-10, 10)
M	(-20, -18)
Δ_M	(-1, 1)
α	(0, 1)
β	(0, 5)
r_d	(140, 160)

Table 2. 1 and 2 σ confidence level got from the MCMC analysis using SN+OHD+BAO data surveys in the case of fourth-order Taylor, (2,2) Padé and (2,1) rational Chebyshev polynomial approximations of d_L .

Parameter	Taylor			Padé			Rational Chebyshev		
	Mean	1 σ	2 σ	Mean	1 σ	2 σ	Mean	1 σ	2 σ
H_0	65.80	+2.09 -2.11	+4.22 -4.00	64.94	+2.11 -2.02	+4.12 -4.13	64.95	+1.89 -1.94	+3.77 -3.77
q_0	-0.276	+0.043 -0.049	+0.093 -0.091	-0.285	+0.040 -0.046	+0.087 -0.084	-0.278	+0.021 -0.021	+0.041 -0.042
j_0	-0.023	+0.317 -0.397	+0.748 -0.685	0.545	+0.463 -0.652	+1.135 -1.025	1.585	+0.497 -0.914	+1.594 -1.453
s_0	-0.745	+0.196 -0.284	+0.564 -0.487	0.118	+0.451 -1.600	+3.422 -1.921	1.041	+1.183 -1.784	+3.388 -3.087
M	-19.16	+0.07 -0.07	+0.14 -0.14	-19.03	+0.02 -0.02	+0.05 -0.05	-19.17	+0.07 -0.07	+0.13 -0.13
Δ_M	-0.054	+0.023 -0.022	+0.044 -0.045	-0.054	+0.022 -0.023	+0.045 -0.045	-0.050	+0.022 -0.022	+0.044 -0.045
α	0.127	+0.006 -0.006	+0.012 -0.012	0.127	+0.006 -0.006	+0.012 -0.012	0.130	+0.006 -0.006	+0.012 -0.012
β	2.624	+0.071 -0.068	+0.136 -0.140	2.625	+0.065 -0.069	+0.137 -0.135	2.667	+0.068 -0.069	+0.137 -0.135
r_d	149.2	+3.7 -4.1	+7.7 -7.5	148.6	+3.5 -3.8	+7.5 -7.1	147.2	+3.7 -4.0	+7.8 -7.5

 Table 3. 68% and 95% errors on the cosmographic outputs got by MCMC analysis in which we used SN+OHD+BAO data in the case of fourth-order Taylor, (2,2) Padé and (2,1) rational Chebyshev polynomial approximations of d_L .

Parameter	Taylor		Padé		Rational Chebyshev	
	1 σ	2 σ	1 σ	2 σ	1 σ	2 σ
H_0	3.19%	6.25%	3.17%	6.35%	2.95%	4.11%
q_0	16.8%	33.5%	15.1%	30.1%	7.66%	14.8%
j_0	1534%	3079%	102%	198%	44.5%	96.1%
s_0	32.2%	70.5%	866%	2258%	142%	311%

5.4. The E_i s method

In this subsection it is relevant to cite a possible approach which consists in testing cosmography with the Hubble parameter, without making use of rational approximations. Formally, the Hubble function in Taylor series around $z = 0$ is

$$E(z) \equiv \frac{H(z)}{H_0} = \sum_i \frac{1}{i!} E_i z^i \quad (203)$$

with $E_i = H^{(i)}(z)/H_0|_{z=0}$. Hereafter we baptize with *eis* coefficients the first four terms in the expansions, which read:

$$\begin{aligned} E_0 &= 1, \\ E_1 &= 1 + q_0, \\ E_2 &= -q_0^2 + j_0, \\ E_3 &= 3q_0^2 + 3q_0^3 - j_0(4q_0 + 3) - s_0. \end{aligned} \quad (204)$$

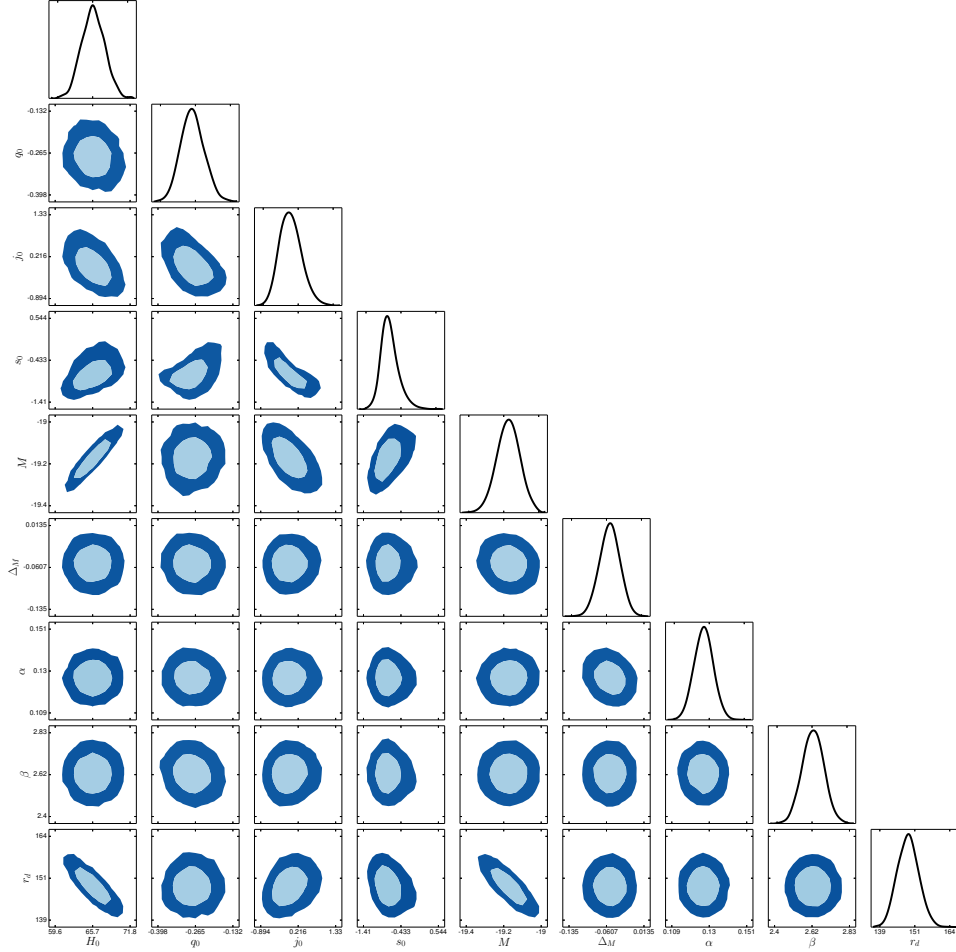
40 *S. Capozziello, R. D'Agostino, O. Luongo*


Fig. 4. 1σ and 2σ confidence level contours and posterior distributions inferred from the MCMC analysis by combining SN+OHD+BAO data surveys. The results have been obtained for fourth-order Taylor approximation of d_L . The units of H_0 are Km/s/Mpc, whereas r_d in Mpc.

To reduce systematics, a possible trick is to use directly the Taylor expansion of $H(z)^{218}$ within the comoving distance $\eta(z) = \int_0^z \frac{dz'}{H(z')}$ and integrate numerically to obtain the luminosity distance. Details of numerical simulations and strategies have been reported in,²¹⁹ in which the estimation of the *eis* parameters through a hierarchical manner has been performed by:

$$\tilde{d}_L(z; E_1, E_2, E_3) = \begin{cases} \tilde{d}_L^{(1)}(z) & z < z_{low} \\ \tilde{d}_L^{(2)}(z) & z_{low} < z < z_{mid} \\ \tilde{d}_L^{(3)}(z) & z_{mid} < z < z_{high}. \end{cases} \quad (205)$$

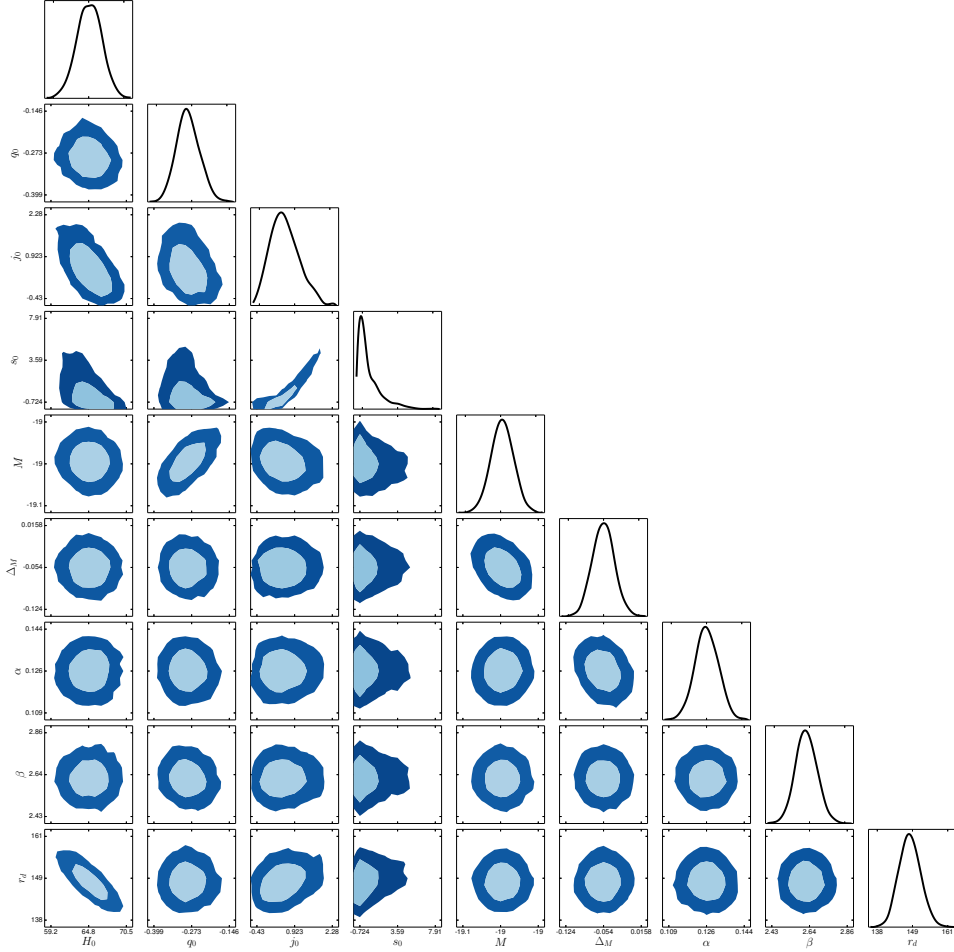


Fig. 5. 68% and 95% confidence levels and corresponding contours with posterior distributions determined from the MCMC analysis. Here, we considered a combined SN+OHD+BAO survey for the (2,2) Padé approximation of d_L . H_0 is written in Km/s/Mpc, while r_d in Mpc.

A good choice for redshift cut-offs is

$$z_{low} = 0.05, \quad z_{mid} = 0.4, \quad z_{high} = 0.9. \quad (206)$$

With simple considerations, adopting binning procedure for Ei's and standard cosmography, one can mix the two approach to reduce significantly the error propagations of every cosmographic analysis. As a genuine example, a module for the code CosmoMC²²⁰ to draw the likelihood distributions for all the methods is available at <https://github.com/alejandroviles/EisCosmography>; also, all the simulated catalogs and further statistics can be found there.

A simple representation of the improvements of the method can be found in Fig.

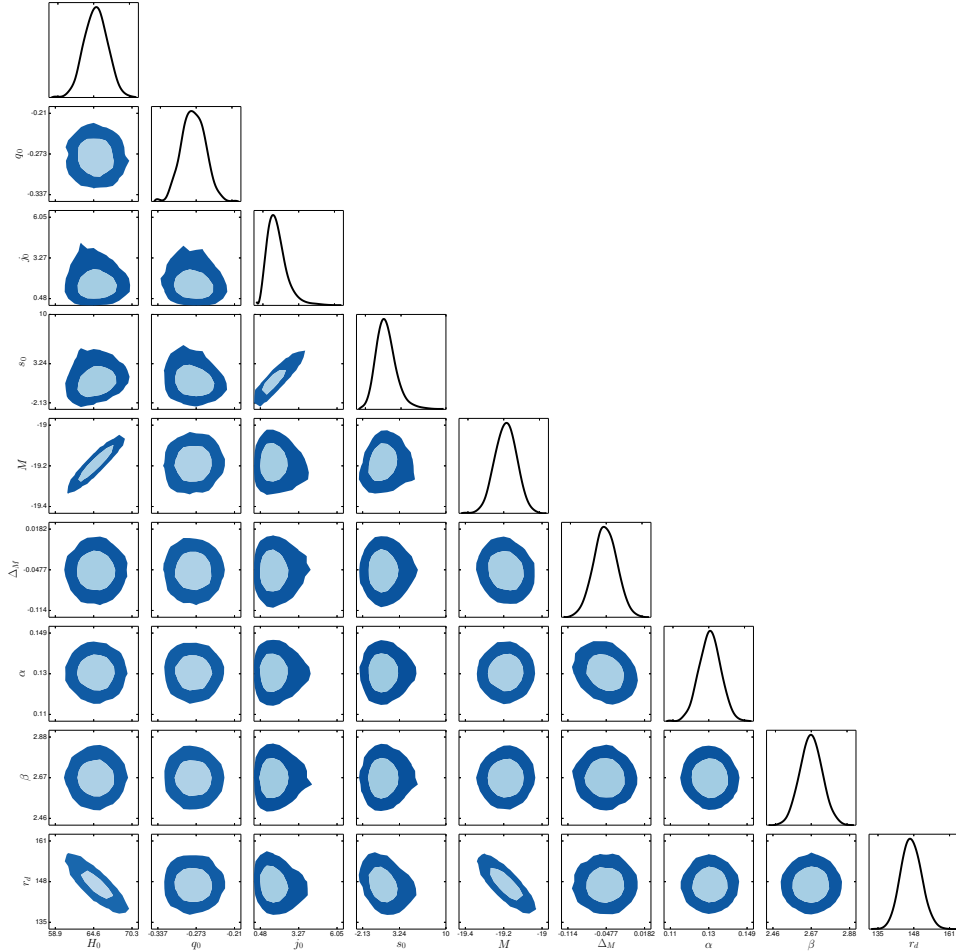


Fig. 6. Contours and posterior distributions for 68% and 95% confidence levels. We got these plots from the MCMC analysis of the whole SN+OHD+BAO data set in the case of (2,1) rational Chebyshev approximation of d_L , with H_0 in Km/s/Mpc, and r_d in Mpc.

(7)

The need of additional methods, different from standard approaches, is essential to overcome the broadening of coefficients due to systematics and error propagation. Often this problem has been imputed to the lacking of cosmic data. However, discussions over this issue are still open.²²¹ An intriguing open challenge would be *unifying* the Ei's method with rational approximations, either with rational approximations or in the framework of extended and/or modified theories of gravity.

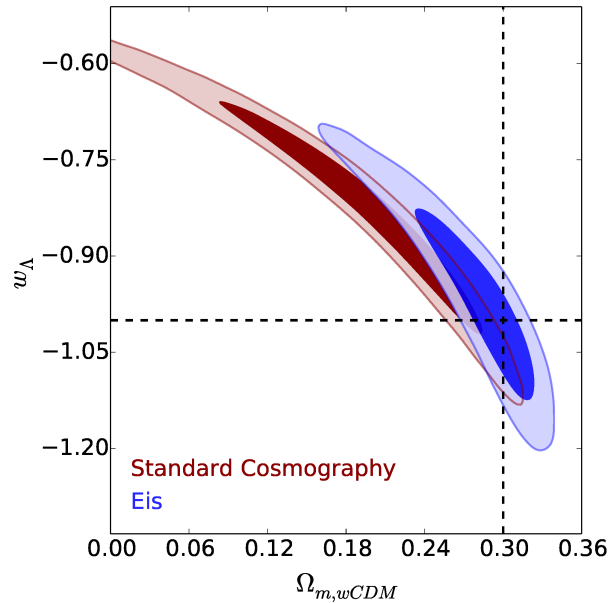


Fig. 7. 2D confidence regions for Ω_m and w , as a pure example for comparing standard cosmography and Eis procedures. It is possible to notice that standard cosmography is unpredictable at 2σ .

6. Model-independent reconstruction of $f(R)$ gravity

The above cosmographic analysis can be adopted to reconstruct dark energy models deriving the functional forms of Lagrangians from observational data. The method can be considered as a sort of *Inverse Scattering* to approach the cosmological problem. In this section, we reconstruct, from cosmography, the $f(R)$ gravity action both in the metric and in the Palatini formalisms, without postulating any specific functional form. A standard procedure in the $f(R)$ studies consists of assuming the gravity action and then finding out the dynamics by solving the modified Friedmann equations. The standard approach relies on postulating the form of $f(R)$ *a priori*, which determines the cosmological model. In what follows, instead, we present a model-independent method to reconstruct the functional form of the action. To this end, we use rational polynomials to obtain accurate cosmographic approximations of the luminosity distance up to high redshifts. We shall study the late-time expansion history of the universe and discuss possible departures from GR and then the Λ CDM model.

6.1. The metric formalism case

Let us start with the model-independent reconstruction of the $f(R)$ action in the metric formalism.²²² The determination of $f(R)$ through the match with cosmic

data has been subject of a wide discussion in the last years.^{92, 223, 224} In particular, the method of Taylor-expanding $f(R)$ for R approaching its late-time values is limited by the short range of redshift characteristic of observational data. Also, the truncation of the Taylor polynomial reproducing the $f(R)$ function unavoidably introduces errors in the analysis. In this respect, Padé polynomials may offer a possible solution to the convergence problem. Motivated by the results already obtained,²¹⁰ let us consider the (2,1) Padé approximation of the Hubble rate:

$$H_{21}(z) = \left[2H_0(1+z)^2(3+z+j_0z-q_0(3+z+3q_0z))^2 \right] \times \left[18(q_0-1)^2 + 6(q_0-1) \right. \\ \left. (-5-2j_0+q_0(8+3q_0))z + (14+2j_0^2+j_0(7-q_0(10+9q_0))+q_0(-40 \right. \\ \left. +q_0(17+9q_0(2+q_0)))z^2 \right]^{-1}. \quad (207)$$

We note that that $H_{21}(z)$ is expressed in terms of the cosmographic series up to the jerk parameter, whereas the third-order Taylor approximation contains also the snap parameter. To apply our strategy, we first convert the time derivatives and the derivatives with respect to R into derivatives with respect to z according to the prescription

$$\frac{d\mathfrak{F}}{dt} = -(1+z)H\mathfrak{F}_z, \quad (208)$$

$$\frac{\partial\mathfrak{F}}{\partial R} = \frac{1}{6} \left[(1+z)H_z^2 + H(-3H_z + (1+z)H_{zz}) \right]^{-1} \mathfrak{F}_z, \quad (209)$$

where $\mathfrak{F}(z)$ is an arbitrary function and we denote derivatives with respect to the redshift by the subscripts ‘ z ’. Then, after determining the values of the cosmographic parameters, one can combine Eq. (39) and Eq. (41) and use Eq. (38). This provides us with the following second-order differential equation for $f(z)$:

$$H^2 f_z = \left[-(1+z)H_z^2 + H(3H_z - (1+z)H_{zz}) \right] \left[-6H_0^2(1+z)^3\Omega_{m0} - f \right. \\ \left. - \frac{Hf_z(2H - (1+z)H_z)}{(1+z)H_z^2 + H(-3H_z + (1+z)H_{zz}^2)} - \frac{f_{zz}((1+z)H_z^2 + H(-3H_z + (1+z)H_{zz}))}{[(1+z)H_z^2 + H(-3H_z + (1+z)H_{zz})]^2} \right] \\ \times (1+z)H^2 - \frac{(1+z)H^2 \left(f_z(2H_z^2 - 3(1+z)H_zH_{zz} + H(2H_{zz} - (1+z)H_{zzz})) \right)}{[(1+z)H_z^2 + H(-3H_z + (1+z)H_{zz})]^2}. \quad (210)$$

The initial conditions needed to solve the above equation can be obtained by combining the condition $f'(R_0) = 1$ together with evaluating Eqs. (39), (41) and (42) at the present time:

$$f_0 = R_0 + 6H_0^2(\Omega_{m0} - 1), \quad (211)$$

$$f_z|_{z=0} = R_z|_{z=0}. \quad (212)$$

In what follows, we fix $\Omega_{m0} = 0.3$. Regarding the cosmographic parameters, for the (2,1) Padé approximation, we use the results found in 210:

$$\begin{cases} h = 0.7064_{-0.0263}^{+0.0277}, \\ q_0 = -0.4712_{-0.1106}^{+0.1224}, \\ j_0 = 0.593_{-0.210}^{+0.216}, \end{cases} \quad (213)$$

and for the third-order Taylor expansion:

$$\begin{cases} h = 0.7253_{-0.0351}^{+0.0353}, \\ q_0 = -0.6642_{-0.1963}^{+0.2050}, \\ j_0 = 1.223_{-0.664}^{+0.644}, \\ s_0 = 0.394_{-0.731}^{+1.335}. \end{cases} \quad (214)$$

Hence, we can reconstruct $f(z)$ numerically by inserting Eq. (207) into Eq. (180). The $f(R)$ function resulting from the reconstruction procedure will be negative due to the metric signature adopted in the analysis. Consistently, $f(z)$ must be a negative function as for the case of upper bound results of (213). In Fig. 8 we show the numerical reconstruction of $f(z)$ for the (2,1) Padé approximation.

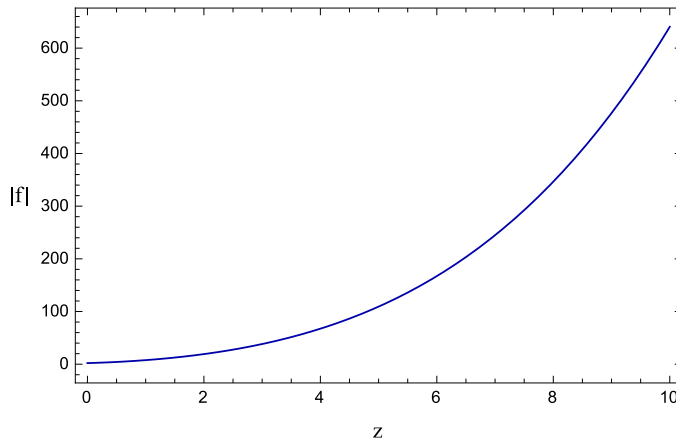


Fig. 8. Plot of the numerical shape of $|f(z)|$ approximated by using the (2,1) Padé polynomial.

To find the analytical match for $f(z)$, we considered the following test-functions

46 *S. Capozziello, R. D'Agostino, O. Luongo*

with three free constant coefficients (\mathcal{A} , \mathcal{B} , \mathcal{C}):

Exponential

$$f_1(z) = \mathcal{A}z + \mathcal{B}z^3 e^{\mathcal{C}z} \quad (215a)$$

$$f_2(z) = \mathcal{A} + \mathcal{B}z^2 \sinh(1 + \mathcal{C}z) \quad (215b)$$

$$f_3(z) = \mathcal{A}z + \mathcal{B}z^3 \cosh(\mathcal{C}z) \quad (215c)$$

$$f_4(z) = \mathcal{A}z^2 + \mathcal{B}z^4 \tanh(\mathcal{C}z) \quad (215d)$$

Trigonometric

$$f_5(z) = \mathcal{A}z^3 + \mathcal{B}z^5 \sin(1 + \mathcal{C}z) \quad (215e)$$

$$f_6(z) = \mathcal{A}z^3 + \mathcal{B}z^4 \cos(1 + \mathcal{C}z) \quad (215f)$$

$$f_7(z) = \mathcal{A}z + \mathcal{B}z^2 \tan(\mathcal{C}z) \quad (215g)$$

Logarithmic

$$f_8(z) = \mathcal{A}z + \mathcal{B}z^3 \ln(1 + \mathcal{C}z) \quad (215h)$$

Then, we perform the \mathcal{F} -statistics:²²⁶

$$\mathcal{F} = \frac{(\text{TSS} - \text{RSS})/p}{\text{RSS}/(n - p - 1)}, \quad (216)$$

where

$$\text{TSS} = \sum_{i=1}^n (y_i - \bar{y})^2, \quad (217)$$

$$\text{RSS} = \sum_{i=1}^n (y_i - \hat{y}_i)^2, \quad (218)$$

and

$$\bar{y} = \frac{1}{n} \sum_{i=1}^n y_i. \quad (219)$$

Here, y_i are the observed value while \hat{y}_i are the values predicted by the model; n is the number of observations and p the number of predictors. The goodness of the model is tested by comparing the null hypothesis (the explanatory power of the model is null as all the regression coefficients are zero) with the case in which there exists at least one non-zero regression coefficient. While in other tests such as t -statistics and p -value the goodness of the model is measured by looking for any association between the individual variables and the response, in the \mathcal{F} -statistics the model is tested through the joint explanatory power of its predictors. For large p it may happen, in fact, that the p -values are small even when there is no real association between the predictors and the response. Furthermore, the advantage of the \mathcal{F} -statistics with respect to \mathcal{R}^2 -test^f relies on the presence of the number of

^fIt is worth noticing that, a part the abuse of notation, \mathcal{R}^2 is not the \mathcal{R} scalar curvature of Palatini formalism.

predictors. Adding more predictors to the model makes \mathcal{R}^2 always increase, even if the association between those variables and the response is weak. It is actually possible to express the \mathcal{F} -statistics in terms of \mathcal{R}^2 as

$$\mathcal{F} = \frac{\mathcal{R}^2/p}{(1 - \mathcal{R}^2)/(n - p - 1)}. \quad (220)$$

The higher the values of \mathcal{F} , the higher the evidence against the null hypothesis, for which we expect very small \mathcal{R}^2 and \mathcal{F} . In this study, $p = 3$ is the number of free

Table 4. \mathcal{F} -statistics on Eqs. (215a)–(215h) for the (2,1) Padé approximation.

Test-function	$(\mathcal{A}, \mathcal{B}, \mathcal{C})$	$\mathcal{F}(\times 10^6)$
$f_1(z)$	$(-8.078, -0.530, 0.005)$	31.7
$f_2(z)$	$(-6.147, -2.148, 0.080)$	13.5
$f_3(z)$	$(-8.046, -0.541, 0.025)$	3.637
$f_4(z)$	$(-3.699, 0.027, -562.2)$	4.535
$f_5(z)$	$(-0.708, -0.001, 1.095)$	0.118
$f_6(z)$	$(-0.717, -0.008, 0.)$	0.142
$f_7(z)$	$(-41.30, 0.002, 1.000)$	0.026
$f_8(z)$	$(-11.69, -0.208, 1.182)$	1.484

parameters and $n = 1000$ are the points generated from the numerical solution of $f(z)$. The results shown in Table 4 indicate that the best analytical match for $f(z)$ is

$$f(z) = \mathcal{A}z + \mathcal{B}z^3 e^{\mathcal{C}z}, \quad (221)$$

where

$$(\mathcal{A}, \mathcal{B}, \mathcal{C}) = (-8.078, -0.530, 0.005). \quad (222)$$

In Fig. 9 we show the comparison between the numerical and the analytical solutions of $f(z)$ in the domain $z \in [0, 10]$.

To determine $f(R)$, we need to invert the function $R(z)$ and insert back into Eq. (221). This procedure can be only done numerically due to the impossibility for an analytical inversion of Eq. (207). Therefore, we used Eq. (38) to find $z(R)$ (see Fig. 10), which we plugged into Eq. (221) to finally obtain $f(R)$ (see Fig. 11).

From Fig. 12 and Fig. 13 we can see that our model fulfils the viability conditions discussed in Sec. 3.1. However, Fig. 12 indicates that $f'(R)$ becomes higher than one for large curvatures, due to the condition imposed on $f'(R_0)$. A correct asymptotic behaviour can be found by relaxing the assumption $f'(R_0) = 1$, i.e. requiring that G_{eff} is slightly different from G , within the limits imposed by the most recent

48 *S. Capozziello, R. D'Agostino, O. Luongo*

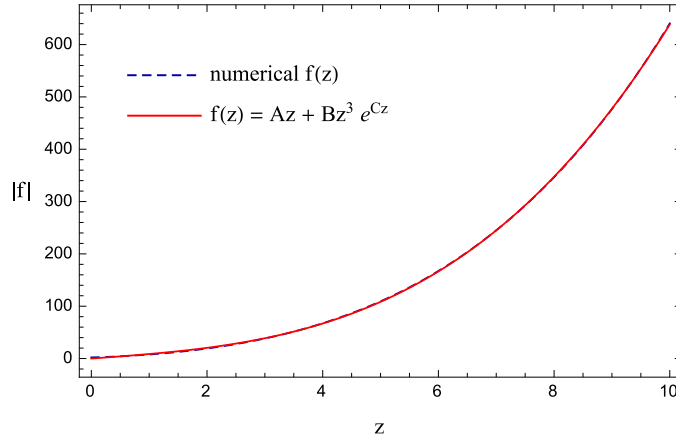


Fig. 9. Comparison between $|f(z)|$ and the functional form Eq. (221) provided by (2,1) Padé approximation.

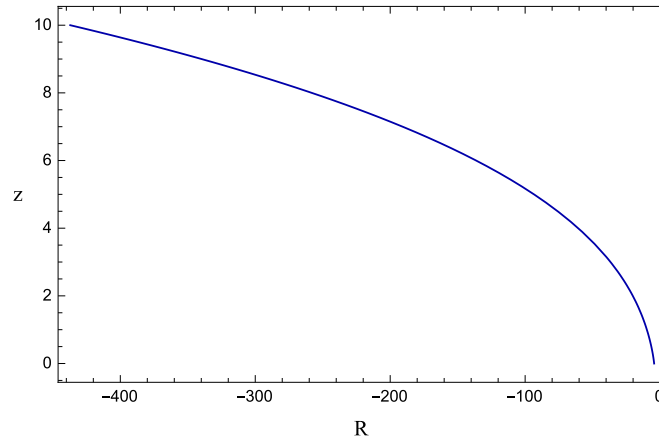


Fig. 10. Framing $z(R)$ out for (2,1) Padé polynomial.

measurements.²²⁷ In light of this, one can modify Eqs. (211) and (212) as follows:

$$f_0 = f'(R_0)(6H_0^2 + R_0) - 6H_0^2\Omega_{m0} , \quad (223)$$

$$f_z|_{z=0} = f'(R_0) R_z|_{z=0} . \quad (224)$$

In Fig. 14 we show the results we obtain by using the above relations to find the auxiliary function $f(z)$. Finally, it is important to stress that the asymptotic value of $f'(R)$ depends on the accuracy of the cosmographic series at high redshifts. The predictive power and the convergence radius of the Padé polynomials could be further improved by considering high-order terms, so that the difference $f'(R)_{numerical} - f'(R)_{exact}$ at large curvatures can be made smaller up to the desired

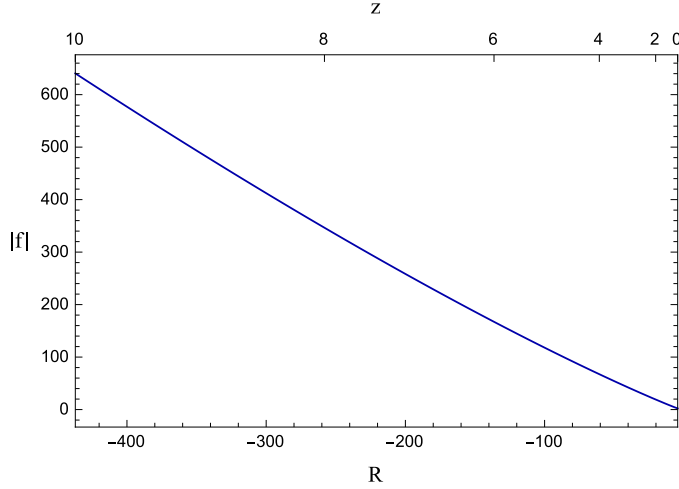


Fig. 11. Reconstructed $|f(R)|$ function developed in the case of (2,1) Padé polynomial inside $z \in [0, 10]$

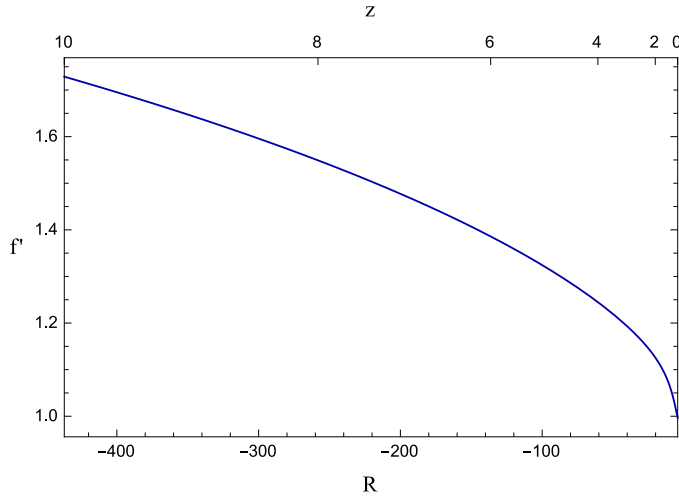


Fig. 12. Behaviour of df/dR as byproduct of (2,1) Padé polynomial inside $z \in [0, 10]$.

level.

We can now study the behaviour of the dark energy equation of state w_{DE} inferred from the reconstructed $f(R)$ function. For this purpose, we rescaled Eq. (221) to take into account the error propagation in the numerical procedure:

$$f(z) \longrightarrow \lambda + f(z). \quad (225)$$

Here, λ does not come as vacuum energy contribution but it plays the role of a

50 *S. Capozziello, R. D'Agostino, O. Luongo*

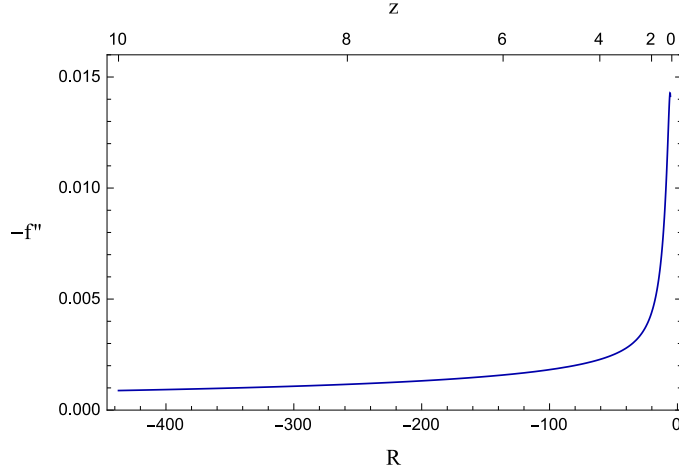


Fig. 13. Behaviour of $|d^2 f/dR^2|$ as byproduct of (2,1) Padé polynomial inside $z \in [0, 10]$.

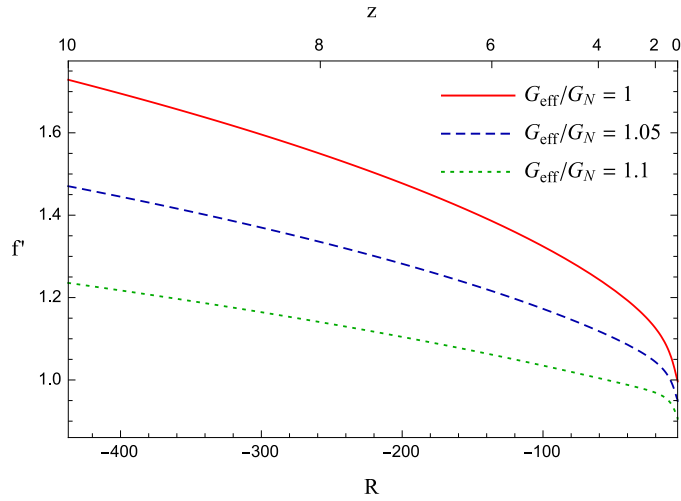


Fig. 14. Behaviour of $f'(R)$ for different values of G_{eff} .

scaling constant which guaranties the matching between the numerical value of $f(z)$ at $z = 0$ and the physical condition $f'(R_0) = 1$. The value of λ can be found by imposing the condition of present acceleration:

$$-1 \leq w_{DE} \Big|_{z=0} < -\frac{1}{3}, \quad (226)$$

which yields

$$\lambda \gtrsim 19.3. \quad (227)$$

The behaviours of curvature density and curvature pressure are displayed in Fig. 15 and Fig. 16 for an indicative value of $\lambda = 100$. Fig. 17 shows the effective dark energy equation of state parameter for various values of λ according to (227).

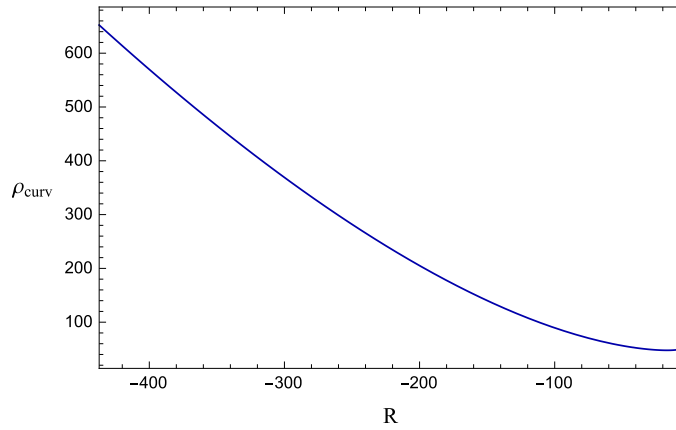


Fig. 15. Curvature density with Padé approximation. Here we use $\lambda = 100$.

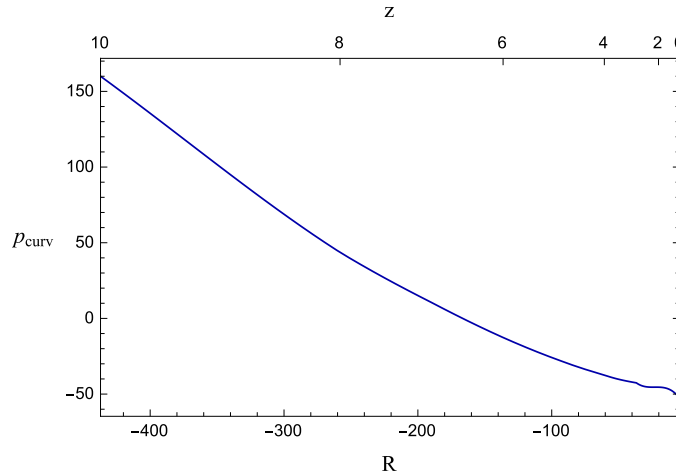


Fig. 16. Curvature pressure with Padé approximation. Here we use $\lambda = 100$.

Finally, to better check the benefits of the analysis based on Padé approximations with respect to the standard approach based on the Taylor series, we used Eq. (246) to solve Eq. (210) with the best-fit results of (214). The comparison between the

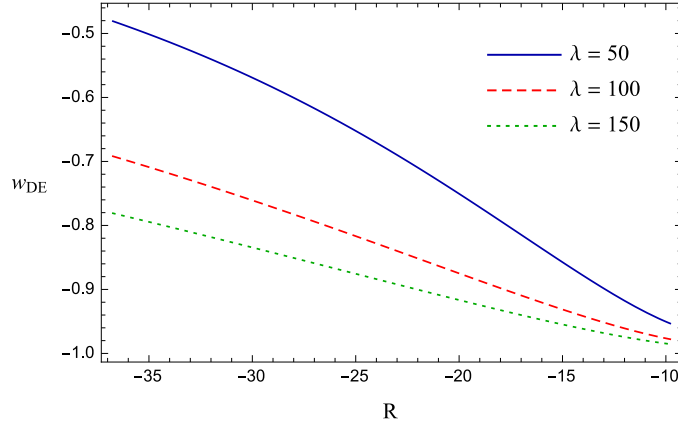


Fig. 17. Dark energy equation of state with different values of λ in Padé approximation

two methods are shown in Fig. 18, from which we see that the Taylor approach is no longer predictive at $z \gtrsim 0.3$. Inverting numerically Eq. (246) with the use of Eq. (38) gives $z(R)$ (see Fig. 19), which we inserted into $f(z)$ to find the $f(R)$ function in the case of the Taylor approximation (see Fig. 20).

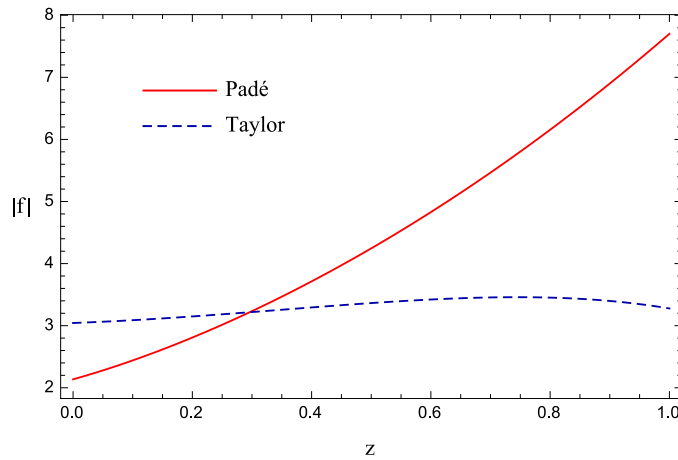


Fig. 18. Comparing $|f(z)|$ with (2,1) Padé (solid red) and third-order Taylor (dashed blue) approximations.

We shall now study the dark energy equation of state parameter for the Taylor approach and compare it with the results of the Padé approximation. Applying to the Taylor approximation the rescaling (225) and the condition (226), one gets

$$\lambda \gtrsim 1196. \quad (228)$$

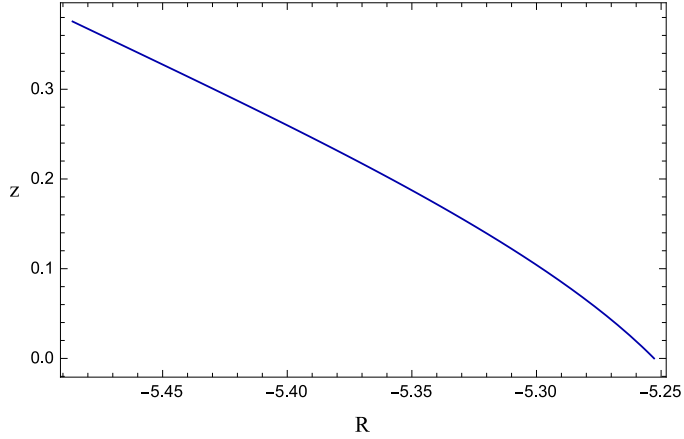


Fig. 19. Numerical shape of $z(R)$ third-order Taylor approximation.

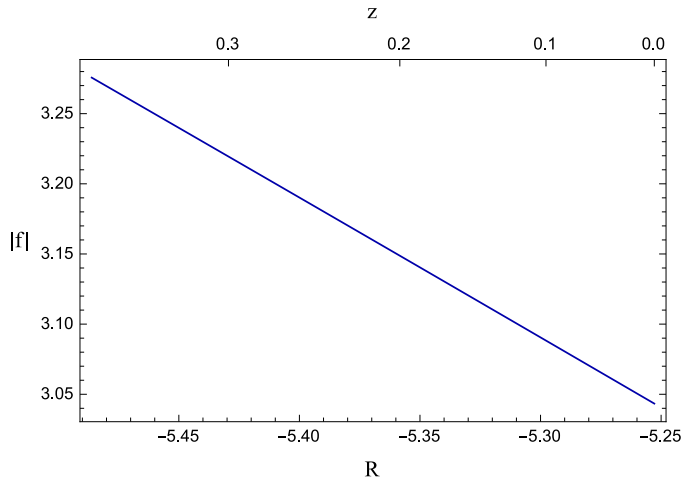


Fig. 20. Reconstructing $f(R)$ models with third-order Taylor approximation.

The dark energy equation of state parameter shown in Fig. 21 experiences a the phantom-line crossing at $z \sim 0.3$. This confirms the problems of the Taylor approach to account for high-redshift observations.

At this point, some important remarks are in order. As discussed in 228, a cosmological reconstruction scheme for $f(R)$ gravity can be developed in terms of e-folding (or, redshift). In such an approach FLRW cosmology emerges from specific $f(R)$ models. The application of this scheme allows a viable unification of inflation with dark energy bypassing the shortcoming related to the Taylor series adopted for the luminosity distance. The reconstruction scheme may be generalized

in presence of scalar fields.²²⁸ By reconstruction techniques applied to $f(R)$ gravity, the transition from matter dominated epoch to dark energy universe can be also achieved.^{84, 229} This fact is extremely relevant in order to obtain viable cosmological models.

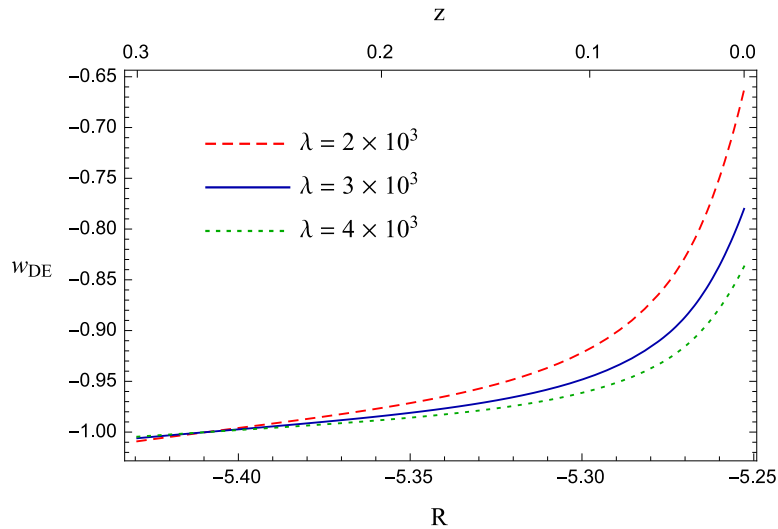


Fig. 21. Dark energy barotropic factor for third-order Taylor approximation with several values of λ .

6.2. The Palatini formalism case

This section is dedicated to the reconstruction of $f(\mathcal{R})$ cosmology within the Palatini formalism. Rational polynomials,²³⁰ such as Padé and ratios of Chebyshev polynomials, can be used to provide accurate information on the thermal properties of the effective cosmic fluid entering the energy-momentum tensor of Palatini's gravity.

In this case, to obtain the cosmological solutions we consider the metric

$$ds^2 = -dt^2 + a(t)^2 \delta_{ij} dx^i dx^j, \quad (229)$$

and the energy-momentum tensor for a perfect fluid of density ρ and pressure p given as

$$T_{\mu\nu} = \text{diag}(-\rho, p, p, p). \quad (230)$$

We thus write down the relation between the Ricci scalar and the Hubble rate in the metric formalism:

$$R = 6(\dot{H} + 2H^2). \quad (231)$$

Converting the time derivative into derivative with respect to the redshift, we get

$$R(z) = -6(1+z)H(z)H'(z) + 12H(z)^2, \quad (232)$$

where the ‘prime’ indicates derivative with respect to z . Inserting Eq. (232) into Eq. (60), we get

$$\mathcal{R}(z) = 12H^2 - 6(1+z)H \left(\frac{HF' + FH'}{F} \right) + 3(1+z)^2 \left[\frac{2HF(HF'' + H'F') - H^2F'^2}{2F^2} \right]. \quad (233)$$

Combining Eqs. (65) and (233) one then obtains

$$F'' - \frac{3F'^2}{2F} + \left(\frac{H'}{H} + \frac{2}{1+z} \right) F' - \frac{2H'}{H(1+z)} F + 3\Omega_{m0}(1+z) \left(\frac{H_0}{H} \right)^2 = 0. \quad (234)$$

Hence, after extracting $H(z)$ from data, we can substitute $z(\mathcal{R})$ found from Eq. (233) into the solution of Eq. (234) to get $F(\mathcal{R})$. Then, the $f(\mathcal{R})$ function can be finally obtained by integrating numerically $F(\mathcal{R})$.

In view of the treatment we proposed in 211, we considered the (2, 2) Padé and the (2, 1) rational Chebyshev approximations of $d_L(z)$ (see Appendix B and Appendix C), from which one can infer the corresponding $H(z)$ by means of Eq. (164). In the following, we fix $\Omega_{m0} = 0.3$ and adopt the best-fit results obtained in 211 for the cosmographic parameters. Thus, in the case of the Padé approximation we used

$$\begin{cases} h_0 = 0.6494_{-0.0202}^{+0.0211}, \\ q_0 = -0.285_{-0.046}^{+0.040}, \\ j_0 = 0.545_{-0.652}^{+0.463}, \\ s_0 = 0.118_{-1.600}^{+0.451}. \end{cases} \quad (235)$$

The initial conditions to solve Eq. (234) are found by requiring that $G_{\text{eff}} = G^{\text{g}}$.^{231, 232} This implies

$$F|_{z=0} = 1, \quad F'|_{z=0} = 0. \quad (236)$$

Fig. 22 shows the behaviour of $F(R)$ using the central values of (235) for the numerical integration of Eq. (234) Then, we integrate this solution by means of the initial condition

$$f_0 = 6(\Omega_{m0} - 1) + \mathcal{R}_0, \quad (237)$$

obtained from evaluating Eq. (65) at the present time. The analytical match to the numerical solution is provided by

$$f(\mathcal{R})_{\text{Padé}} = a + b\mathcal{R}^n, \quad (238)$$

^gRelaxing this condition and allowing for slight departures from G^{227} would ensure to recover the asymptotic Λ CDM behaviour.^{92, 93}

56 *S. Capozziello, R. D'Agostino, O. Luongo*

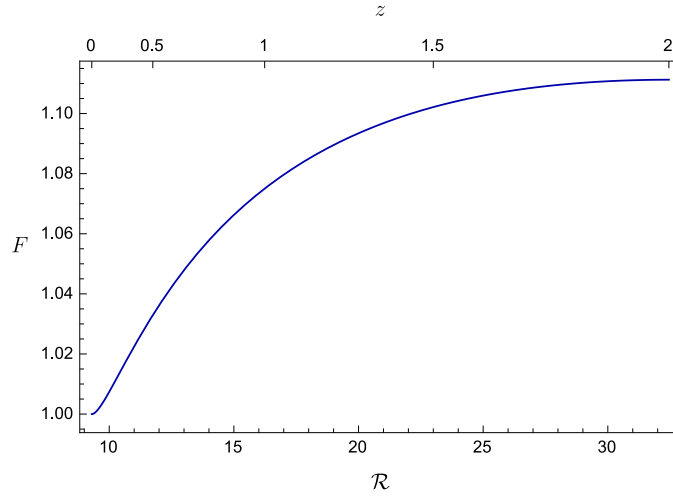


Fig. 22. Padé approximation of $F(\mathcal{R})$ inside $[0, 2]$.

where

$$(a, b, n) = (-1.627, 0.866, 1.074) . \quad (239)$$

We show the Padé reconstruction of $f(\mathcal{R})$ in Fig. 23. Taking into account the 1σ

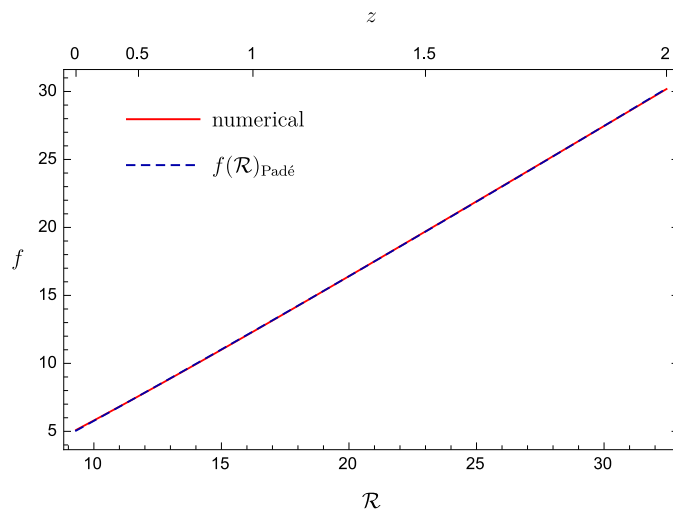


Fig. 23. Padé reconstruction of $f(\mathcal{R})$ with the corresponding most suitable analytical approximation (cf. Eq. (238)).

values of 235, one finds the following bounds:

$$\begin{cases} a \in [-1.627, -1.326] , \\ b \in [0.733, 0.951] , \\ n \in [1.025, 1.123] . \end{cases} \quad (240)$$

In the case of rational Chebyshev approximation we used²¹¹

$$\begin{cases} h = 0.6495^{+0.0189}_{-0.0194} , \\ q_0 = -0.278^{+0.021}_{-0.021} , \\ j_0 = 1.585^{+0.497}_{-0.914} , \\ s_0 = 1.041^{+1.183}_{-1.784} . \end{cases} \quad (241)$$

Following a similar procedure as the one seen above, we show in Fig. 24 $F(\mathcal{R})$ reconstructed using the central values of (241). In this case, the analytical function

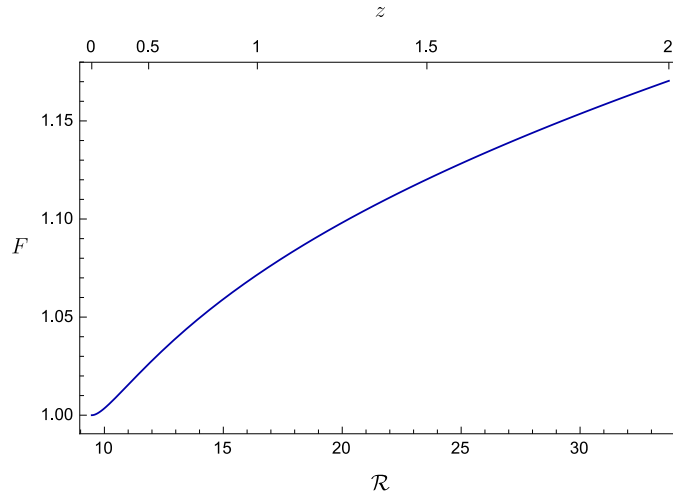


Fig. 24. Chebyshev reconstruction of $F(\mathcal{R})$ inside $z \in [0, 2]$

matching the numerical integration of $F(\mathcal{R})$ is

$$f(\mathcal{R})_{\text{Cheb}} = \alpha + \beta \mathcal{R}^m , \quad (242)$$

where

$$(\alpha, \beta, m) = (-1.332, 0.749, 1.124) . \quad (243)$$

The rational Chebyshev reconstruction of $f(\mathcal{R})$ is finally shown in Fig. 25. If also

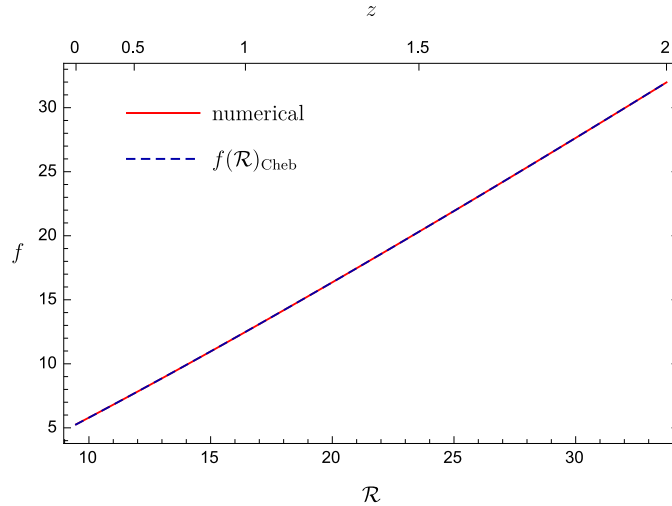


Fig. 25. Comparison between the rational Chebyshev approximation on $f(\mathcal{R})$ with its most suitable analytical approximation (cf. Eq. (242)).

the lower and upper 1σ bounds are considered, we find

$$\begin{cases} \alpha \in [-1.481, -1.332] , \\ \beta \in [0.749, 0.818] , \\ m \in [1.096, 1.124] . \end{cases} \quad (244)$$

An interesting exercise is to compare the obtained results with the cosmological predictions of the standard Λ CDM model. Fig. 26 shows the best $f(\mathcal{R})$ reconstructed through the rational approximations compared to the action of Λ CDM assuming $\{h, \Omega_{m0}\} = \{0.7, 0.3\}$. Moreover, one can calculate the effective equation of state parameter as

$$w_{\text{eff}}(z) = -1 + \frac{2}{3}(1+z)\frac{H'(z)}{H(z)} . \quad (245)$$

In Fig. 27 we show the results for the different models.

7. Model-independent reconstruction of $f(T)$ gravity

In this section, we apply the cosmographic method to reconstruct the $f(T)$ function of teleparallel gravity in a model-independent way. As above, we reconstruct¹⁴⁴ the $f(T)$ function from cosmological observations, without *a priori* assumptions over the model. To do that, we assume the flat FLRW metric and consider the Taylor series expansion of the luminosity distance up to the fourth order (cf. Eq. (163)). Then, making use of Eq. (164) we can write down the Taylor expansion of the

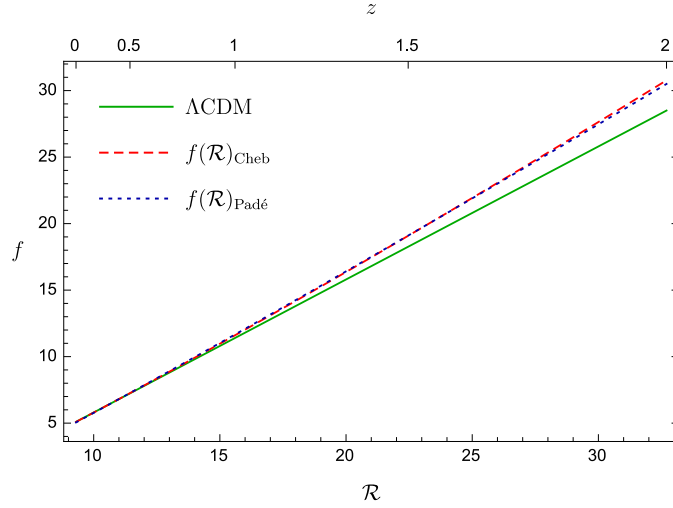


Fig. 26. Confront among $f(\mathcal{R})$ actions of Λ CDM, Padé and rational Chebyshev approximations.

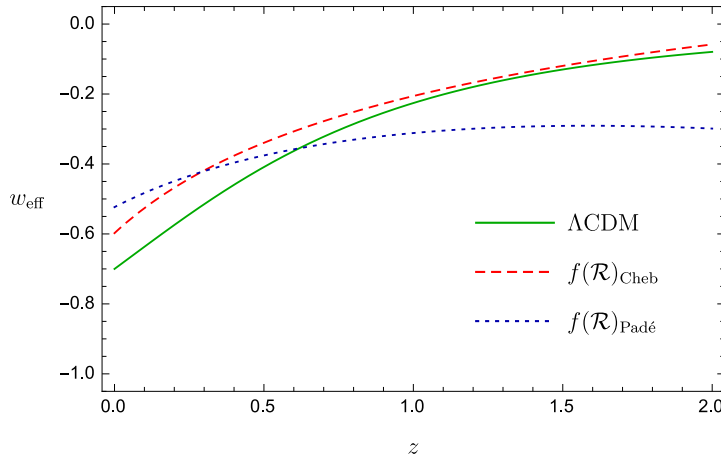


Fig. 27. Comparison between the Λ CDM barotropic factor and the Padé and the rational Chebyshev approximations.

Hubble rate as a function of the cosmographic parameters:

$$H(z) \simeq H_0 \left[1 + z(1 + q_0) + \frac{z^2}{2}(j_0 - q_0^2) + \frac{z^3}{6}(-3q_0^2 - 3q_0^3 + j_0(3 + 4q_0) + s_0) \right]. \quad (246)$$

Hence, once the parameters (H_0, q_0, j_0, s_0) are known, one can infer $f(T(z)) = f(z)$ numerically by combining the modified Friedmann equations (144) and (145). To do that, one need to convert the derivatives with respect to time and the derivatives

60 *S. Capozziello, R. D'Agostino, O. Luongo*

with to respect to the torsion scalar into derivatives with respect to the redshift. For any function $\mathfrak{F}(z)$, we have

$$\frac{d}{dt}\mathfrak{F}(z) = -(1+z)H(z)\frac{d}{dz}\mathfrak{F}(z), \quad (247)$$

$$\frac{\partial}{\partial T}\mathfrak{F}(z) = -12H(z)H'(z)\frac{d}{dz}\mathfrak{F}(z), \quad (248)$$

where we have used Eq. (143) in the latter equation. Thus, if we combine Eqs. (144) and (247) we obtain a differential equation for $f(z)$:

$$\left(\frac{df}{dz}\right)^{-1} \left[H(1+z)\frac{d^2f}{dz^2} + 3f\frac{dH}{dz} \right] = \frac{1}{H} \left(\frac{dH}{dz}\right)^{-1} \left[3\frac{dH}{dz} + (1+z)\frac{d^2H}{dz^2} \right]. \quad (249)$$

One possibility to solve this equation is to assume a particular cosmological model and impose the form of $H(z)$. This, however, would introduce a bias in the analysis and would drive the resulting dynamics towards solutions only slightly deviating from the postulated model. Our idea is, instead, to reconstruct the Hubble expansion as model-independent as possible, and this can be done through cosmography. It is, in fact, possible to perform a model-independent procedure by using the kinematic expansion given in Eq. (246) to solve Eq. (249) as a function of z only. Specifically, two initial conditions are needed to find $f(z)$. The first one is obtained by imposing the equivalence between the effective gravitation constant and the Newton constant:

$$\left.\frac{df}{dz}\right|_{z=0} = 1. \quad (250)$$

The second initial condition comes from Eqs. (143) and (250):

$$f(T(z=0)) = f(z=0) = 6H_0^2(\Omega_{m0} - 2). \quad (251)$$

Therefore, we follow the strategy presented in 233 and recast the cosmographic parameters as

$$q_0 = -1 + \frac{3\tilde{\Omega}_{m0}}{2(1+2\tilde{F}_2)}, \quad (252)$$

$$j_0 = 1 - \frac{9\tilde{\Omega}_{m0}^2(3\tilde{F}_2 + 2\tilde{F}_3)}{2(1+2\tilde{F}_2)^3}, \quad (253)$$

$$s_0 = 1 - \frac{9\tilde{\Omega}_{m0}}{2(1+2\tilde{F}_2)} + \frac{45\tilde{\Omega}_{m0}^2(3\tilde{F}_2 + 2\tilde{F}_3)}{2(1+2\tilde{F}_2)^3} + \frac{27\tilde{\Omega}_{m0}^3(3\tilde{F}_2 + 12\tilde{F}_3 + 4\tilde{F}_4)}{4(1+2\tilde{F}_2)^4} - \frac{81\tilde{\Omega}_{m0}^3(3\tilde{F}_2 + 2\tilde{F}_3)^2}{2(1+2\tilde{F}_2)^5}, \quad (254)$$

where

$$\begin{aligned} \tilde{\Omega}_{m0} &= \frac{\Omega_{m0}}{F_1}, & \tilde{F}_i &= \frac{F_i}{F_1} \quad (i = 2, 3, 4) \\ F_i &= T_0^{i-1} f^{(i)}(T_0) \quad (i = 1, 2, 3, 4). \end{aligned} \quad (255)$$

In order to numerically solve Eq. (249), we adopt the following results:²³³

$$\begin{cases} \Omega_{m0} = 0.289 \\ h = 0.692 \\ q_0 = -0.545 \\ j_0 = 0.776 \\ s_0 = -0.192 \end{cases} \quad (256)$$

where $h \equiv H_0/(100 \text{ km/s/Mpc})$. These values are compatible with the observational bounds obtained through a comparison with different data sets.²³⁴ Then, the first step is to consider a second-order expansion of the Hubble rate, *i.e.* up to the jerk coefficient of the cosmographic series. In Fig. 28 we show the results for different sets of cosmographic parameters. To match the numerical behaviours, we used the

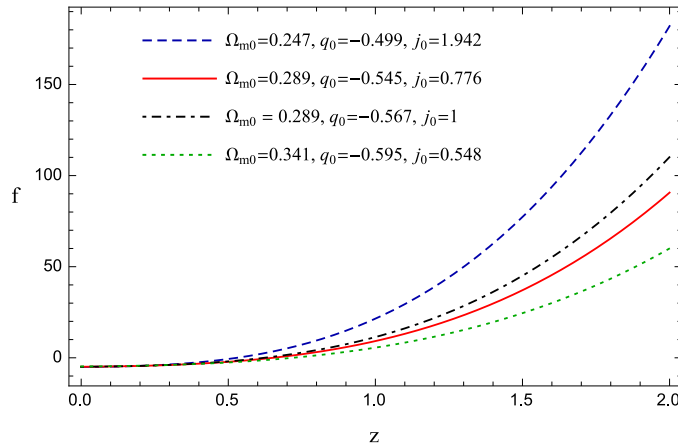


Fig. 28. Reconstructing $f(z)$ for different (Ω_{m0}, q_0, j_0) based on Table 6 outcomes in 233. The solid red, the dashed blue and the dotted green lines correspond, respectively, to the best-fit values, the upper 2σ bounds and the lower 2σ constraints imposed over $(\tilde{\Omega}_{m0}, \tilde{F}_2, \tilde{F}_3)$. The Λ CDM paradigm is due to dot-dashed black line and $h = 0.692$.

62 *S. Capozziello, R. D'Agostino, O. Luongo*

following test-functions^h:

$$f_1(z) = \mathcal{A} + z(\mathcal{B} + \mathcal{C}z) \ln(1 + z^2) \quad (257a)$$

$$f_2(z) = \mathcal{A} + \mathcal{B}z^2 e^{\mathcal{C}z} \quad (257b)$$

$$f_3(z) = \mathcal{A}z^2 + \mathcal{B}z \sin(1 + \mathcal{C}z^2) \quad (257c)$$

$$f_4(z) = \mathcal{A} + \mathcal{B}z^2 \cos(1 + \mathcal{C}z) \quad (257d)$$

$$f_5(z) = \mathcal{A} + \mathcal{B} \sinh(1 + \mathcal{C}z) \quad (257e)$$

$$f_6(z) = \mathcal{A} + \mathcal{B}z^3 \tanh(\mathcal{C}z^2) \quad (257f)$$

where the values of the free coefficients \mathcal{A} , \mathcal{B} and \mathcal{C} are found through a comparison with the numerical curves. To obtain information on how well the test-functions approximate the numerical $f(z)$, we performed the \mathcal{R}^2 -test.²³⁵ If f_i^{obs} are the numerical values of $f(z_i)$, and f_i are the correspondent analytical values, one can define

$$\mathcal{R}^2 \equiv 1 - \frac{\sum_{i=1}^n (f_i^{obs} - f_i)^2}{\sum_{i=1}^n (f_i^{obs} - \bar{f})^2}, \quad (258)$$

where

$$\bar{f} = \frac{1}{n} \sum_{i=1}^n f_i^{obs}, \quad (259)$$

being n the number of points. The ideal case $\mathcal{R}^2 = 1$ occurs when the test-function and $f(z)$ agree exactly. In the case of the best-fit red curve of Fig. 28, the \mathcal{R}^2 -test indicates the function (257b) as the most suitable choice (cf. Table 5):

$$f(z) = \mathcal{A} + \mathcal{B}z^2 e^{\mathcal{C}z}, \quad (260)$$

where

$$(\mathcal{A}, \mathcal{B}, \mathcal{C}) = (-5.024, 8.651, 0.512). \quad (261)$$

We show in Fig. 29 the comparison between the numerical solution of $f(z)$ and its best analytical approximation given by 260. From Table 5 we note that also the functions 257a and 257f represents very good approximations of $f(z)$: their \mathcal{R}^2 values are only 0.024% and 0.038% far from the best one, respectively.

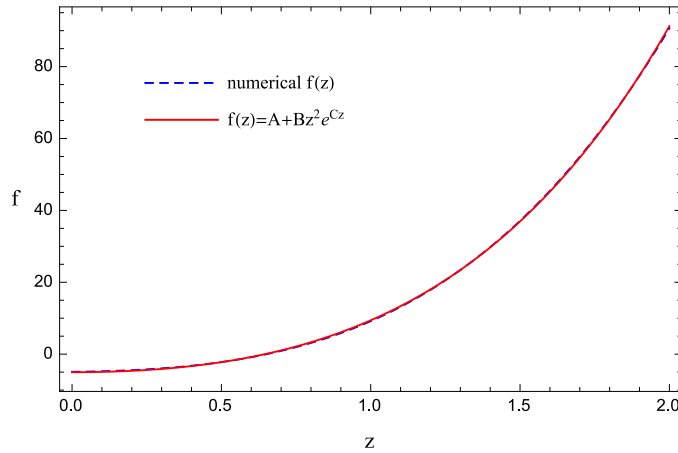
The second step of the analysis considers the expansion of $H(z)$ up to the third order. We thus show in Fig. 30 the behaviour of $f(z)$ for different values of s_0 within the interval $[-1, 0]$, while we fix the other cosmographic parameters to their best-fit results. As in the previous case, the best approximation of $f(z)$ is given by the function 260 with the following values of the free parameters:

$$(\mathcal{A}, \mathcal{B}, \mathcal{C}) = (-5.022, 8.577, 0.532). \quad (262)$$

^hThe forms of the test-functions have been chosen *a posteriori* to match the shapes of the curves gotten from the numerical analysis.

Table 5. Outcomes of the \mathcal{R}^2 -test on the test-functions Eqs. (257a)–(257f) for the best-fit curve of Fig. 28 .

Test-function	(A, B, C)	\mathcal{R}^2
$f_1(z)$	(−3.897, 10.88, 7.185)	0.99974
$f_2(z)$	(−5.024, 8.651, 0.512)	0.99997
$f_3(z)$	(15.73, −9.286, 1.112)	0.99102
$f_4(z)$	(−3.152, −21.52, 1.114)	0.99630
$f_5(z)$	(−10.93, 3.173, 1.593)	0.99909
$f_6(z)$	(−3.463, 11.89, 4.143)	0.99959


 Fig. 29. Confront between numerical and analytical solutions on $f(z)$, with best fit parameters $(\Omega_{m0}, h, q_0, j_0)$ as in 233, while the coefficients (A, B, C) are given in Eq. (261).

We finally describe the strategy to reconstruct the function $f(T)$. We plug the expansion of $H(z)$ up to the snap parameter into Eq. (143), which can be inverted to find $z(T)$. Therefore, inserting the obtained result back into Eq. (260) provides us with the function $f(T)$. In this procedure one takes into account the error propagation due to the uncertainties in cosmographic parameters through redefining $f(z)$ by a rescaling factor α :

$$\alpha f(z) \longrightarrow f(z) . \quad (263)$$

The value of the constant α will be determined from cosmological constraints. One

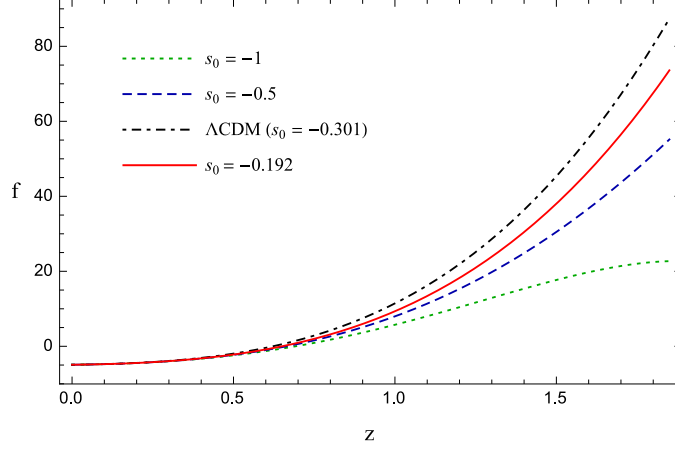


Fig. 30. Different $f(z)$ shapes with distinct snap parameters and $(\Omega_{m0}, h, q_0, j_0)$ fixed by best-fit results as in 233. The solid red line is due to the best-fit value of s_0 , while the dot-dashed black line to the Λ CDM model, assuming that $\Omega_{m0} = 0.289$.

thus gets

$$z(T) = \frac{1}{2\mathcal{Q}} \left[2(q_0^2 - j_0) + \left(\frac{4\mathcal{M}(T)}{H_0^3} \right)^{1/3} + \left(\frac{16H_0^3}{\mathcal{M}(T)} \right)^{1/3} \left(j_0^2 + q_0^2(6 + 12q_0 + 7q_0^2) - 2j_0(3 + 7q_0 + 5q_0^2) - 2s_0(1 + q_0) \right) \right], \quad (264)$$

and

$$f(T) = \alpha\mathcal{A} + \frac{\alpha\mathcal{B}}{4\mathcal{Q}^2} \left[2(q_0^2 - j_0) + \left(\frac{4\mathcal{M}(T)}{H_0^3} \right)^{1/3} + \left(\frac{16H_0^3}{\mathcal{M}(T)} \right)^{1/3} \left(j_0^2 + q_0^2(6 + 12q_0 + 7q_0^2) - 2j_0(3 + 7q_0 + 5q_0^2) - 2s_0(1 + q_0) \right) \right]^2 \exp \left\{ \frac{\mathcal{C}}{2\mathcal{Q}} \left[2(q_0^2 - j_0) + \left(\frac{4\mathcal{M}(T)}{H_0^3} \right)^{1/3} + \left(\frac{16H_0^3}{\mathcal{M}(T)} \right)^{1/3} \left(j_0^2 + q_0^2(6 + 12q_0 + 7q_0^2) - 2j_0(3 + 7q_0 + 5q_0^2) - 2s_0(1 + q_0) \right) \right] \right\}, \quad (265)$$

where

$$\mathcal{M}(T) \equiv H_0^2 \sqrt{2\mathcal{P}(T)}\mathcal{Q} - 2H_0^3\mathcal{N} + \sqrt{-6T}H_0^2\mathcal{Q}^2, \quad (266)$$

$$\begin{aligned}
 \mathcal{P}(T) \equiv & 2H_0^2 \left[6j_0^3 - 6q_0^2(2 + q_0(4 + q_0))^2 + 3j_0^2(8 + q_0(28 + 17q_0)) + 4 \left(2 + q_0(6 - q_0(3 \right. \right. \\
 & \left. \left. + 7q_0)) \right) s_0 + 9s_0^2 + 2j_0 \left(6(2 + 3s_0) + q_0(52 + q_0(60 - q_0(6 + 17q_0)) + 27s_0) \right) \right] \\
 & - 2\sqrt{-6T}H_0 \left(j_0^3 + 3j_0^2(1 + q_0)(6 + 11q_0) - 3j_0q_0^2(12 + q_0(29 + 16q_0)) + q_0^4(18 \right. \\
 & \left. + q_0(36 + 17q_0)) - 15q_0^2(1 + q_0)s_0 + 3j_0(5 + 7q_0)s_0 + 3s_0^2 \right) - 3T \left(-3q_0^2(1 + q_0) \right. \\
 & \left. + j_0(3 + 4q_0) + s_0 \right)^2, \tag{267}
 \end{aligned}$$

$$\mathcal{Q} \equiv -3q_0^2(1 + q_0) + j_0(3 + 4q_0) + s_0, \tag{268}$$

$$\begin{aligned}
 \mathcal{N} \equiv & j_0^3 + 3j_0^2(1 + q_0)(6 + 11q_0) - 3j_0q_0^2(12 + q_0(29 + 16q_0)) + q_0^4(18 + q_0(36 + 17q_0)) \\
 & - 15q_0^2(1 + q_0)s_0 + 3j_0(5 + 7q_0)s_0 + 3s_0^2. \tag{269}
 \end{aligned}$$

The obtained $f(T)$ can be used to study the torsional density and pressure, and compare the above results with the cosmological findings in the literature.²³⁶ From Eqs. (146) and (147) we get

$$\rho_T = -\frac{1}{2} \left[T + \alpha \left(\mathcal{A} + \frac{\mathcal{B} \xi(T)}{4\mathcal{Q}^2} e^{\frac{c\xi(T)}{2\mathcal{Q}}} \right) \right] + \frac{2^{1/3} \alpha \mathcal{B} T G(T)}{24H_0^3 \mathcal{Q}^3 \mathcal{M}(T)^2} X(T) Y(T) \mathcal{M}'(T) e^{\frac{c\xi(T)}{2\mathcal{Q}}}, \tag{270}$$

$$\begin{aligned}
 p_T = & \left[e^{-\frac{c\xi(T)}{2\mathcal{Q}}} H_0^4 \mathcal{Q}^4 \mathcal{M}(T)^{10/3} \left(72\mathcal{A} + \frac{18\mathcal{B}\xi(T)^2}{\mathcal{Q}^2} e^{\frac{c\xi(T)}{2\mathcal{Q}}} - \frac{3 \times 2^{1/3} \mathcal{B} T G(T) X(T) Y(T) \mathcal{M}'(T)}{H_0^3 \mathcal{Q}^3 \mathcal{M}(T)^2} \right) \right. \\
 & \times e^{\frac{c\xi(T)}{2\mathcal{Q}}} + \frac{2^{1/3} \mathcal{B} T^2}{H_0^3 \mathcal{Q}^4 \mathcal{M}(T)^{10/3}} \times e^{\frac{c\xi(T)}{2\mathcal{Q}}} \left(2^{1/3} \mathcal{C} G(T)^2 X(T) Y(T) \mathcal{M}'(T)^2 + 2^{7/3} H_0 \mathcal{Q} \right. \\
 & \times X(T) Y(T) \mathcal{M}(T) \mathcal{M}'(T)^2 + 2H_0 \mathcal{Q} G(T) \mathcal{M}(T)^{1/3} \times \left(-6X(T) Y(T) \mathcal{M}'(T)^2 \right. \\
 & \left. \left. + 2^{5/3} (\mathcal{C} X(T) + Y(T)) \mathcal{M}(T)^{2/3} \mathcal{M}'(T)^2 + 2H_0 ((2\mathcal{Q} + \mathcal{C}(q_0^2 - j_0)) X(T) + (q_0^2 - j_0) \right. \right. \\
 & \left. \left. \times Y(T)) \mathcal{M}(T)^{1/3} \mathcal{M}'(T)^2 + 3X(T) Y(T) \mathcal{M}(T) \mathcal{M}''(T) \right) \right) \left. \right] \times \left[2^{4/3} \mathcal{B} \left(2^{1/3} \mathcal{C} G(T)^2 \right. \right. \\
 & \times X(T) Y(T) \mathcal{M}'(T)^2 + 2^{7/3} H_0 \mathcal{Q} T X(T) Y(T) \mathcal{M}(T) \mathcal{M}'(T)^2 + H_0 \mathcal{Q} G(T) \mathcal{M}(T)^{1/3} \\
 & \times \left(-12T X(T) Y(T) \mathcal{M}'(T)^2 + 2^{7/3} (\mathcal{C} X(T) + Y(T)) T \mathcal{M}(T)^{2/3} \mathcal{M}'(T)^2 + 4H_0 \right. \\
 & \times ((2\mathcal{Q} + \mathcal{C}(q_0^2 - j_0)) X(T) + (q_0^2 - j_0) Y(T)) T \mathcal{M}(T)^{1/3} \mathcal{M}'(T)^2 + 3X(T) Y(T) \mathcal{M}(T) \\
 & \left. \left. \times (\mathcal{M}'(T) + 2T \mathcal{M}''(T)) \right) \right], \tag{271}
 \end{aligned}$$

66 *S. Capozziello, R. D'Agostino, O. Luongo*

where

$$\xi(T) \equiv 2(q_0^2 - j_0) + \left(\frac{4\mathcal{M}(T)}{H_0^3}\right)^{1/3} + \left(\frac{16H_0^3}{\mathcal{M}(T)}\right)^{1/3}, \quad (272)$$

$$X(T) \equiv 2^{4/3}H_0^2\mu + 2H_0(q_0^2 - j_0)\mathcal{M}(T)^{1/3} + 2^{2/3}\mathcal{M}(T)^{2/3}, \quad (273)$$

$$Y(T) \equiv 2^{4/3}\mathcal{C}H_0^2\mu + 2H_0(2\mathcal{Q} + \mathcal{C}(q_0^2 - j_0))\mathcal{M}(T)^{1/3} + 2^{2/3}\mathcal{C}\mathcal{M}(T)^{2/3}, \quad (274)$$

$$G(T) \equiv -2H_0^2\mu + 2^{1/3}\mathcal{M}(T)^{2/3}, \quad (275)$$

$$\mu \equiv j_0^2 + q_0^2(6 + 12q_0 + 7q_0^2) - 2j_0(3 + 7q_0 + 5q_0^2) - 2s_0(1 + q_0), \quad (276)$$

and

$$\mathcal{M}'(T) \equiv \frac{\partial \mathcal{M}}{\partial T} = \frac{1}{\sqrt{2}} \left[\frac{\sqrt{3}H_0^2\mathcal{Q}^2T}{(-T)^{3/2}} + \frac{H_0^2\mathcal{Q}}{\sqrt{\mathcal{P}(T)}}\mathcal{P}'(T) \right], \quad (277)$$

$$\mathcal{M}''(T) \equiv \frac{\partial^2 \mathcal{M}}{\partial T^2} = -\frac{\sqrt{-3T}H_0^2\mathcal{Q}^2\mathcal{P}(T)^2 + H_0^2\mathcal{Q}T^2\mathcal{P}(T)^{1/2}\mathcal{P}'(T)^2 - 2H_0^2\mathcal{Q}T^2\mathcal{P}(T)^{3/2}\mathcal{P}''(T)}{2\sqrt{2}T^2\mathcal{P}(T)^2} \quad (278)$$

$$\begin{aligned} \mathcal{P}'(T) \equiv \frac{\partial \mathcal{P}}{\partial T} &= -3(-3q_0^2(1 + q_0) + j_0(3 + 4q_0) + s_0)^2 + \frac{\sqrt{6}H_0}{\sqrt{-T}} [j_0^3 + 3j_0^2(1 + q_0)(6 + 11q_0) \\ &\quad - 3j_0q_0^2(12 + q_0(29 + 16q_0)) + q_0^4(18 + q_0(36 + 17q_0)) - 15q_0^2(1 + q_0)s_0 \\ &\quad + 3j_0(5 + 7q_0)s_0 + 3s_0^2], \end{aligned} \quad (279)$$

$$\begin{aligned} \mathcal{P}''(T) \equiv \frac{\partial^2 \mathcal{P}}{\partial T^2} &= \sqrt{\frac{3}{2}} \frac{H_0}{(-T)^{3/2}} [j_0^3 + 3j_0^2(1 + q_0)(6 + 11q_0) - 3j_0q_0^2(12 + q_0(29 + 16q_0)) \\ &\quad + q_0^4(18 + q_0(36 + 17q_0)) - 15q_0^2(1 + q_0)s_0 + 3j_0(5 + 7q_0)s_0 + 3s_0^2]. \end{aligned} \quad (280)$$

We note that p_T does not actually depend on the rescaling factor α . To constrain the value of this coefficient, we impose the condition $w_{DE} < -1/3$ implying present accelerated expansion. We thus find

$$0 < \alpha \lesssim 0.936. \quad (281)$$

In Fig. 31 we show the reconstructed $f(T)$ assuming an indicative $\alpha = 0.5$. Figs. 32 and 33 show the behaviours of the ρ_T and p_T , while the effective dark energy equation of state parameter for different values of α is displayed in Fig. 34.

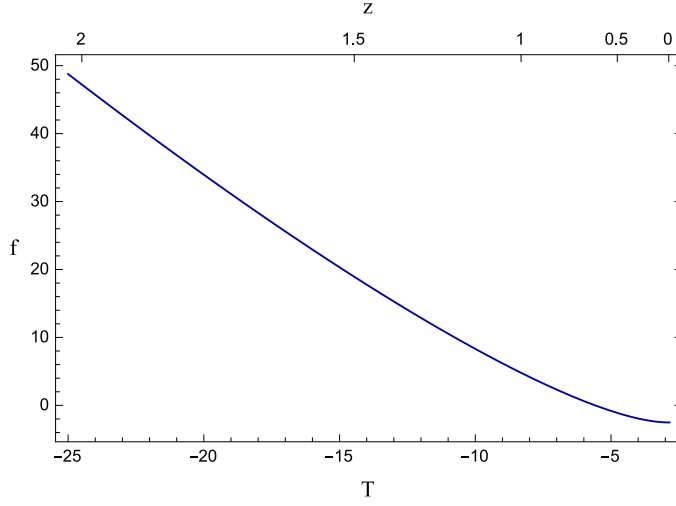


Fig. 31. Numerical shape of $f(T)$ imposed from best-fit values and $\alpha = 0.5$ inside $0 \leq z \leq 2$.

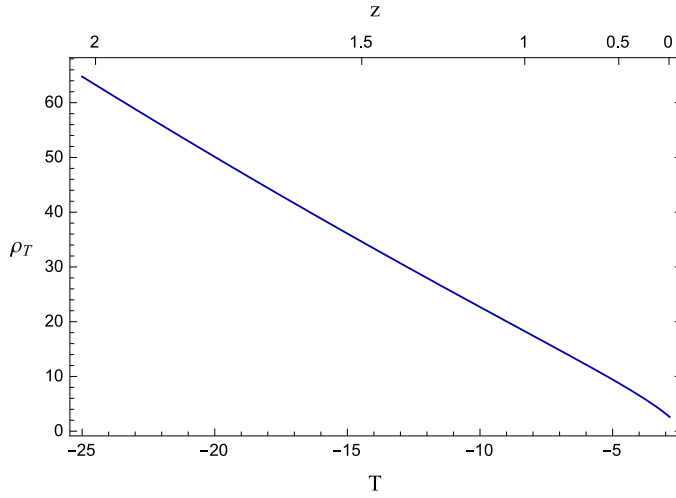


Fig. 32. Torsion density with mean values of cosmographic parameters got from the experimental analysis with $\alpha = 0.5$ inside $0 \leq z \leq 2$.

7.1. Comparison with previous $f(T)$ models

We here compare the $f(T)$ model we have obtained with the cosmographic reconstruction found in 146. In fact, testing the consistency of the two models in the valid redshift interval provides a measure of the goodness of the present approach.

68 *S. Capozziello, R. D'Agostino, O. Luongo*

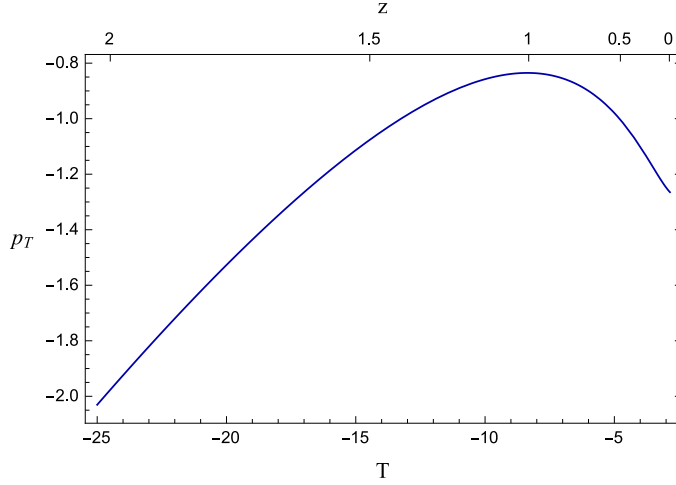


Fig. 33. P_T with the best-fit values of the cosmographic parameters inside $0 \leq z \leq 2$.

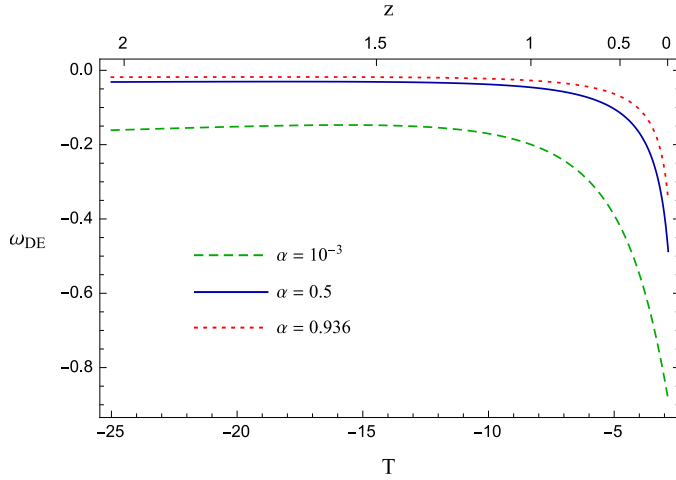


Fig. 34. Dark energy equation of state inside $0 \leq z \leq 2$, with different values of α (cf. Eq. (281)).

To this end, we report the model proposed in 146:

$$f(T)_{\text{ABCL}} = c_0 T + (T - T_0) \left[c_1 + c_3 \cosh(T - T_0) + (T - T_0) \left(c_2 + c_4 (T - T_0) \sinh(T - T_0) \right) \right] \quad (282)$$

where $T_0 = -6H_0^2$. The above model is made of different functions which dominate over each other in different redshift domains. The free coefficients c_i ($i = 0, \dots, 4$) have been determined through imposing the conditions $f(T_0) = 6H_0^2(\Omega_{m0} - 2)$ and $f'(T_0) = 1$ as for the initial settings. In particular, an experimental analysis

performed on different data sets provided

$$c_0 = 2 - \Omega_{m0} , \quad (283a)$$

$$c_1 = \Omega_{m0} - 1 , \quad (283b)$$

$$c_2 = -3 \times 10^{-6} , \quad (283c)$$

$$c_3 = \frac{1}{15} \times 10^{-9} , \quad (283d)$$

$$c_4 = \frac{3}{4} \times 10^{-14} . \quad (283e)$$

along with

$$\Omega_{m0} = 0.364 , \quad H_0 = 71.47 \text{ km/s/Mpc} . \quad (284)$$

Let us compare Eq. (282) to the above model without caring about the sign of T . Fig. 35 clearly shows the compatibility between the two models for $z \leq 1$. The 10% – 15% level discrepancies are due to bigger uncertainties in the estimate of the cosmographic series present in the previous model. Both curves indicate slight departures from the standard model, which become more evident as the redshift increases. We can then conclude that the limits of the model (282) are overcome by adopting the numerical analysis performed in here.

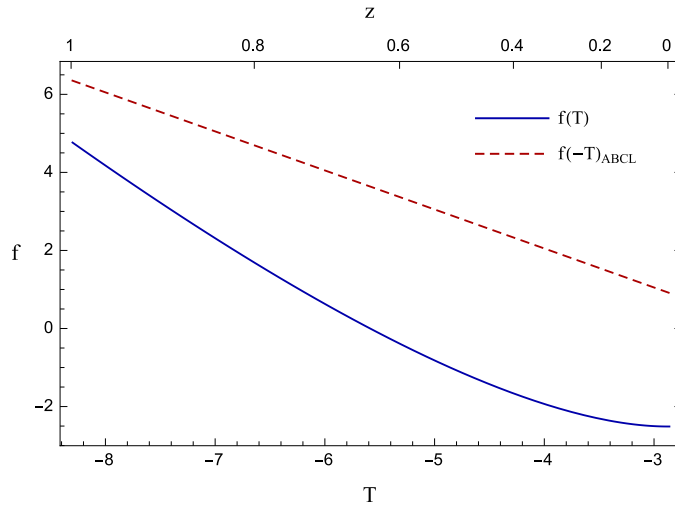


Fig. 35. Comparison between $f(T)$ functions. The first got for $\alpha = 0.5$ (solid blue line), whereas the second by 146 (dashed red line) inside $0 \leq z \leq 1$.

8. Final outlook

In this review paper, we discussed the cosmographic method and its applications to cosmological models derived from extended or modified theories of gravity. The

philosophy is going beyond Einstein's gravity to cure the shortcomings of the standard cosmological model.³ Specifically, the observational evidence that almost the entire energy density of the cosmic fluid is in the form of dark components might be the sign that standard GR breaks down at IR cosmological scales. One way to address this issue is to modify the Einstein-Hilbert action and introduce higher-order curvature invariants and minimally or non-minimally coupled terms between scalar fields and geometry. The ETG scenarios represent a semi-classical approach where GR is recovered in the low-energy limit.

With this recipe in mind, we focused on $f(R)$ gravity in the metric and Palatini formalisms. We showed the equivalence between these paradigms and the scalar-tensor theories, analyzing the role of conformal transformations in the Einstein and Jordan frames. We thus described the dynamics of the $f(R)$ cosmological models and discussed the observational viability of such theories.

Then, we discuss an alternative description of the gravitational interaction in terms of torsion. Assuming torsion instead of curvature as dynamical field leads to the equivalent teleparallel formulation of GR (TEGR). We show that the features of a late-time accelerating universe can be reproduced by modifying the gravity action to include a generic function of the torsion scalar. Moreover, scalar field non-minimally coupled to torsion can be considered.

Furthermore, it is possible to develop model-independent techniques to describe the expansion of the universe without postulating the dark terms a priori. We showed how cosmography can be used to break the degeneracy among cosmological models. We thus proposed the use of rational polynomials to overcome the convergence issues and reduce the error propagations typical of the standard cosmographic approach. The latest cosmic data can be used to place bounds on the cosmographic series through different Monte Carlo integrations. This new cosmographic method can be adopted to accurately describe the late-time history of the universe.

These cosmographic techniques can be adopted to derive cosmological consistent models of $f(R)$ and $f(T)$ gravity. The approach allows to reconstruct the extended/modified gravity actions in different formalisms by assuming only the validity of the cosmological principle. Hence, we discussed the dynamical features of the reconstructed models and their consequences at the level of background cosmology. The results indicated slight departures from GR (that is the Λ CDM model) and dark energy terms evolving in time.

To conclude, the current state of the art suggests that it is not yet possible to falsify the Λ CDM model by robust statements adopting only cosmography. The degeneracy among the dark energy models is still unavoidable and the need of more precise measurements (eventually at very high redshift) from forthcoming observations remains crucial. As reported in 200, a redshift of the order $z \sim 1.5$ is crucial to discriminate among concurring models while the issue of determining the physical frame, i.e. the Einstein or the Jordan frame, may be addressed in cosmography.²⁴⁹ Finally, the models have also to be confronted with perturbations

to be consistent with observations of large scale structure. These topics will be the arguments of future works.

Acknowledgments

This work is based upon the COST action CA15117 (CANTATA), supported by COST (European Cooperation in Science and Technology). S.C. is supported by Istituto Nazionale di Fisica Nucleare (INFN), *iniziative specifiche* QGSKY and MOONLIGHT2. R.D. thanks Anna Silvia Baldi for useful discussions. O.L. acknowledges the financial support by MES of the RK, Program Center of Excellence for Fundamental and Applied Physics IRN: BR05236454, and by the MES Program IRN: BR05236494.

Appendix A. Experimental data compilations

Table 6. $H(z)$ measurements got from differential age treatment, in which $H(z)$ is given by km/s/Mpc.

z	$H \pm \sigma_H$	Ref.
0.0708	69.00 ± 19.68	237
0.09	69.0 ± 12.0	215
0.12	68.6 ± 26.2	237
0.17	83.0 ± 8.0	238
0.179	75.0 ± 4.0	239
0.199	75.0 ± 5.0	239
0.20	72.9 ± 29.6	237
0.27	77.0 ± 14.0	238
0.28	88.8 ± 36.6	237
0.35	82.1 ± 4.85	240
0.352	83.0 ± 14.0	241
0.3802	83.0 ± 13.5	241
0.4	95.0 ± 17.0	238
0.4004	77.0 ± 10.2	241
0.4247	87.1 ± 11.2	241
0.4497	92.8 ± 12.9	241
0.4783	80.9 ± 9.0	241
0.48	97.0 ± 62.0	242
0.593	104.0 ± 13.0	239
0.68	92.0 ± 8.0	239
0.781	105.0 ± 12.0	239
0.875	125.0 ± 17.0	239
0.88	90.0 ± 40.0	242
0.9	117.0 ± 23.0	238
1.037	154.0 ± 20.0	239
1.3	168.0 ± 17.0	238
1.363	160.0 ± 33.6	243
1.43	177.0 ± 18.0	238
1.53	140.0 ± 14.0	238
1.75	202.0 ± 40.0	238
1.965	186.5 ± 50.4	243

Table 7. Baryon acoustic oscillations measurements.

z	$d_V \pm \sigma_{d_V}$	Ref.
0.106	0.336 ± 0.015	244
0.15	0.2239 ± 0.0084	245
0.32	0.1181 ± 0.0023	246
0.57	0.0726 ± 0.0007	246
2.34	0.0320 ± 0.0016	247
2.36	0.0329 ± 0.0012	248

Appendix B. Padé approximations of the luminosity distance

$$P_{1,1}(z) = \frac{1}{H_0} \left[\frac{2z}{2 + (-1 + q_0)z} \right]. \quad (\text{B.1})$$

$$P_{1,2}(z) = \frac{1}{H_0} \left[\frac{12z}{12 + 6(-1 + q_0)z + (5 + 2j_0 - q_0(8 + 3q_0))z^2} \right]. \quad (\text{B.2})$$

$$P_{2,1}(z) = \frac{1}{H_0} \left[\frac{z(6(-1 + q_0) + (-5 - 2j_0 + q_0(8 + 3q_0))z)}{-2(3 + z + j_0z) + 2q_0(3 + z + 3q_0z)} \right]. \quad (\text{B.3})$$

$$P_{1,3}(z) = \frac{24z}{H_0} / (24 + 12(-1 + q_0)z + 2(5 + 2j_0 - q_0(8 + 3q_0))z^2 - (9 + j_0(9 + 6q_0) - q_0(19 + 2q_0(7 + 3q_0)) + s_0)z^3). \quad (\text{B.4})$$

$$P_{2,2}(z) = \frac{1}{H_0} (6z(10 + 9z - 6q_0^3z + s_0z - 2q_0^2(3 + 7z) - q_0(16 + 19z) + j_0(4 + (9 + 6q_0)z)) / (60 + 24z + 6s_0z - 2z^2 + 4j_0^2z^2 - 9q_0^4z^2 - 3s_0z^2 + 6q_0^3z(-9 + 4z) + q_0^2(-36 - 114z + 19z^2) + j_0(24 + 6(7 + 8q_0)z + (-7 - 23q_0 + 6q_0^2)z^2) + q_0(-96 - 36z + (4 + 3s_0)z^2)). \quad (\text{B.5})$$

$$P_{3,1}(z) = \frac{1}{H_0} (z(24(1 + j_0 - q_0(1 + 3q_0)) + 6(4 + j_0(7 + 8q_0) - q_0(6 + q_0(19 + 9q_0)) + s_0)z + (2 - 4j_0^2 + j_0(7 + (23 - 6q_0)q_0) + q_0(-4 + q_0(-19 + 3q_0(-8 + 3q_0)) - 3s_0) + 3s_0)z^2) / (24(1 + j_0 - q_0(1 + 3q_0)) + 6(2 + 5j_0(1 + 2q_0) - q_0(2 + 15q_0(1 + q_0)) + s_0)z). \quad (\text{B.6})$$

Appendix C. Rational Chebyshev approximations of the luminosity distance

$$R_{1,1}(z) = -\frac{1}{H_0} \left[(3(2 - 2q_0 - 15q_0^2 - 15q_0^3 + 5j_0(1 + 2q_0) + s_0) + (1/(7 - j_0 + q_0 + 3q_0^2))(-72(7 - j_0 + q_0 + 3q_0^2)^2 + 3(18 + 5j_0(1 + 2q_0) - 3q_0(6 + 5q_0(1 + q_0)) + s_0)(14 + 5j_0(1 + 2q_0) - q_0(14 + 15q_0(1 + q_0)) + s_0) + 2(14 + 5j_0(1 + 2q_0) - q_0(14 + 15q_0(1 + q_0)) + s_0)^2)z) / (576(1 - ((14 + 5j_0(1 + 2q_0) - q_0(14 + 15q_0(1 + q_0)) + s_0)z)/(3(7 - j_0 + q_0 + 3q_0^2)))) \right]. \quad (\text{C.1})$$

74 *S. Capozziello, R. D'Agostino, O. Luongo*

$$\begin{aligned}
 R_{1,2}(z) = & \frac{1}{H_0} (-(44184 + 5j_0^3(1 + 2q_0)(1 + 10q_0)(9 + 10q_0) - 3q_0(32024 + q_0(26948 + q_0(4780 \\
 & + q_0(-15938 + q_0(2134 + 15q_0(565 + 3q_0(249 + 25q_0(3 + q_0))))))))) + 7148s_0 + q_0(-5272 \\
 & + q_0(-16 + 3q_0(-32 + 3q_0(439 + 75q_0(2 + q_0))))s_0 - 3(-38 + q_0(38 + 15q_0(1 + q_0)))s_0^2 \\
 & + s_0^3 + j_0(49884 + q_0(34880 + q_0(-41632 + q_0(-9472 + 135q_0(125 + q_0(332 + 25q_0(5 \\
 & + 2q_0)))))) + 916s_0 - 2q_0(-586 + 3q_0(439 + 75q_0(3 + 2q_0)))s_0 + 15(1 + 2q_0)s_0^2 + j_0^2(-222 \\
 & + 59s_0 + q_0(8422 - 5q_0(17 + 15q_0(211 + 60q_0(2 + q_0)) - 60s_0) + 300s_0))/(8(-1 - j_0 + q_0 \\
 & + 3q_0^2)(7 - j_0 + q_0 + 3q_0^2) + 24(7 - j_0 + q_0 + 3q_0^2)^2 - (18 + 5j_0(1 + 2q_0) - 3q_0(6 + 5q_0(1 \\
 & + q_0)) + s_0)(14 + 5j_0(1 + 2q_0) - q_0(14 + 15q_0(1 + q_0))s_0))) + 4(271 - 17j_0 + 17q_0 + 51q_0^2 \\
 & + (4(39106 - 56j_0^3 + j_0^2(1665 + q_0(193 + 454q_0)) + 5s_0 - j_0(14469 - 5s_0 + q_0(3492 + q_0(10127 \\
 & + q_0(1033 + 1287q_0)) + 5s_0)) + q_0(14282 - 10s_0 + q_0(45365 - 10s_0 + q_0(10501 + 3q_0(5082 \\
 & + q_0(479 + 429q_0)) + 15s_0)))))/(-868 + j_0^2(-7 + 100q_0(1 + q_0)) + q_0(-888 + q_0(-1412 \\
 & + 3q_0(-64 + q_0(139 + 75q_0(2 + q_0)))))) + 32s_0 - 2q_0(16 + 15q_0(1 + q_0))s_0 + s_0^2 + j_0(544 \\
 & + 10s_0 - 2q_0(q_0(139 + 75q_0(3 + 2q_0)) - 2(56 + 5s_0))))z) / (576(1 - (4(214 - 5j_0^2(1 + 2q_0) \\
 & + j_0(65 + 5q_0(33 + q_0(8 + 9q_0)) - s_0) + 15s_0 + q_0(-204 - 5q_0(41 + 3q_0(18 + q_0(4 + 3q_0))) \\
 & + s_0 + 3q_0s_0))z) / (8(-1 - j_0 + q_0 + 3q_0^2)(7 - j_0 + q_0 + 3q_0^2) + 24(7 - j_0 + q_0 + 3q_0^2)^2 - (18 \\
 & + 5j_0(1 + 2q_0) - 3q_0(6 + 5q_0(1 + q_0)) + s_0)(14 + 5j_0(1 + 2q_0) - q_0(14 + 15q_0(1 + q_0)) + s_0)) \\
 & - (4(12(-1 - j_0 + q_0 + 3q_0^2)(7 - j_0 + q_0 + 3q_0^2) + 4(1 + j_0 - q_0(1 + 3q_0))^2 - (14 + 5j_0(1 \\
 & + 2q_0) - q_0(14 + 15q_0(1 + q_0)) + s_0)^2)(-1 + 2z^2)) / (3(8(-1 - j_0 + q_0 + 3q_0^2)(7 - j_0 + q_0 \\
 & + 3q_0^2) + 24(7 - j_0 + q_0 + 3q_0^2)^2 - (18 + 5j_0(1 + 2q_0) - 3q_0(6 + 5q_0(1 + q_0)) + s_0)(14 \\
 & + 5j_0(1 + 2q_0) - q_0(14 + 15q_0(1 + q_0)) + s_0)))) . \tag{C.2}
 \end{aligned}$$

$$\begin{aligned}
 R_{2,1}(z) = & \frac{1}{H_0} (-(3(16(-1 - j_0 + q_0 + 3q_0^2)(7 - j_0 + q_0 + 3q_0^2) - (18 + 5j_0(1 + 2q_0) - 3q_0(6 \\
 & + 5q_0(1 + q_0)) + s_0)(14 + 5j_0(1 + 2q_0) - q_0(14 + 15q_0(1 + q_0)) + s_0)) / (14 + 5j_0(1 + 2q_0) \\
 & - q_0(14 + 15q_0(1 + q_0)) + s_0)) + 4(47 - j_0 + q_0 + 3q_0^2 - (12(-1 + q_0)(1 + j_0 - q_0(1 + 3q_0)))) / \\
 & (14 + 5j_0(1 + 2q_0) - q_0(14 + 15q_0(1 + q_0)) + s_0))z - (4(12(-1 - j_0 + q_0 + 3q_0^2)(7 - j_0 + q_0 \\
 & + 3q_0^2) + 4(1 + j_0 - q_0(1 + 3q_0))^2 - (14 + 5j_0(1 + 2q_0) - q_0(14 + 15q_0(1 + q_0)) + s_0)^2)(-1 \\
 & + 2z^2)) / (14 + 5j_0(1 + 2q_0) - q_0(14 + 15q_0(1 + q_0)) + s_0)) / (192(1 + (4(1 + j_0 - q_0(1 \\
 & + 3q_0))z) / (14 + 5j_0(1 + 2q_0) - q_0(14 + 15q_0(1 + q_0)) + s_0))) . \tag{C.3}
 \end{aligned}$$

$$\begin{aligned}
 R_{2,2}(z) = & -\frac{1}{H_0} \left[(2808 + 3828s_0 + 474s_0^2 + 15s_0^3 + 891712z + 115776s_0z + 4560s_0^2z + 753744z^2 \right. \\
 & + 142392s_0z^2 + 4284s_0^2z^2 + 90s_0^3z^2 - 50625q_0^9(1 + 6z^2) - 10125q_0^8(15 - 16z + 90z^2) \\
 & - 135q_0^7(1723 - 2800z + 12738z^2) + 135q_0^6(-845 + 10688z - 7470z^2 + 75s_0(1 + 6z^2)) \\
 & - q_0^3(-13140 + 440320z - 79608z^2 + 675s_0^2(1 + 6z^2) + 576s_0(2 + 275z + 12z^2)) + 18q_0^5(4463 \\
 & + 117160z + 23082z^2 + 75s_0(15 - 16z + 90z^2)) + 5j_0^3(183 - 688z + 1098z^2 + 3000q_0^3(1 \\
 & + 6z^2) + 300q_0^2(15 - 16z + 90z^2) + 6q_0(311 - 800z + 1866z^2)) - 3q_0^2(9420 + 555072z \\
 & + 541384z^2 + 15s_0^2(15 - 16z + 90z^2) + 8s_0(385 + 5300z + 2718z^2)) + 9q_0^4(15158 + 229520z \\
 & + 214372z^2 + s_0(2513 - 3200z + 19878z^2)) - 6q_0(s_0^2(79 - 40z + 714z^2) + 4s_0(319 + 4624z \\
 & + 5594z^2) + 4(351 + 61768z + 69386z^2)) - 3j_0^2(s_0(-311 + 800z - 1866z^2) + 22500q_0^5(1 \\
 & + 6z^2) + 3000q_0^4(15 - 16z + 90z^2) + 125q_0^3(313 - 544z + 2262z^2) - 2(1079 + 6040z \\
 & + 12986z^2) - 5q_0^2(-293 + 37264z - 1758z^2 + 300s_0(1 + 6z^2)) - 2q_0(6181 + 71720z \\
 & + 62254z^2 + 50s_0(15 - 16z + 90z^2))) + 3j_0(33750q_0^7(1 + 6z^2) + 5625q_0^6(15 - 16z + 90z^2) \\
 & + 5s_0^2(15 - 16z + 90z^2) + 4s_0(363 + 3400z + 3634z^2) + 60q_0^5(1723 - 2800z + 12738z^2) \\
 & + 4(1019 + 62496z + 78914z^2) - 15q_0^4(-1745 + 39664z - 15270z^2 + 300s_0(1 + 6z^2)) \\
 & + 2q_0(75s_0^2(1 + 6z^2) + 64(36 + 1895z + 1520z^2) + 2s_0(427 + 8200z + 3762z^2)) - 2q_0^3(225s_0(15 \\
 & - 16z + 90z^2) + 8(2477 + 42040z + 19398z^2)) - 2q_0^2(s_0(2513 - 3200z + 19878z^2) + 12(1433 \\
 & + 18780z + 21502z^2)))) / (384(-2348 - 324s_0 - 15s_0^2 - 784z - 200s_0z + 104z^2 + 136s_0z^2 \\
 & + 10s_0^2z^2 + 1125q_0^6(-3 + 2z^2) + 90q_0^5(-75 - 4z + 50z^2) + q_0^4(-6795 - 480z + 3138z^2) \\
 & - 6q_0^3(25s_0(-3 + 2z^2) + 8(-20 - 35z + 16z^2)) - 4q_0(-982 - 296z + 52z^2 + s_0(-81 - 2z \\
 & + 34z^2)) + j_0^2(-215 - 40z + 122z^2 + 500q_0^2(-3 + 2z^2) + 20q_0(-75 - 4z + 50z^2)) + q_0^2(8(578 \\
 & + 475z - 146z^2) - 6s_0(-75 - 4z + 50z^2)) - 2j_0(1034 + 700z - 212z^2 + s_0(75 + 4z - 50z^2) \\
 & + 750q_0^4(-3 + 2z^2) + 45q_0^3(-75 - 4z + 50z^2) + q_0^2(-2265 - 160z + 1046z^2) + q_0(970 + 780z \\
 & - 468z^2 - 50s_0(-3 + 2z^2))))). \tag{C.4}
 \end{aligned}$$

References

1. S. Weinberg, *Gravitation and Cosmology* (Wiley, New York, 1972).
2. A. H. Guth, *Phys. Rev. D* **23** (1981) 347.
3. S. Capozziello and V. Faraoni, *Beyond Einstein Gravity: A Survey of Gravitational Theories for Cosmology and Astrophysics*, *Fundam. Theor. Phys.* **170** (2010).
4. S. Capozziello and M. Francaviglia, *Gen. Rel. Grav.* **40** (2008) 35.
5. I. L. Buchbinder, S. D. Odintsov and I. Shapiro, *Effective Action in Quantum Gravity* (IOP Publishing, Bristol, 1992).
6. N. D. Birrell and P. C. W. Davies, *Quantum Fields in Curved Space* (Cambridge University Press, Cambridge, 1982).
7. S. Perlmutter *et al.*, *Astrophys. J.* **517** (1999) 565.
8. A. G. Riess *et al.*, *Astron. J.* **116** (1998) 1009; B. Schmidt *et al.*, *Astrophys. J.* **507** (1998) 46.
9. B. S. Haridasu, V. V. Luković, R. D'Agostino and N. Vittorio, *Astron. Astrophys.* **600** (2017) L1.
10. WMAP Collab. (G. Hinshaw *et al.*), *Astrophys. J. Supp. Ser.* **208** (2013) 2.
11. Planck Collab. (P. A. R. Ade *et al.*), *Astron. Astrophys.* **594** (2016) A132015.
12. V. Sahni and A. Starobinsky, *Int. J. Mod. Phys. D* **9** (2000) 373.
13. S. Weinberg, *Rev. Mod. Phys.* **61** (1989) 1.
14. P. J. E. Peebles and B. Ratra, *Rev. Mod. Phys.* **75** (2003) 559.
15. I. Zlatev, L. Wang and P. J. Steinhardt, *Phys. Rev. Lett.* **82** (1999) 896.
16. V. Sahni, *Class. Quant. Grav.* **19** (2002) 3435.
17. S. M. Carroll, *Living Rev. Rel.* **4** (2001) 1.
18. D. Huterer and M. S. Turner, *Phys. Rev. D* **64** (2001) 123527.
19. T. Padmanabhan, *Phys. Rept.* **380** (2003) 235.
20. R. R. Caldwell, M. Kamionkowski and N. N. Weinberg, *Phys. Rev. Lett.* **91** (2003) 071301.
21. E. J. Copeland, M. Sami and S. Tsujikawa, *Int. J. Mod. Phys. D* **15** (2006) 1753.
22. M. Li, X. D. Li, S. Wang and Y. Wang, *Commun. Theor. Phys.* **56** (2011) 525.
23. A. Y. Kamenshchik, U. Moschella and V. Pasquier, *Phys. Lett. B* **511** (2001) 265.
24. T. Padmanabhan, *Phys. Rev. D* **66** (2002) 021301.
25. S. Capozziello, *Int. J. Mod. Phys. D* **11** (2002) 483.
26. Y. F. Cai, S. Capozziello, M. De Laurentis and E. N. Saridakis, *Rept. Prog. Phys.* **79** (2016) 106901.
27. A. Friedmann, *Zeitschrift für Physik* **10** (1922) 377.
28. G. Lemaître, *Mon. Not. Roy. Astron. Soc.*, **91** (1931) 483.
29. H. P. Robertson, *Astrophys. J.* **82** (1935) 284.
30. A. G. Walker, *Proc. London Math. Soc.* **s2-42** (1937) 90.
31. V. V. Luković, R. D'Agostino and N. Vittorio, *Astron. Astrophys.* **595** (2016) A109.
32. E. Hubble, *Proc. Nat. Acad. Sci.*, **15** (1929) 168.
33. W. L. Freedman *et al.*, *Astrophys. J.* **553** (2001) 47.
34. A. G. Riess *et al.*, *Astrophys. J.* **826** (2016) 56.
35. V. Bonvin *et al.*, *Mon. Not. Roy. Astron. Soc.* **465** (2017) 4914.
36. O. Luongo, M. Muccino, *Phys. Rev. D* **98** (2018) 103520.
37. O. Luongo, H. Quevedo, *Int. J. Mod. Phys. D*, **23**, (2014) 1450012.
38. O. Luongo, H. Quevedo, *Astroph. sp. sci.*, **338**, (2012) 345.
39. P. K. S. Dunsby, O. Luongo, L. Reverberi, *Phys. Rev. D*, **94**, (2016) 083525.
40. A. Aviles, N. Cruz, J. Klapp, O. Luongo, *Gen. Rel. Grav.*, **47**, (2015), 63.
41. S. Capozziello, R. D'Agostino, O. Luongo, *Phys. Dark Univ.*, **20**, (2018), 12.
42. S. Capozziello, R. D'Agostino, R. Giambo', O. Luongo, *Phys. Rev. D*, **99**, (2019),

- 023532.
43. K. Boshkayev, R. D'Agostino, O. Luongo, ArXiv[gr-qc]:1901.01031, (2019).
 44. A. D. Linde, Phys. Lett. B **108** (1982) 389.
 45. A. Albrecht and P. J. Steinhardt, Phys. Rev. Lett. **48** (1982) 1220.
 46. P. J. Peebles and R. Ratra, Astrophys. J. **325** (1988) 1220; B. Ratra and P. J. E. Peebles, Phys. Rev. D **37** (1988) 3406.
 47. R. R. Caldwell, R. Dave and P. J. Steinhardt, Phys. Rev. Lett. **80** (1998) 1582.
 48. C. Armendariz-Picon, V. Mukhanov and P. J. Steinhardt, Phys. Rev. Lett. **85** (2000) 4438.
 49. P. G. Ferreira and M. Joyce, Phys. Rev. D **58** (1998) 023503.
 50. E. J. Copeland, A. R. Liddle and D. Wands, Phys. Rev. D **57** (1998) 4686.
 51. P. J. Steinhardt, L. Wang and I. Zlatev, Phys. Rev. D **59** (1999) 123504.
 52. G. Lemaitre, Ann. Soc. Sci. Bruxelles **53** (1933) 51.
 53. R. C. Tolman, Proc. Nat. Acad. Sci. **20** (1934) 169.
 54. H. Bondi, Mon. Not. Roy. Astron. Soc. **107** (1947) 410.
 55. S. Nadathur and S. Sarkar, Phys. Rev. D **83** (2011) 063506.
 56. S. Capozziello and M. De Laurentis, Phys. Rept. **509** (2011) 167.
 57. S. Nojiri, S. D. Odintsov and V. K. Oikonomou, Phys. Rept. **692** (2017) 1.
 58. S. Nojiri and S. D. Odintsov, Int. J. Geom. Meth. Mod. Phys. **4** (2007) 115.
 59. LIGO Scientific and Virgo Collab. (B. P. Abbott *et al.*), Phys. Rev. Lett. **116** (2016) 061102.
 60. A. A. Starobinsky, Phys. Lett. B **91** (1980) 99.
 61. J. P. Duruisseau, R. Kerner and P. Eysseric, Gen. Rel. Grav. **15** (1983) 797.
 62. D. La and P. J. Steinhardt, Phys. Rev. Lett. **62** (1989) 1066.
 63. K. Maeda, Phys. Rev. D **39** (1989) 3159.
 64. D. Wands, Class. Quant. Grav. **11** (1994) 269.
 65. S. Capozziello, R. de Ritis and A. A. Marino, Gen. Rel. Grav. **30** (1998) 1247.
 66. R. Utiyama and B. S. De Witt, J. Math. Phys. **3** (1962) 608.
 67. S. Capozziello, Int. J. Mod. Phys. D **11** (2002) 483; S. Capozziello, V. F. Cardone, S. Carloni and A. Troisi, Int. J. Mod. Phys. D **12** (2003) 1969; S. Capozziello, V. F. Cardone and A. Troisi, Phys. Rev. D **71** (2005) 043503.
 68. S. M. Carroll, V. Duvvuri, M. Trodden and M. S. Turner, Phys. Rev. D **70** (2004) 043528.
 69. T. P. Sotiriou and V. Faraoni, Rev. Mod. Phys. **82** (2010) 451.
 70. A. De Felice and S. Tsujikawa, Living Rev. Rel. **13** (2010) 3.
 71. S. Nojiri and S. D. Odintsov, Phys. Rept. **505** (2011) 59.
 72. A. Palatini, Rend. Circ. Mat. Palermo **43** (1919) 203.
 73. M. Ferraris, M. Francaviglia and I. Volovich, Class. Quant. Grav. **11** (1994) 1505.
 74. G. Magnano and L. M. Sokolowski, Phys. Rev. D **50** (1994) 5039.
 75. M. Borunda, B. Janssen and M. Bastero-Gil, J. Cosm. Astrop. Phys. **0811** (2008) 008.
 76. F. W. Hehl and G. D. Kerlick, Gen. Rel. Gravit. **9** (1978) 691.
 77. S. Capozziello, R. Cianci, C. Stornaiolo and S. Vignolo, Class. Quant. Grav. **24** (2007) 6417.
 78. T. P. Sotiriou and S. Liberati, Ann. Phys. **322** (2007) 935.
 79. Y. Wang, Phys. Rev. D **42** (1990) 2541.
 80. S. Nojiri and S. D. Odintsov, Phys. Rev. D **68** (2003) 123512.
 81. A. D. Dolgov and M. Kawasaki, Phys. Lett. B, **1573** (2003) 1.
 82. M. E. Sousa and R. P. Woodard, Gen. Rel. Grav. **36** (2004) 855.
 83. L. Amendola, D. Polarski and S. Tsujikawa, Phys. Rev. Lett. **98** (2007) 131302; L.

78 *S. Capozziello, R. D'Agostino, O. Luongo*

- Amendola, D. Polarski, and S. Tsujikawa, *Int. J. Mod. Phys. D* **16** (2007) 1555.
84. S. Capozziello, S. Nojiri, S. D. Odintsov and A. Troisi, *Phys. Lett. B* **639** (2006) 135.
85. G. J. Olmo, *Phys. Rev. D* **72** (2005) 083505.
86. V. Faraoni, *Phys. Rev. D* **74** (2006) 023529.
87. L. Amendola, R. Gannouji, D. Polarski and S. Tsujikawa, *Phys. Rev. D*, **75** (2007) 083504.
88. S. M. Carroll, I. Sawicki, A. Silvestri, M. Trodden, *New J. Phys.*, **8**, 323 (2006).
89. Y. S. Song, W. Hu, I. Sawicki, *Phys. Rev. D*, **75**, 044004 (2007).
90. R. Bean, D. Bernat, L. Pogosian, A. Silvestri, M. Trodden, *Phys. Rev. D*, **75**, 064020 (2007).
91. T. Chiba, T. L. Smith and A. L. Erickcek, *Phys. Rev. D*, **75**, 124014 (2007).
92. W. Hu and I. Sawicki, *Phys. Rev. D* **7676** (2007) 064004.
93. S. A. Appleby and R. A. Battye, *Phys. Lett. B* **654** (2007) 7.
94. G. Cognola, E. Elizalde, S. Nojiri, S.D. Odintsov, L. Sebastiani, S. Zerbini, *Phys.Rev. D* **77** (2008) 046009.
95. S. Nojiri, S. D. Odintsov, *Phys.Rev. D* **77** (2008) 026007.
96. E. Elizalde, S. Nojiri, S.D. Odintsov, L. Sebastiani, S. Zerbini, *Phys. Rev. D* **83** (2011) 086006.
97. D. N. Vollick, *Phys. Rev. D* **68** (2003) 063510.
98. X. Meng and P. Wang, *Gen. Rel. Grav.* **36** (2004) 2673.
99. C. Brans and R. H. Dicke, *Phys. Rev.* **124** (1961) 925.
100. T. Chiba, *Phys. Lett. B* **575** (2003) 1.
101. V. Faraoni and S. Nadeau, *Phys. Rev. D* **75** (2007) 023501.
102. S. Capozziello and S. Vignolo, *Class. Quant. Grav.* **26**, 175013 (2009).
103. F. Briscese, E. Elizalde, S. Nojiri, S.D. Odintsov, *Phys.Lett. B* **646** (2007) 105.
104. S. Bahamonde, S.D. Odintsov, V.K. Oikonomou, *Annals Phys.* **373** (2016) 96.
105. S. Bahamonde, S. D. Odintsov, V.K. Oikonomou, P. V. Tretyakov, *Phys.Lett. B* **766** (2017) 225.
106. T. Harko, T. S. Koivisto, F. S. N. Lobo and G. J. Olmo, *Phys. Rev. D* **85** (2012) 084016
107. S. Capozziello, T. Harko, T. S. Koivisto, F. S. N. Lobo and G. J. Olmo, *Universe* **1**, 199 (2015).
108. S. Capozziello, T. Harko, T. S. Koivisto, F. S. N. Lobo and G. J. Olmo. *JCAP* **1304**, 011 (2013).
109. S. Capozziello, T. Harko, F. S. N. Lobo and G. J. Olmo, *Int. J. Mod. Phys. D* **22** (2013) 1342006.
110. X. H. Meng and P. Wang, *Class. Quant. Grav.* **20** (2003) 4949.
111. X. H. Meng and P. Wang, *Class. Quant. Grav.* **21** (2004) 951.
112. S. Fay, R. Tavakol and S. Tsujikawa, *Phys. Rev. D* **75** (2007) 063509.
113. M. Amarzguioui, O. Elgaroy, D. F. Mota and T. Multamaki, *Astron. Astrophys.* **454** (2006) 707.
114. T. Koivisto, *Phys. Rev. D* **73** (2006) 083517.
115. B. Li and M. C. Chu, *Phys. Rev. D* **74** (2006) 104010.
116. S. Tsujikawa, K. Uddin and R. Tavakol, *Phys. Rev. D* **77** (2008) 043007.
117. E. E. Flanagan, *Phys. Rev. Lett.* **92** (2004) 071101.
118. F. W. Hehl, P. Von Der Heyde, G. D. Kerlick and J. M. Nester, *Rev. Mod. Phys.*, **48** (1976) 393.
119. M. B. Green, J. H. Schwarz and E. Witten, *Superstring Theory* (Cambridge University Press, Cambridge, 1987).
120. R. Hammond, *Nuovo Cim. B* **109** (1994) 319.

121. V. de Sabbata and C. Sivaram, *Ann. Phys.* **48** (1991) 419.
122. V. de Sabbata, C. Sivaram and Twistors, *Nuovo Cim. A*, **109** (1996) 377.
123. P. S. Howe, A. Opfermann and G. Papadopoulos, *Commun. Math. Phys.* **197** (1998) 713.
124. C. M. Hull, G. Papadopoulos and P. K. Townsend, *Phys. Lett. B* **316** (1993) 291.
125. G. Papadopoulos and P. K. Townsend, *Nucl. Phys. B*, **444** (1995) 245.
126. H. Gonner and F. Mueller-Hoissen, *Class. Quant. Grav.* **1** (1984) 651.
127. P. Chatterjee and B. Bhattacharya, *Mod. Phys. Lett. A* **8** (1993) 2249.
128. C. Wolf, *Gen. Rel. Grav.* **27** (1995) 1031.
129. D. K. Ross, *Int. J. Theor. Phys.* **28** (1989) 1333.
130. L. C. Garcia de Andrade, *Mod. Phys. Lett. A* **12** (1997) 2005.
131. S. Vignolo, S. Carloni and L. Fabbri, *Phys. Rev. D* **91** (2015) 043528.
132. S. Capozziello and C. Stornaiolo, *Nuovo Cim. B* **113** (1998) 879.
133. S. Capozziello, G. Lambiase and C. Stornaiolo, *Ann. Phys.* **10** (2001) 713.
134. A. Trautman, *Nature* **242** (1973) 7.
135. S. W. Hawking and G. F. R. Ellis, *The large scale structure of space-time* (Cambridge University Press, Cambridge, 1973).
136. C. Møller, *Nordita Publ.* **64** (1961) 50.
137. J. W. Maluf, *J. Math. Phys.* **35** (1994) 335.
138. A. Unzicker and T. Case, physics/0503046 (2005).
139. R. Weitzenböck, *Invariantentheorie* (Noordhoff, Groningen, 1923).
140. S. Kobayashi and K. Nomizu, *Foundations of Differential Geometry* (Interscience, New York, 1963).
141. V. C. de Andrade, L. C. T. Guillen and J. G. Pereira, *Phys. Rev. Lett.* **84** (2000) 4533.
142. K. S. Virbhadra, *Phys. Rev. D* **42** (1990) 2919.
143. T. Shirafuji, G. G. L. Nashed and Y. Kobayashi, *Prog. Theor. Phys.* **96** (1996) 933.
144. S. Capozziello, R. D'Agostino and O. Luongo, *Gen. Rel. Grav.* **49** (2017) 141.
145. S. Capozziello, O. Luongo and E. N. Saridakis, *Phys. Rev. D* **91** (2015) 124037.
146. A. Aviles, A. Bravetti, S. Capozziello and O. Luongo, *Phys. Rev. D* **87** (2013) 064025.
147. H. Abedi, M. Wright and A. M. Abbassi, *Phys. Rev. D* **95** (2017) 064020.
148. R. Ferraro and F. Fiorini, *Phys. Rev. D* **75** (2007) 084031.
149. G. R. Bengochea and R. Ferraro, *Phys. Rev. D* **79** (2009) 124019.
150. E. V. Linder, *Phys. Rev. D* **81** (2010) 127301.
151. C. Q. Geng, C. C. Lee, E. N. Saridakis and Y. P. Wu, *Phys. Lett. B* **704** (2011) 384.
152. C. Xu, E. N. Saridakis and G. Leon, *J. Cosm. Astrop. Phys.* **07** (2012) 005.
153. R. D'Agostino and O. Luongo, *Phys. Rev. D* **98** (2018) 124013.
154. J. P. Uzan, *Phys. Rev. D* **59** (1999) 123510.
155. N. Bartolo and M. Pietroni, *Phys. Rev. D* **61** (1999) 023518.
156. V. Faraoni, *Phys. Rev. D* **62** (2000) 023504.
157. V. Vardanyan and L. Amendola, *Phys. Rev. D* **92** (2015) 024009.
158. D. I. Kaiser, *Phys. Rev. D* **81** (2010) 084044.
159. H. Abedi and A. M. Abbassi, *J. Cosm. Astrop. Phys.* **05** (2015) 026.
160. R. J. Yang, *Europhys. Lett.* **93** (2011) 60001.
161. M. Wright, *Phys. Rev. D* **93** (2016) 103002.
162. H. Abedi, S. Capozziello, R. D'Agostino and O. Luongo, *Phys. Rev. D* **97** (2018) 084008.
163. M. Visser, *Gen. Rel. Grav.* **37** (2005) 1541; M. Visser, *Class. Quant. Grav.* **32** (2015) 135007.
164. P. K. S. Dunsby and O. Luongo, *Int. J. Geom. Meth. Mod. Phys.* **13** (2016) 1630002.

80 *S. Capozziello, R. D'Agostino, O. Luongo*

165. E. R. Harrison, *Nature* **260** (1976) 591.
166. O. Luongo, *Phys. Lett. A*, **28** (2013) 1350080.
167. S. Capozziello, M. De Laurentis, O. Luongo and A. C. Ruggeri, *Galaxies* **1** (2013) 216.
168. A. Mukherjee, N. Paul and H. K. Jassal, *J. Cosm. Astrop. Phys.* **1901** (2019) 005.
169. S. Capozziello, O. Farooq, O. Luongo and B. Ratra, *Phys. Rev D* **90** (2014) 044016.
170. A. Aviles, A. Bravetti, S. Capozziello and O. Luongo, *Phys. Rev. D* **87** (2013) 044012.
171. S. Capozziello, M. De Laurentis and O. Luongo, *Int. J. Mod. Phys. D* **24** (2014) 1541002.
172. O. Luongo, *Entropy* **19** (2017) 55.
173. O. Luongo and H. Quevedo, *Gen. Rel. Grav.* **46** (2014) 1649.
174. H. Velten, S. Gomes and V. C. Busti, *Phys. Rev. D* **97** (2018) 083516.
175. U. Andrade, C. A. P. Bengaly, J. S. Alcaniz and B. Santos, *Phys. Rev. D* **97** (2018) 083518.
176. C. Rodrigues Filho, Edesio M. Barboza, *J. Cosm. Astrop. Phys.* **1807** (2018) 037.
177. O. Luongo, G. B. Pisani and A. Troisi, *Int. J. Mod. Phys. D* **26** (2016) 1750015.
178. Z. Y. Yin and H. Wei, e-Print: arXiv:1902.00289, (2019).
179. A. Al Mamon and K. Bamba, *Eur. Phys. J. C* **78** (2018) 862.
180. A. Piloyan, S. Pavluchenko and L. Amendola, *Particles* **1** (2018) 23.
181. F. Montanari and S. Rasanen, *J. Cosm. Astrop. Phys.* 1711 (2017) 032.
182. X. B. Zou, H. K. Deng, Z. Y. Yin and H. Wei, *Phys. Lett. B* **776** (2018) 284.
183. W. Yang, L. Xu, H. Li, Y. Wu and J. Lu, *Entropy* **19** (2017) 327.
184. C. S. Carvalho, S. Basilakos, *Astron. Astrophys.* **592** (2016) A152.
185. O. Luongo and H. Quevedo, *Found. of Phys.* **48** (2017) 1.
186. I. Semiz and A. K. Camlibel, *J. Cosm. Astrop. Phys.* **1512** (2015) 038.
187. Y. L. Bolotin, V. A. Cherkaski and O. A. Lemets, *Int. J. Mod. Phys. D* **25** (2016) 1650056.
188. B. Bochner, D. Pappas, M. Dong, *Astrophys. J.* **814** (2015) 7.
189. S. Nesseris and J. Garcia-Bellido, *Phys. Rev. D* **88** (2013) 063521.
190. O. Farooq, S. Crandall and B. Ratra, *Phys. Lett. B* **726** (2013) 72.
191. F. A. Teppa Pannia and S. E. Perez Bergliaffa, *J. Cosm. Astrop. Phys.* **1308** (2013) 030.
192. C. J. A. P. Martins, M. Martinelli, E. Calabrese and M. P. L. P. Ramos, *Phys. Rev. D* **94** (2016) 043001.
193. F. Piazza and T. Schucker, *Gen. Rel. Grav.* **48** (2016) 41.
194. K. Bamba, S. Capozziello, S. Nojiri and S. D. Odintsov, *Astrop. Sp. Sci.* **342** (2012) 155.
195. S. Capozziello, V. F. Cardone, H. Farajollahi and A. Ravanpak, *Phys. Rev. D* **84** (2011) 043527.
196. J. C. Carvalho and J. S. Alcaniz, *Mon. Not. Roy. Astron. Soc.* **418** (2011) 1873.
197. M. Bouhmadi-Lopez, S. Capozziello and V. F. Cardone, *Phys. Rev. D* **82** (2010) 103526.
198. S. Capozziello, V. F. Cardone and V. Salzano, *Phys. Rev. D* **78** (2008) 063504.
199. M. V. John, *Astrophys. J.* **630** (2005) 667.
200. S. Capozziello, Ruchika and A. A. Sen, *Mon. Not. Roy. Astron. Soc.* **484** (2019) 4484.
201. C. Cattoen and M. Visser, *Phys. Rev. D* **78** (2008) 063501.
202. A. Aviles, C. Gruber, O. Luongo and H. Quevedo, *Phys. Rev. D* **86** (2012) 123516.
203. C. Clarkson, M. Cortes and B. A. Bassett, *J. Cosm. Astrop. Phys.* **0708** (2007) 011.
204. A. Pavlov, S. Westmoreland, K. Saaidi and B. Ratra, *Phys. Rev. D* **88** (2013) 123513.
205. G. A. Baker Jr. and P. Graves-Morris, *Padé Approximants* (Cambridge University

- Press, 1996).
206. G. L. Litvinov, *Appl. Russ. J. Math. Phys.* **1** (1993) 313.
 207. C. Gruber and O. Luongo, *Phys. Rev. D* **89** (2014) 103506.
 208. H. Wei, X. P. Yan and Y. N. Zhou, *J. Cosm. Astrop. Phys.* **1401** (2014) 045.
 209. K. Dutta, Ruchika, A. Roy, A. A. Sen and M. M. Sheikh-Jabbari, e-Print: arXiv:1808.06623 (2018).
 210. A. Aviles, A. Bravetti, S. Capozziello and O. Luongo, *Phys. Rev. D* **90** (2014) 043531.
 211. S. Capozziello, R. D'Agostino and O. Luongo, *Mon. Not. Roy. Astron. Soc.* **476** (2018) 3924.
 212. P. L. Chebyshev, *Mémoires des Savants étrangers présentés à l'Académie de Saint-Petersbourg* **7** (1854) 539.
 213. B. Obsieger, *Numerical Methods III - Approximations of Functions* (University of Rijeka, 2013).
 214. M. Betoule *et al.*, *Astron. Astrophys.* **568** (2014) A22.
 215. R. Jimenez and A. Loeb, *Astrophys. J.* **573** (2002) 37.
 216. SDSS Collab. (D. J. Eisenstein *et al.*), *Astrophys. J.* **633** (2005) 560.
 217. B. Audren, J. Lesgourgues, K. Benabed and S. Prunet, *J. Cosm. Astrop. Phys.* **02** (2013) 001.
 218. O. Luongo, *Mod. Phys. Lett. A*, **26** (2011) 1459.
 219. A. Aviles, J. Klapp, O. Luongo, *Phys. Dark Univ.*, **17** (2017) 25.
 220. A. Lewis and S. Bridle, *Phys. Rev. D*, **66** (2002) 103511.
 221. V. C. Busti, P. K. S. Dunsby, A. de la Cruz-Dombriz, D. Saez-Gomez, *Phys. Rev. D*, **92** (2015) 123512.
 222. S. Capozziello, R. D'Agostino and O. Luongo, *J. Cosm. Astrop. Phys.* **1805** (2018) 008.
 223. A. A. Starobinsky, *JETP Lett.* **86** (2007) 157.
 224. G. Cognola, E. Elizalde, S. Nojiri, S. D. Odintsov, L. Sebastiani and S. Zerbini, *Phys. Rev. D* **77** (2008) 046009.
 225. S. Tsujikawa, *Phys. Rev. D* **77** (2008) 023507.
 226. G. James, D. Witten, T. Hastie and R. Tibshirani, *An Introduction to Statistical Learning* (Springer-Verlag, New York, 2013).
 227. C. J. A. P. Martins, *Rep. Prog. Phys.* **80** (2017) 12.
 228. S. Nojiri, S.D. Odintsov, D. Saez-Gomez, *Phys. Lett. B* **681** (2009) 74.
 229. S. Nojiri and S.D. Odintsov, *Phys. Rev. D* **74** (2006) 086005.
 230. S. Capozziello, R. D'Agostino and O. Luongo, *Gen. Rel. Grav.* **51** (2019) 2.
 231. R. Dick, *Gen. Rel. Grav.* **36** (2004) 217.
 232. A. E. Dominguez and D. E. Barraco, *Phys. Rev. D* **70** (2004) 043505.
 233. A. de la Cruz-Dombriz, P. K. S. Dunsby, O. Luongo and L. Reverberi, *J. Cosm. Astrop. Phys.* **1612** (2016) 042.
 234. D. Muthukrishna and D. Parkinson, *J. Cosm. Astrop. Phys.* **1611** (2016) 052.
 235. N. R. Draper and H. Smith, *Applied Regression Analysis* (Wiley-Interscience, 1998).
 236. S. Nesseris, S. Basilakos, E. N. Saridakis and L. Perivolaropoulos, *Phys. Rev. D* **88** (2013) 103010.
 237. C. Zhang *et al.*, *Res. Astron. Astrophys.* **14** (2014) 1221.
 238. J. Simon, L. Verde and R. Jimenez, *Phys. Rev. D* **71** (2005) 123001.
 239. M. Moresco *et al.*, *J. Cosm. Astrop. Phys.* **8** (2012) 006.
 240. C. H. Chuang, *Mon. Not. Roy. Astron. Soc.* **426** (2012) 006.
 241. M. Moresco *et al.*, *J. Cosm. Astrop. Phys.* **05** (2016) 014.
 242. D. Stern *et al.*, *J. Cosm. Astrop. Phys.* **1002** (2010) 008.
 243. M. Moresco, *Mon. Not. Roy. Astron. Soc.* **450** (2015) L16.

82 *S. Capozziello, R. D'Agostino, O. Luongo*

- 244. F. Beutler *et al.*, *Mon. Not. Roy. Astron. Soc.* **416** (2011) 3017.
- 245. A. Ross *et al.*, *Mon. Not. Roy. Astron. Soc.* **449** (2015) 835.
- 246. BOSS Collab. (L. Anderson *et al.*), *Mon. Not. Roy. Astron. Soc.* **441** (2014) 24.
- 247. BOSS Collab. (T. Delubac *et al.*) *Astron. Astrophys.* **574** (2015) A59.
- 248. BOSS Collab. (A. Font-Ribera *et al.*), *J. Cosm. Astrop. Phys.* **1405** (2014) 27.
- 249. L. Del Vecchio, L. Fatibene, S. Capozziello, M. Ferraris, P. Pinto and S. Camera, *Eur. Phys. J. Plus* **134** (2019) 5